Superconducting RF-I
- Basics for SRF Cavity -

K.Saito KEK

1. Superconductivity Basics
2. Niobium Material
3. SRF Cavity Design
4. HOM Issue
5. Lorentz Detuning
6. RF input coupler
7. Cavity Dressing
8. Cryomodule
9. Cryogenics

1. Superconductivity   Basics

1.1 Superconductivity

1.2 SRF Specifics and Constrains

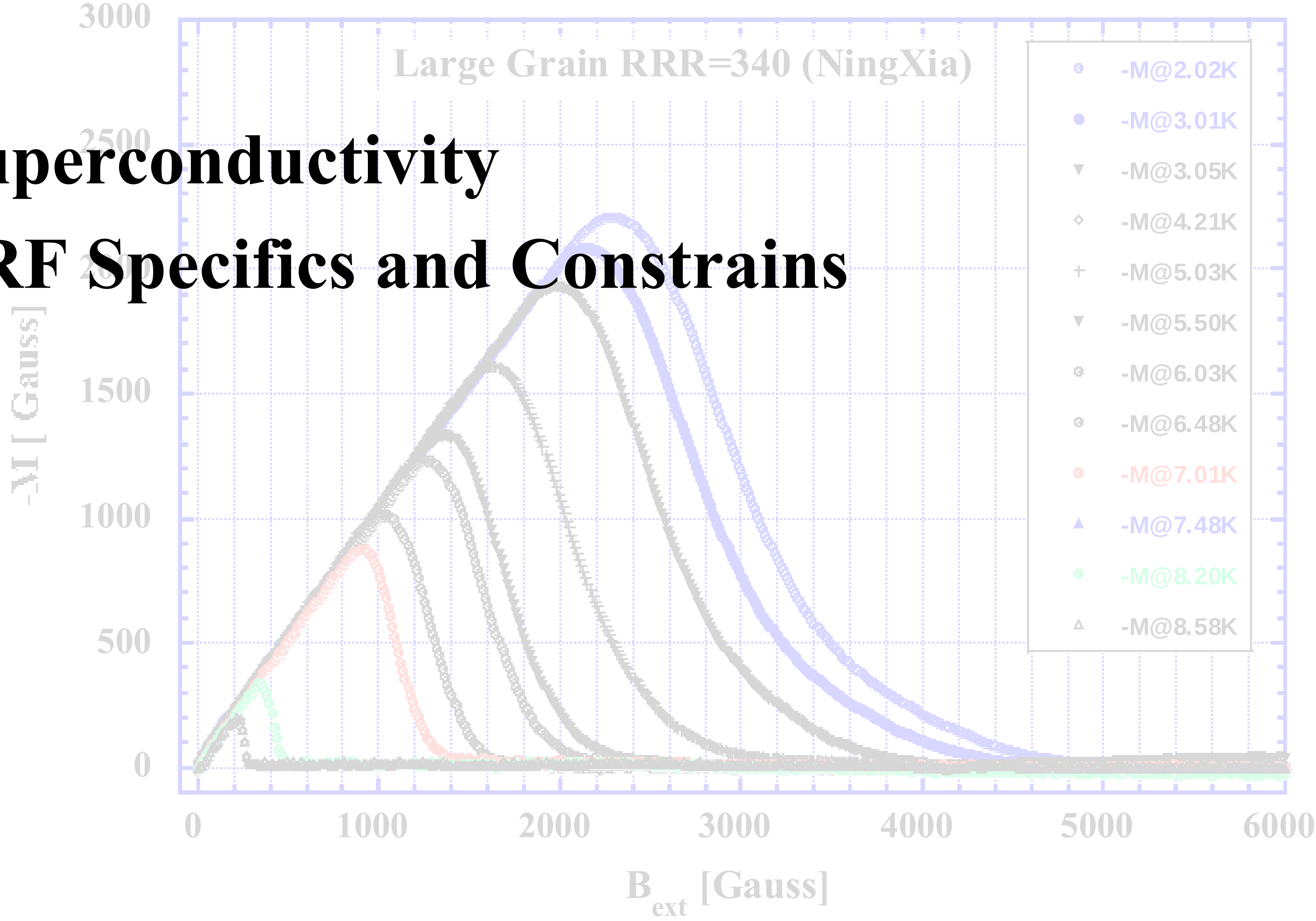

1.1 Superconductivity

1911 by K.Onnes

19933 by Meissner and Ochsenfeld (experiment)
1935 Phenomenological theory by F.and H.London

Zero resistance @ Tc

Perfect diamagnetism < Hc

Miessner effect

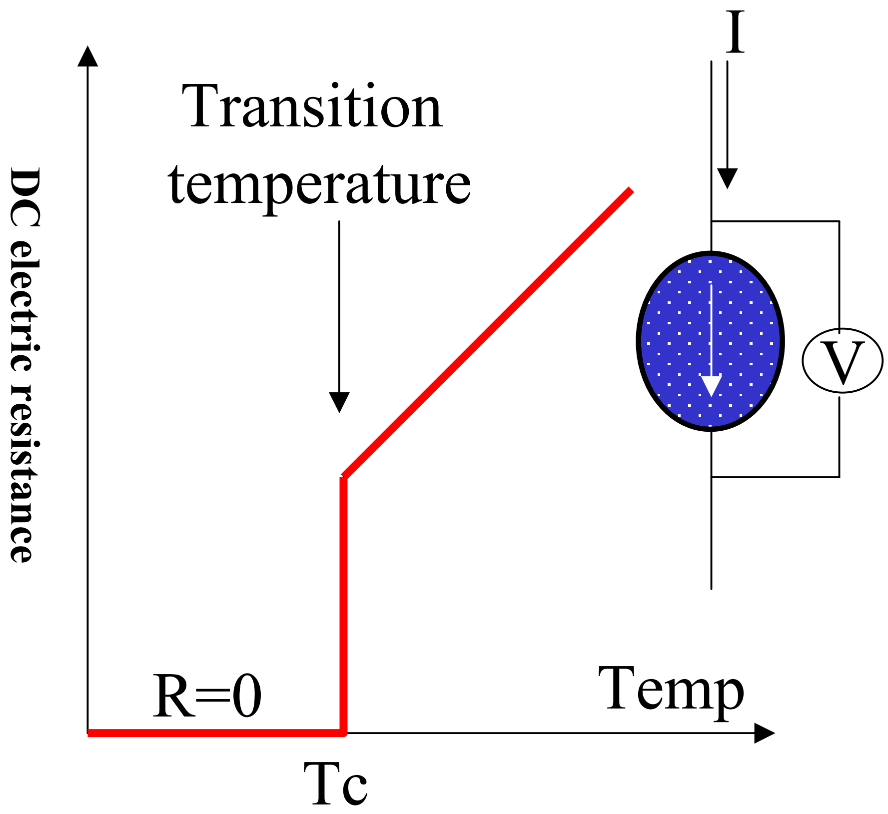

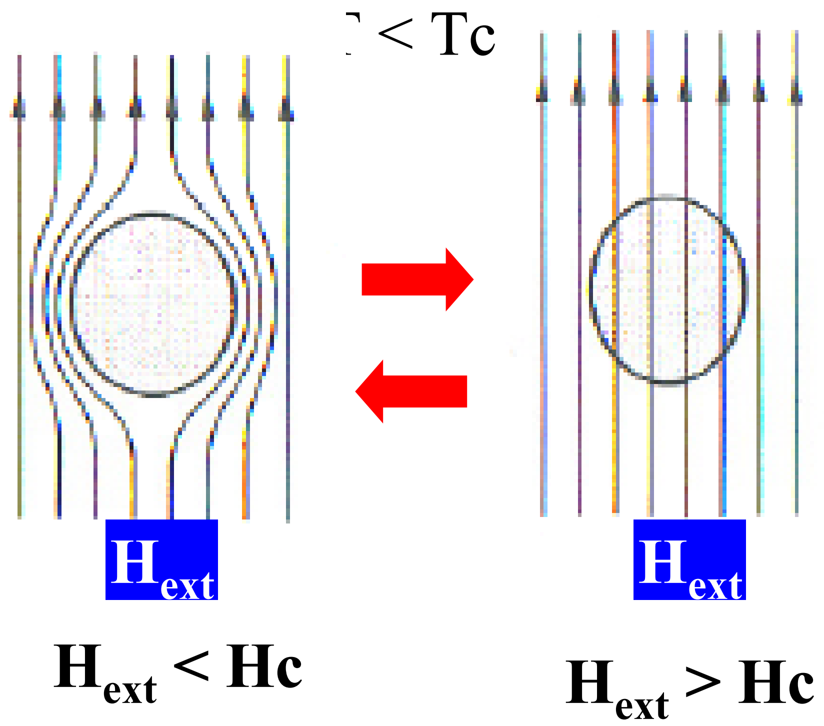

Microscopic Theory

Two electrons having opposite spin and momentum get an attractive interaction through lattice/electron interaction.

Attractive interaction through electron-lattice interaction

$$V = \frac{\left|V_{\mathbf{p}-\hbar\mathbf{k},\mathbf{p}}\right|^2}{\varepsilon(\mathbf{p}) - \varepsilon(\mathbf{p}-\hbar\mathbf{k}) - \hbar\omega(\mathbf{k})}$$

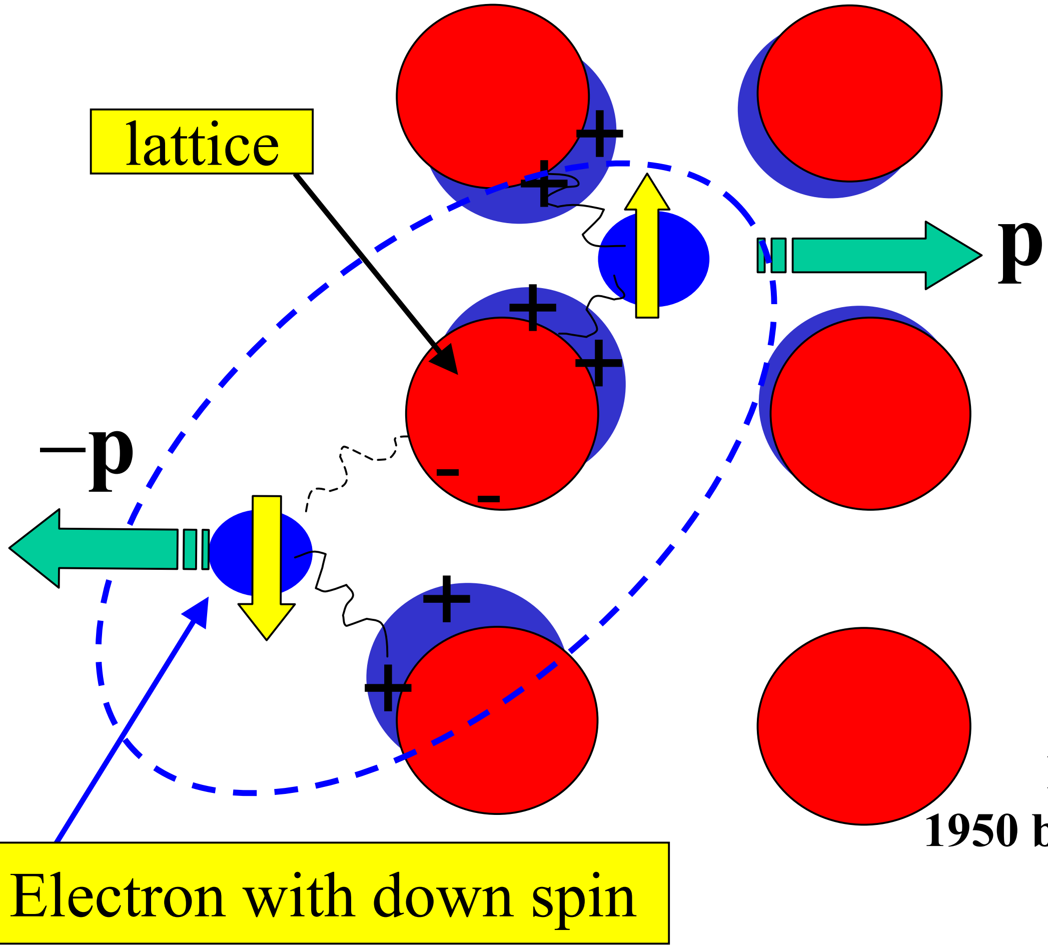

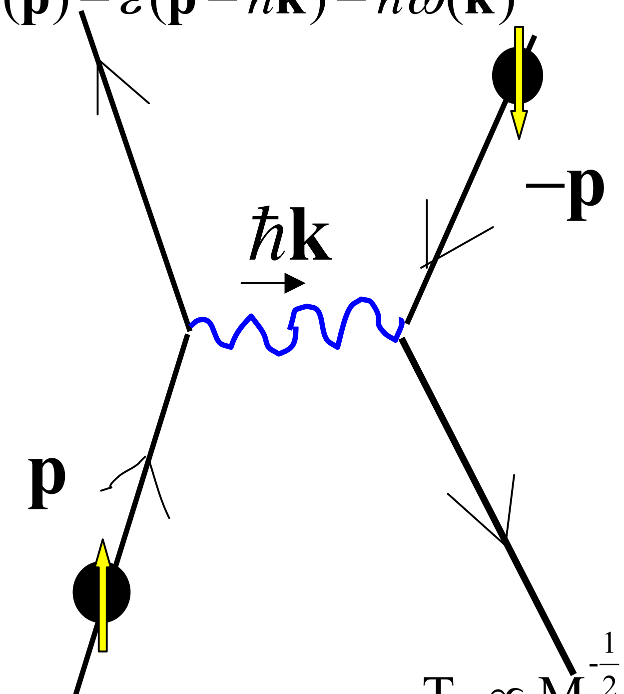

Isotope effect of Tc
1950 by Reynolds and Maxwell

$T_C \propto M^{-\frac{1}{2}}$,

$H_C \propto M^{-\frac{1}{2}}$

BCS theory
1957 by Bardeen, Cooper, and Schrieffer

Two Types of Superconductor

1937 by Schubnikov (experiment), 1957 Abrikosov (theory)

Type-I

$$\frac{\lambda}{\xi} \leq \frac{1}{\sqrt{2}}$$

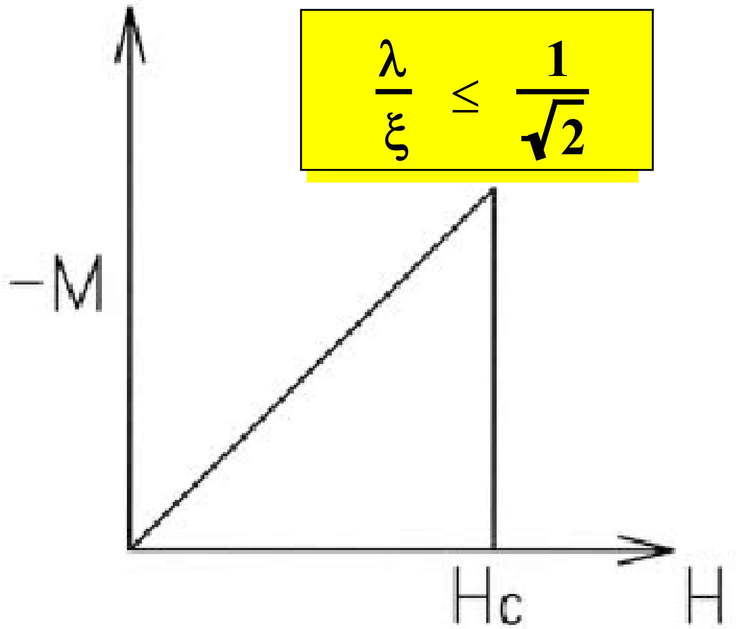

Type-II

$$\frac{\lambda}{\xi} > \frac{1}{\sqrt{2}}$$

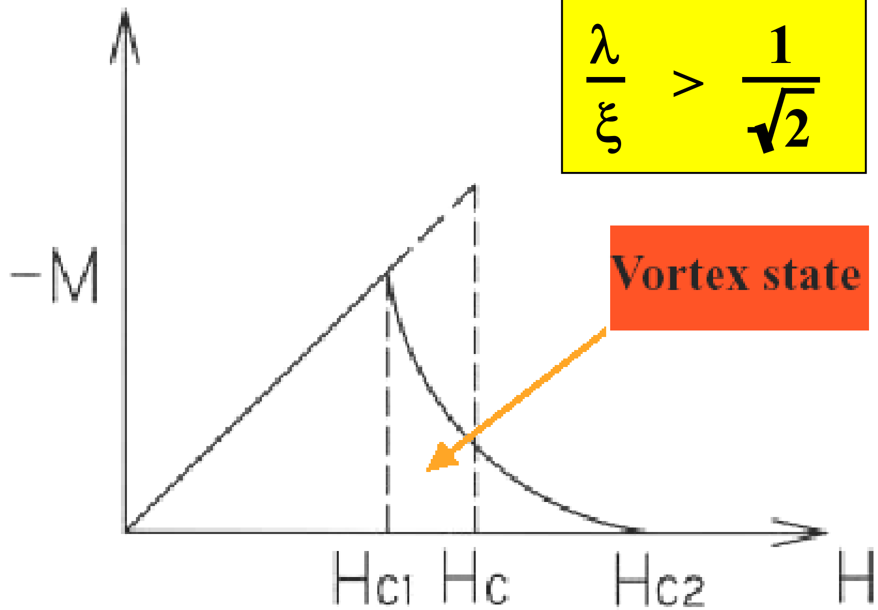

$$G_n - G_s = \frac{1}{2}\mu \mathrm{H}_\mathrm{C}^2 \equiv \int_0^{\mathrm{H}_{c2}} \mathrm{MdH}$$

Vortex state

Flux quantization, 1961 by Deaver and Fairbank

Observed by iron powder

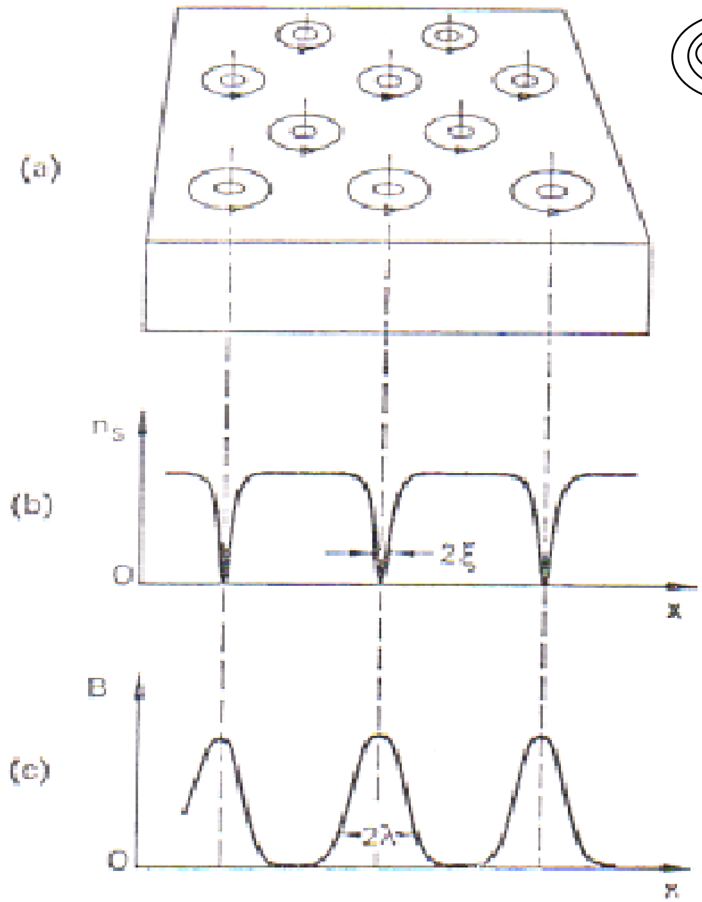

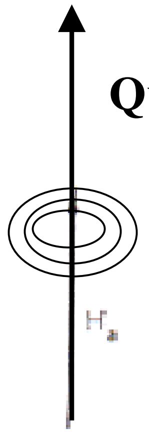

Quantized magnetic flux

supercurrent

Vortex state

Figure 19 Triangular lattice of fluxoids through top surface of a superconducting cylinder. The points of exit of the flux lines are decorated with fine ferromagnetic particles. The electron microscope image is at a magnification of 8300, by U. Essmann and H. Träuble.

ξ : Coherence length

a distance within which the superconducting electron concentration cannot change drastically in a spatially-varying magnetic field

λ_L : London penetration depth

Depth of penetration of the magnetic field

Critical magnetic field measurement

$$V = V_A + V_B = -\frac{d}{dt}\Phi_A + \frac{d}{dt}\Phi_B$$

$$(\,-nS_0\mu\frac{d}{dt}B_{ext} + \frac{d}{dt}M\,) + nS_0\mu\frac{d}{dt}B_{ext}$$

$$= \frac{d}{dt}M$$

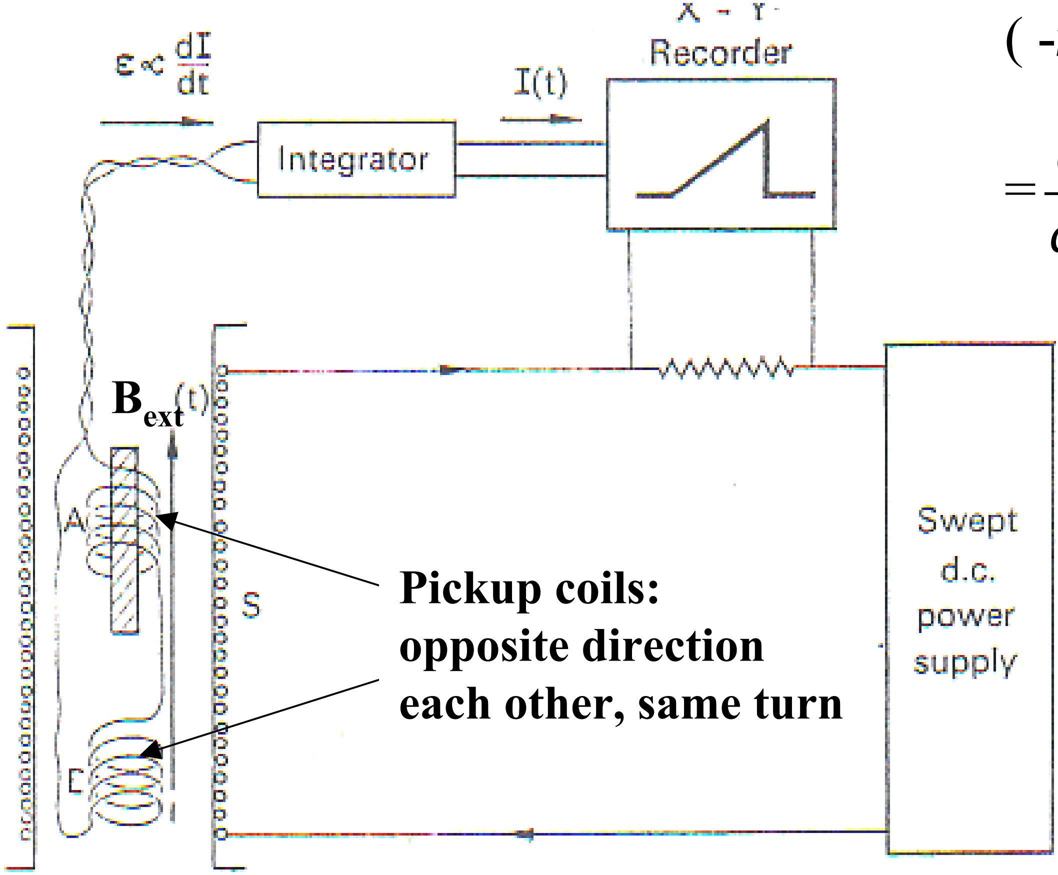

$$M = \int_0^t V dt$$

Example of demagnetization curve on Niobium
(NingXia, Large Grain RRR=340)

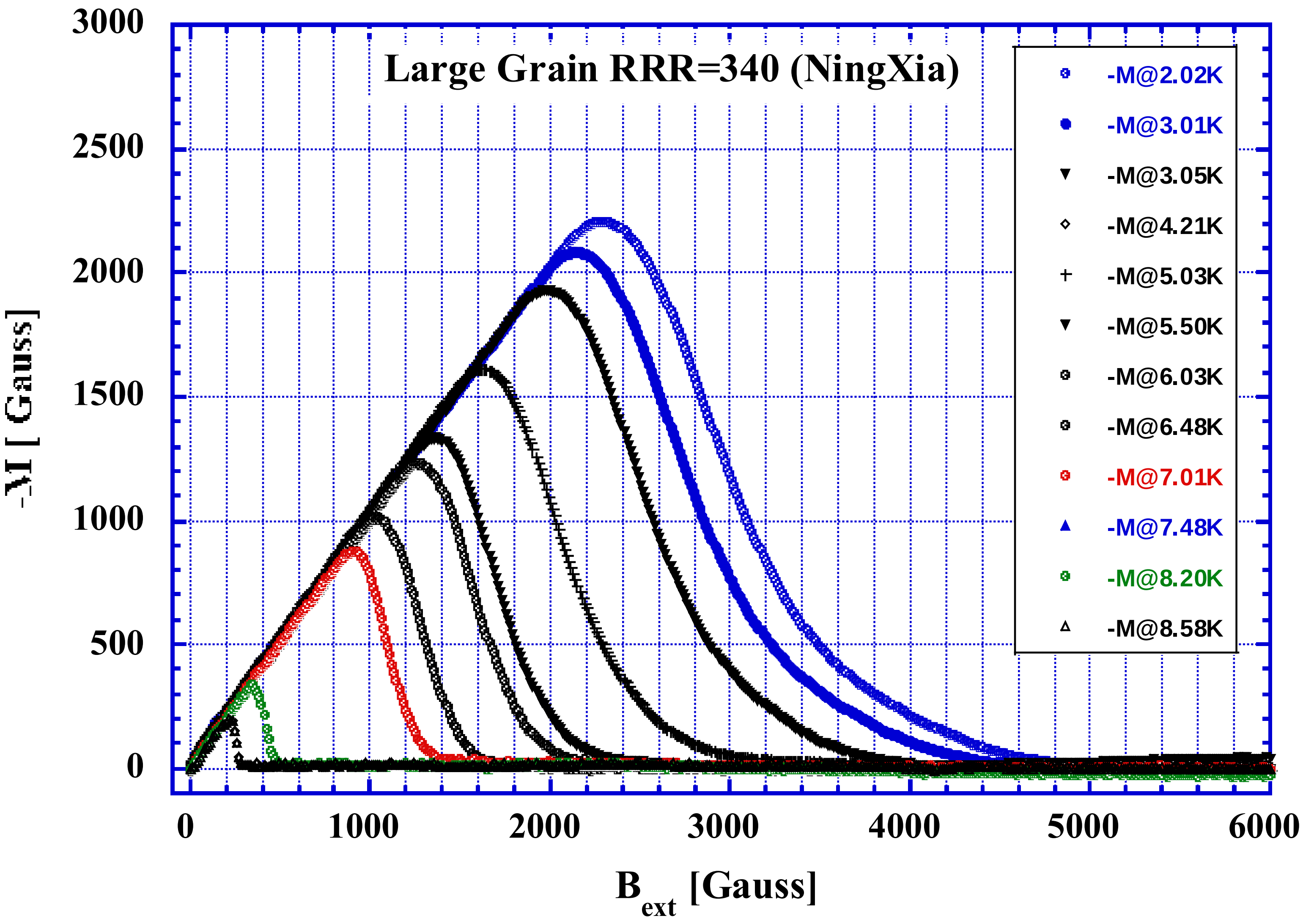

Abrikosov's Theory for Type-II

$$H_c = \frac{\kappa}{\lambda^2}\frac{\hbar c}{\sqrt{2}e^*} = \frac{\kappa}{\lambda^2}\frac{(hc/2e)}{2\pi\sqrt{2}} = \frac{\phi_0}{2\pi\sqrt{2}\lambda\xi}$$

$$H_{c2} = \sqrt{2}\frac{\lambda}{\xi}\frac{\phi_0}{2\pi\sqrt{2}\lambda\xi} = \frac{\phi_0}{2\pi\xi^2}$$

$$H_{c1} = \frac{\phi_o}{4\pi\lambda^2}\ln(\frac{\lambda}{\xi} + 0.08)$$

$$\phi_0 = hc/2e = 2.0678 \times 10^{-7} Gauss \cdot cm^2$$
$$= 2.0678 \times 10^{-15}\ T \cdot m^2$$

Perturbation theory T ~Tc

$$H_C(T) = H_C(0)\left[1-(T/T_C)^2\right]$$

$$\lambda(T) = \frac{\lambda(0)}{\sqrt{1-(T/T_C)^4}}$$

Exercise I.
Show the formulas for ξ, λ by Hc,Hc2.
Get the T-dependences for ξ, H_{C2}, κ, H_C^{RF}.

Expand for all T range (assumption)

$$\xi(T) = \xi(0)\cdot\sqrt{\frac{1+(T/T_C)^2}{1-(T/T_C)^2}} \qquad \kappa(T) = \frac{\kappa(0)}{1+(T/T_C)^2}$$

T-dependence of H_{C1}, H_C, H_{C2}

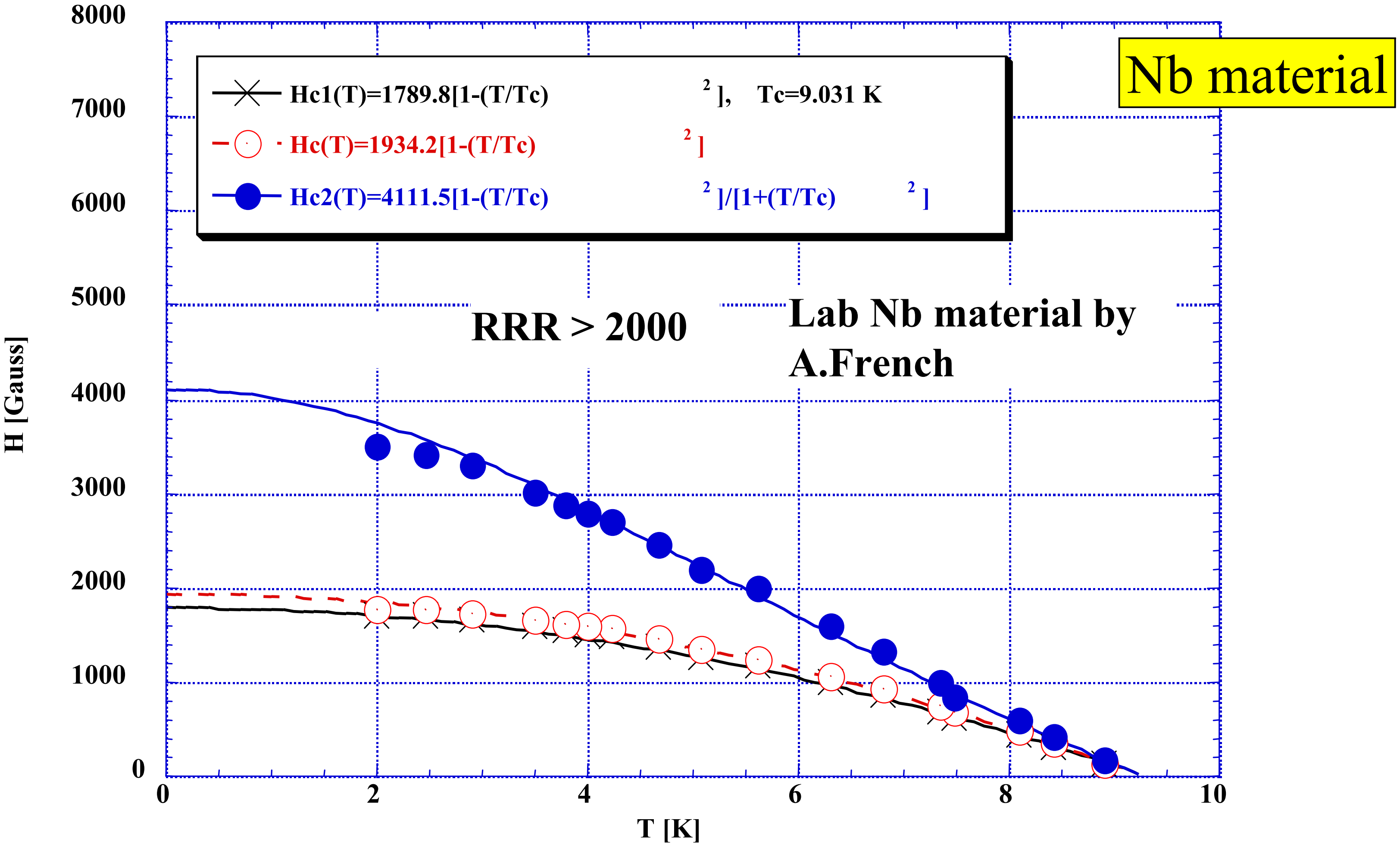

$$H_c(T) = H_c(0) \cdot \left[\, 1 - \left(\frac{T}{T_c}\right)^2 \right]$$

T–dependence of λ and ξ

Lab material, RRR>2000

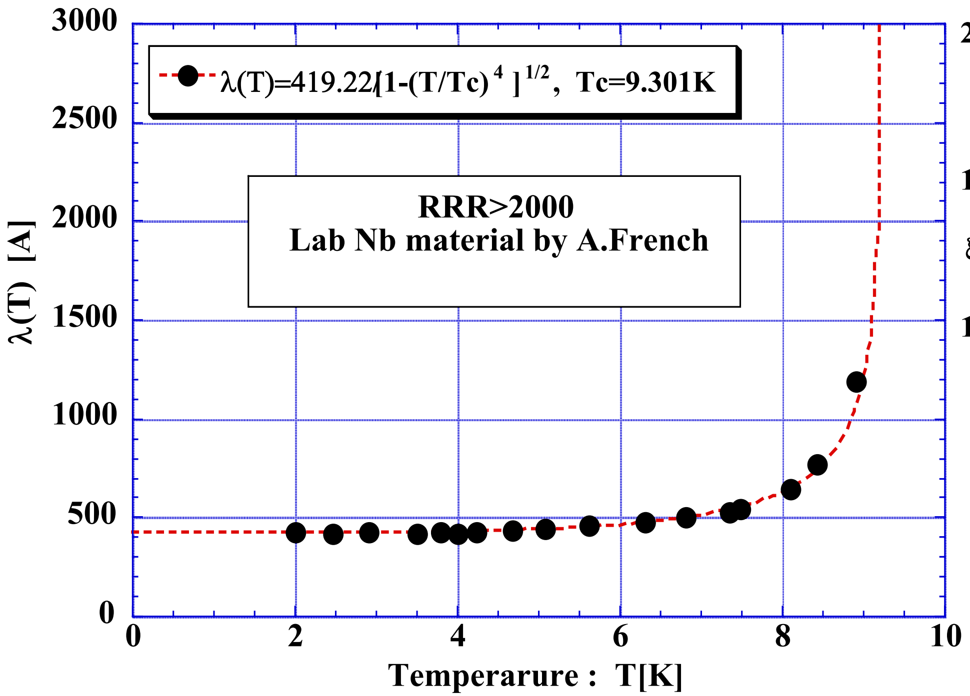

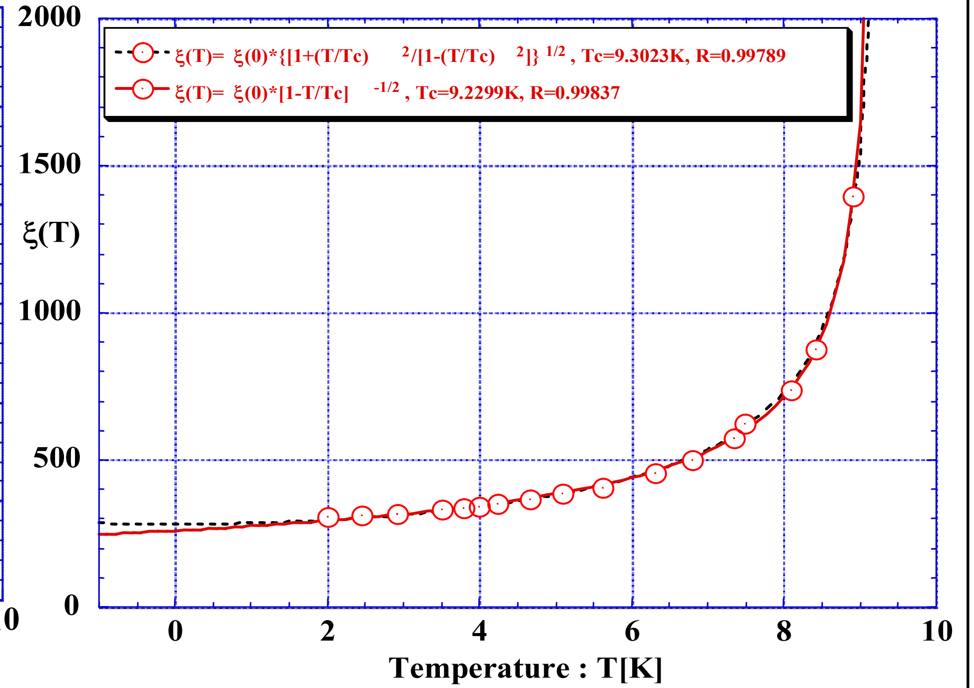

$$\lambda(T) = \frac{\lambda(0)}{\sqrt{1-(T/T_C)^4}}, \qquad \xi(T) = \xi(0)\cdot\sqrt{\frac{1+(T/T_C)^2}{1-(T/T_C)^2}}$$

T-dependence of κ with Lab material

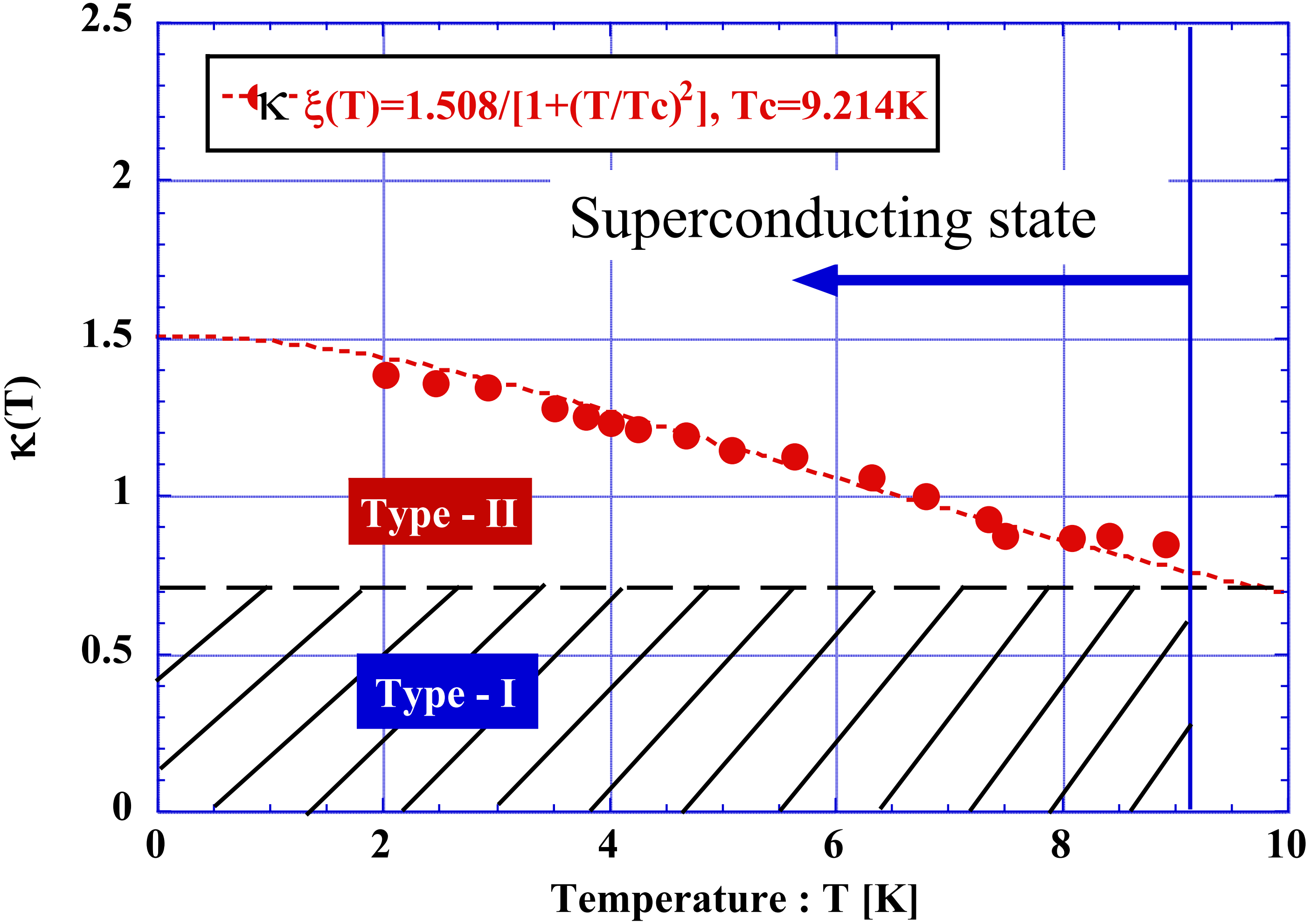

$$\kappa(T) = \frac{\kappa(0)}{1 + (T/T_C)^2}$$

Attempt for RF Field limitation model

$$\frac{1}{2}\mu H^2\lambda^2 - \frac{1}{2}\mu H_c^2\xi^2 = 0$$

$$H_c^{Line} = \frac{\xi}{\lambda} H_c = \frac{H_c}{\kappa}$$

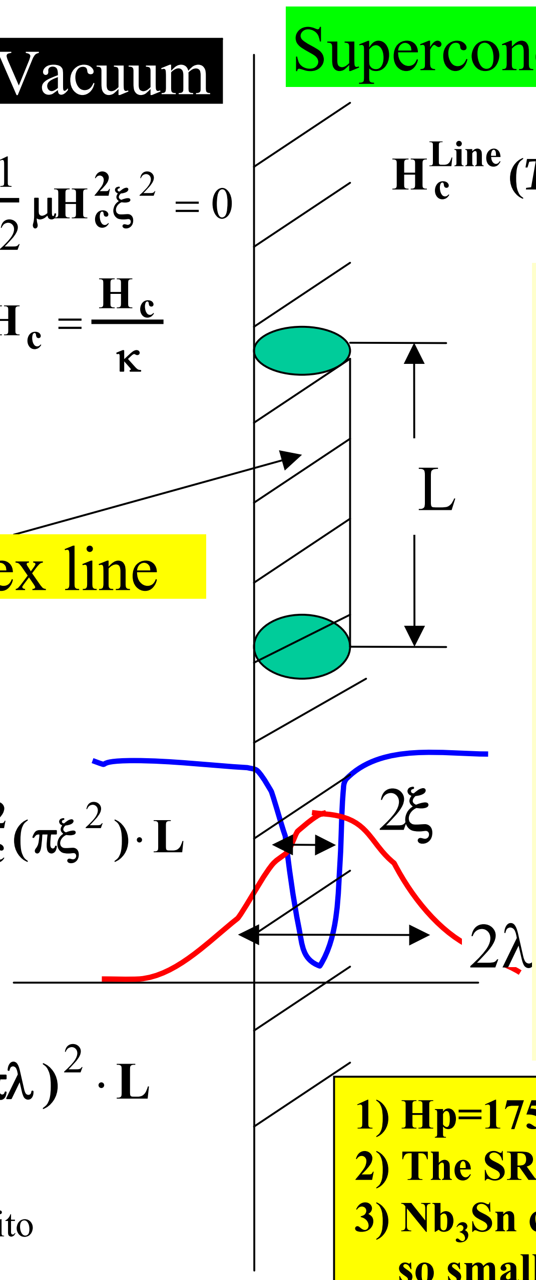

$$-\frac{1}{2}\mu H_c^2(\pi\xi^2)\cdot L$$

$$\frac{1}{2}\mu H^2(\pi\lambda)^2\cdot L$$

K.Saito

Effective field strength

$$H_c^{Line}(T) = \frac{\xi(T)}{\lambda(T)}\cdot\sqrt{2}H_c(T) = \frac{\sqrt{2}H_c(T)}{\kappa(T)} = \sqrt{2}\frac{H_c(0)}{\kappa(0)}\cdot\left[1-\left(\frac{T}{T_c}\right)^4\right]$$

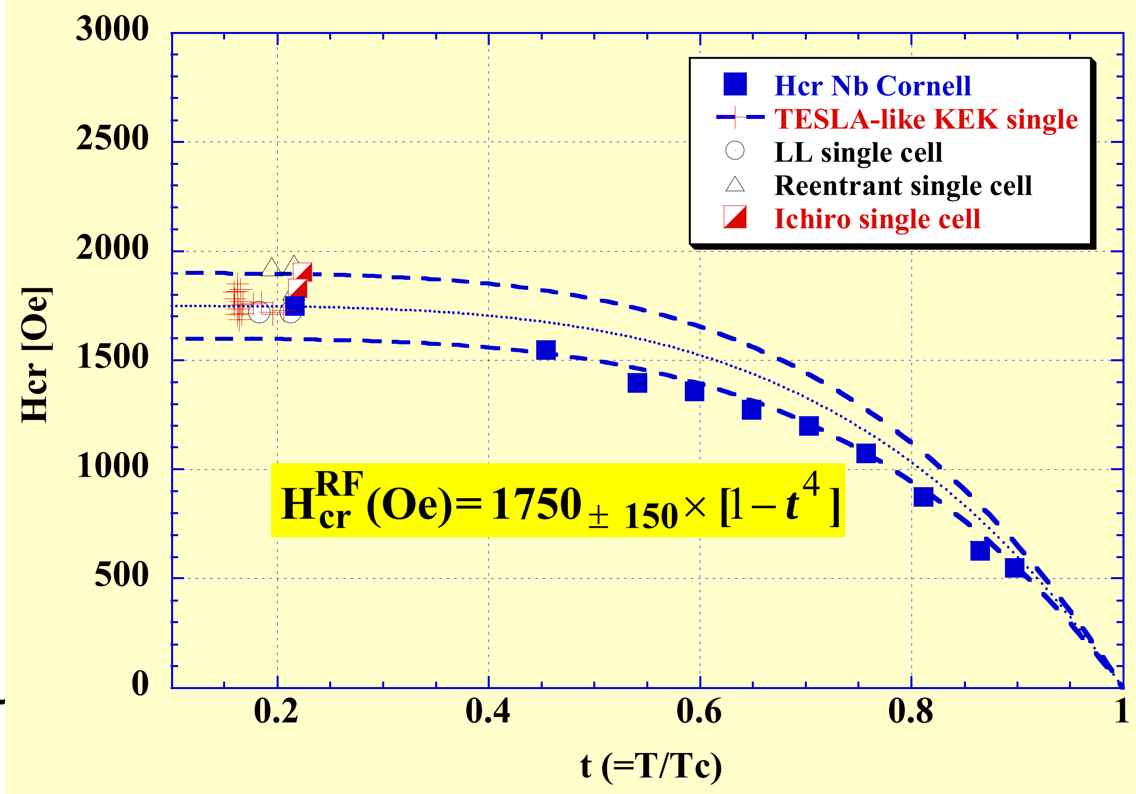

1) Hp=1750±100 Oe with Nb cavity ⟶ Eacc ~ 40MV/m
2) The SRF technology is meeting the theoretical limit.
3) Nb_3Sn cavity has a very larger k(0), therefore the critical field is so small.

Checking of the model for other materials

The model looks good for the type-II material cavity !

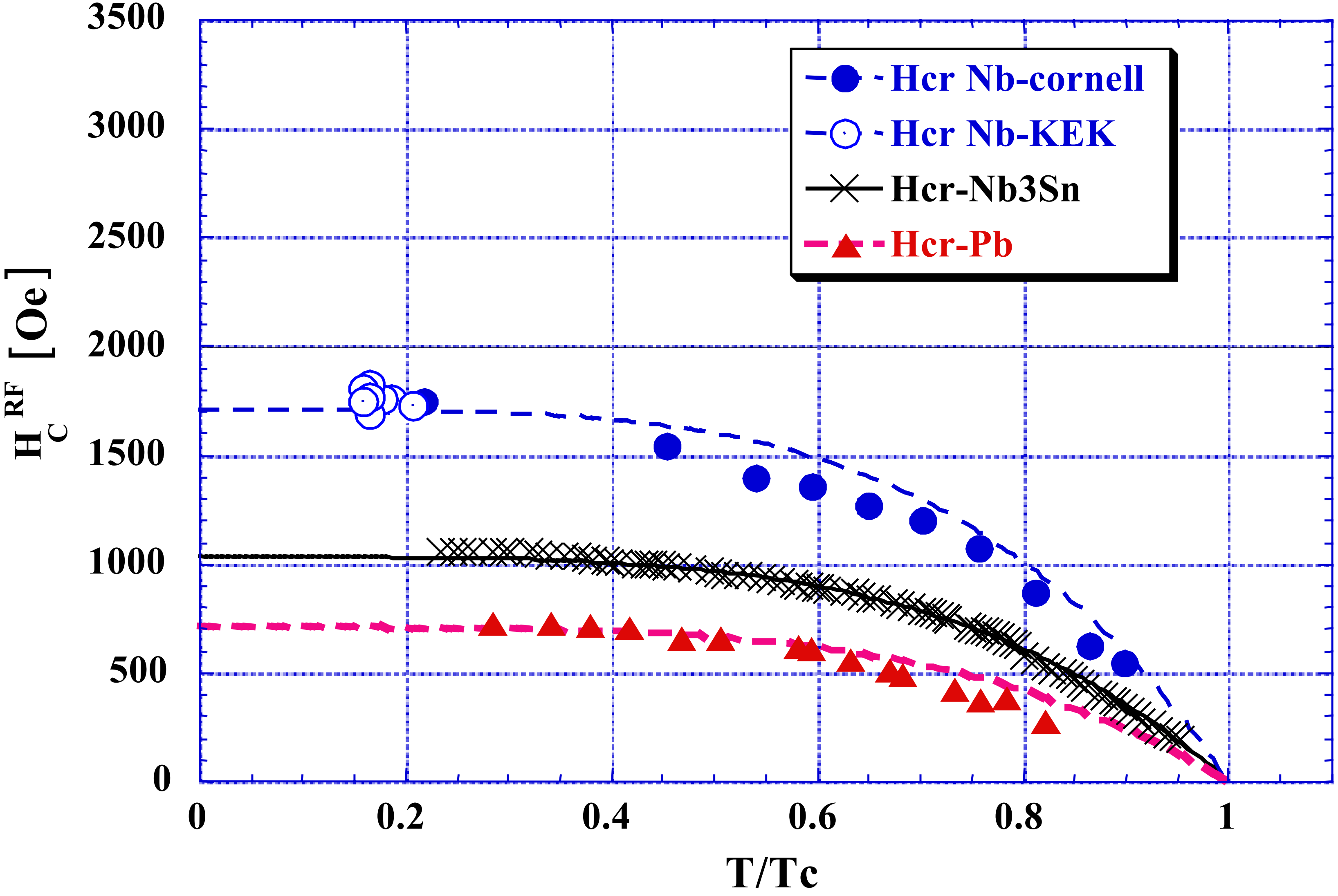

What material is best for SRF cavity?

Material point of view:

- Smaller heat loading for refrigerator → Higher T_C
- High gradient

  $H_{RF} > H_C^{RF}$, then normal conducting

$$H_c^{RF} = \sqrt{2} \cdot \frac{H_c}{\kappa}, \ \kappa : \text{G - L parameter}$$

  The material with higher Hc and smaller κ-value

This is very much different from superconducting magnet

If Hc is high enough, Type-I material is better because of the smaller κ-value.

- Good formability

Materials	Tc [K]	Hc, Hc1 [Gauss]	Type	Fabrication
Pb	7.2	803	I	Electroplating
Nb	9.25	1900, 1700	II	Deep drawing, film
Nb_3Sn	18.2	5350, 300	II	Film
MgB_2	39	4290, 300	II	Film

Niobium has higher Tc, Hc and enough formability.

Now, niobium is widely used for RF sc cavity production.

1.2 SRF Specifics and Constrains

What happens when microwave is input a cavity?

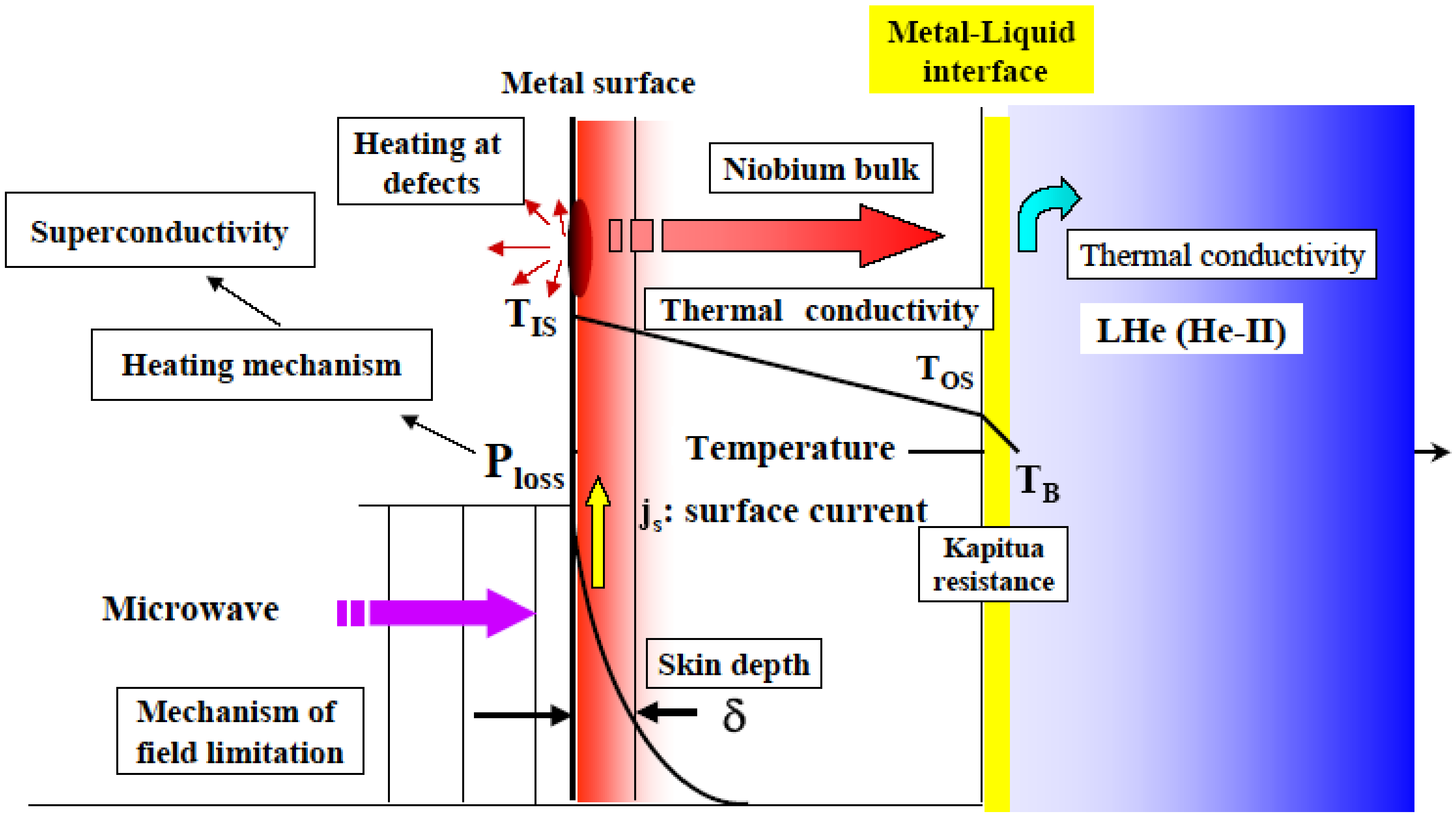

Surface resistance **is very very small.**

➡ Cavity performance strongly depends on the surface.

Thermal conductivity @ superconducting state is very small.

➡ *High thermal conductivity* is very important.

Surface resistance of normal conducting Case

Maxwell Equations for conductor (ε, μ, ρ = 0)

$$\nabla \cdot \vec{B} = 0,\ \nabla \times \vec{E} + \mu \frac{\partial \vec{H}}{\partial t} = 0$$

$$\nabla \cdot \vec{D} = 0,\ \nabla \times \vec{H} - \varepsilon \frac{\partial \vec{E}}{\partial t} - \sigma \vec{E} = 0$$

$$\vec{J} = \sigma \vec{E} \quad \text{(Ohm's Law)}$$

$$\vec{E}(\vec{x},t) = \vec{E}_\ell(\vec{x},t) + \vec{E}_t(\vec{x},t),$$

$$\vec{H}(\vec{x},t) = \vec{H}_\ell(\vec{x},t) + \vec{H}_t(\vec{x},t)$$

From Maxwell Equation,

$$\frac{\partial \vec{H}_\ell}{\partial t} = 0,\quad \vec{E}_\ell(x,t) = \vec{E}_\ell(0) \cdot e^{-\frac{\sigma t}{\varepsilon}}$$

For the transvers,

Plane wave : $\vec{E}_t(\vec{x},t) = \vec{E}_t(0) \cdot \exp(i\vec{k} \cdot \vec{x} - \omega t)$

$$\vec{H}_t(x,t) = \frac{1}{\mu\omega}[\vec{k} \times \vec{E}_t(\vec{x},t)],$$

$$[\ k^2 - (\varepsilon\mu\omega^2 + i\mu\omega\sigma)\ ]\begin{Bmatrix} \vec{E}_t(\vec{x},t) \\ \vec{H}_t(\vec{x},t) \end{Bmatrix} = 0$$

Normal Conducting Case, continued

$$k^2 - (\varepsilon\mu\omega^2 + i\mu\omega\sigma) = 0,$$

$$k = \alpha + i\beta,$$

$$\begin{Bmatrix} \alpha \\ \beta \end{Bmatrix} = \sqrt{\varepsilon\mu} \cdot \omega \left[\frac{\sqrt{1+\left(\frac{\sigma}{\omega\varepsilon}\right)^2} \pm 1}{2} \right]^{\frac{1}{2}}$$

For good electric conductor

$$\frac{\sigma}{\omega\varepsilon} >> 1$$

$$k \approx (1+i)\sqrt{\frac{\mu\sigma\omega}{2}}$$

$$\delta = \frac{1}{\beta} = \sqrt{\frac{2}{\mu\sigma\omega}}$$: Skin depth

Surface Impedance for normal conducting case

$$Z \equiv R_s + iX_s \equiv \left.\frac{E_t}{H_t}\right|_{Surface} = \frac{\mu\omega}{k}$$

Exercise II.
Get the formula of Rs
for good electric conductor

$$\mathbf{R_s} = \sqrt{\frac{\mu\omega}{2\sigma}} = \frac{1}{\sigma}\sqrt{\frac{\mu\sigma\omega}{2}} = \frac{1}{\sigma\delta}$$

$$P_{loss} = \frac{1}{2} R_S \cdot \int_S H_S{}^2 dS$$

Surface resistance in superconductor (Two Fluid model)

General equation: $m\dfrac{\partial \mathbf{v}}{\partial t} = q(\mathbf{E} + \mathbf{v}\times\mathbf{B}) - m\nu\,\mathbf{v}$

Two-fluid model by Gorter and Casimir in 1933

$\mathbf{J} = \mathbf{J}_s + \mathbf{J}_\mathbf{n}$, $\mathbf{J}_s = n_s q_s \mathbf{v}$, $\mathbf{J}_\mathbf{n} = n_n q_n \mathbf{v}$

Maxwell equation: neglecting the Lorentz term, $\mathbf{v}\times\mathbf{B} \ll 1$

$$m_s\frac{\partial \mathbf{v}_s}{\partial t} = q_s\mathbf{E} \;,\; m_s = 2m_e \;,\; q_s = -2e$$

$$m_e\frac{\partial \mathbf{v}_n}{\partial t} = q_n\mathbf{E} - m_e\nu\,\mathbf{v}_n \;,\quad q_n = -e$$

$$\mathbf{E} = \mathbf{E}_0 e^{i\omega t} \Rightarrow \mathbf{J}_s = \frac{n_s q_s^2}{i\omega m_s}\mathbf{E} \;,\; \mathbf{J}_n = \frac{n_n q_n^2}{i(\omega - i\nu)m_e}\mathbf{E}$$

$$\mathbf{J} = \left(\frac{n_s q_s^2}{i\omega m_s} + \frac{n_n e^2}{i(\omega - i\nu)m_e}\right)\mathbf{E}$$

$$\nu \gg \omega \;\Rightarrow\; \mathbf{J} = \left(\frac{n_n e^2}{\nu m_e} - i\frac{n_s q_s^2}{\omega m_s}\right)\mathbf{E} = \sigma E, \quad \sigma = \sigma_\mathrm{n} - i\sigma_s \;\Rightarrow\; \mathrm{R}_\mathrm{s} = \sqrt{\frac{\mu\omega}{2\sigma}}$$

Surface resistance in superconductor

$$\sigma_n = \frac{n_n \cdot e^2 \cdot l}{m \cdot v_F} = \frac{e^2 \cdot l}{m \cdot v_F} \cdot n_s(T=0) \cdot e^{-\frac{\Delta}{k_B \cdot T}}$$

Exercise III.
Get this formula.

$$R_S = \frac{1}{2} \cdot (2\pi)^2 \cdot \mu^2 \cdot f^2 \cdot \lambda_L^3 \cdot l \cdot \frac{n_s(0)}{m v_F} \cdot e^{-\frac{\Delta}{k_B T}}$$

$$= A \cdot f^2 \cdot e^{-\frac{\Delta}{k_B T}}$$

At a finite temperature T

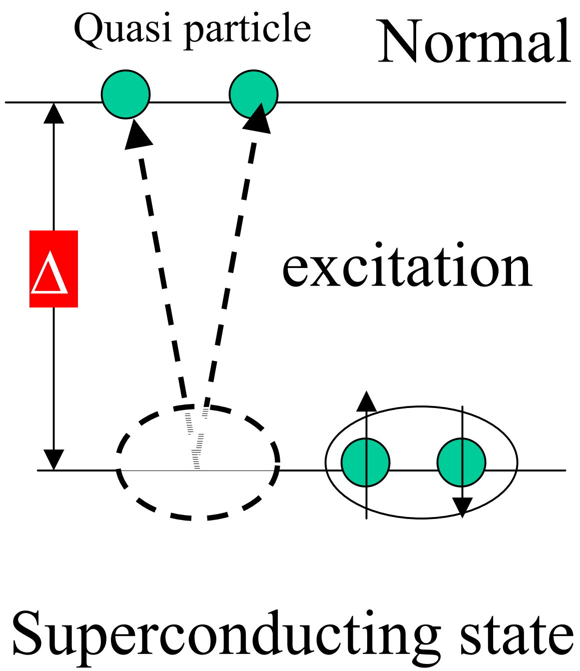

BCS Theory

$$R_S^{BCS}(T,\omega) = A(\lambda, \xi, \ell, T_c) \cdot \exp(-\frac{\Delta}{k_B T})$$

"Very Small" Surface Resistance in SRF Cavity

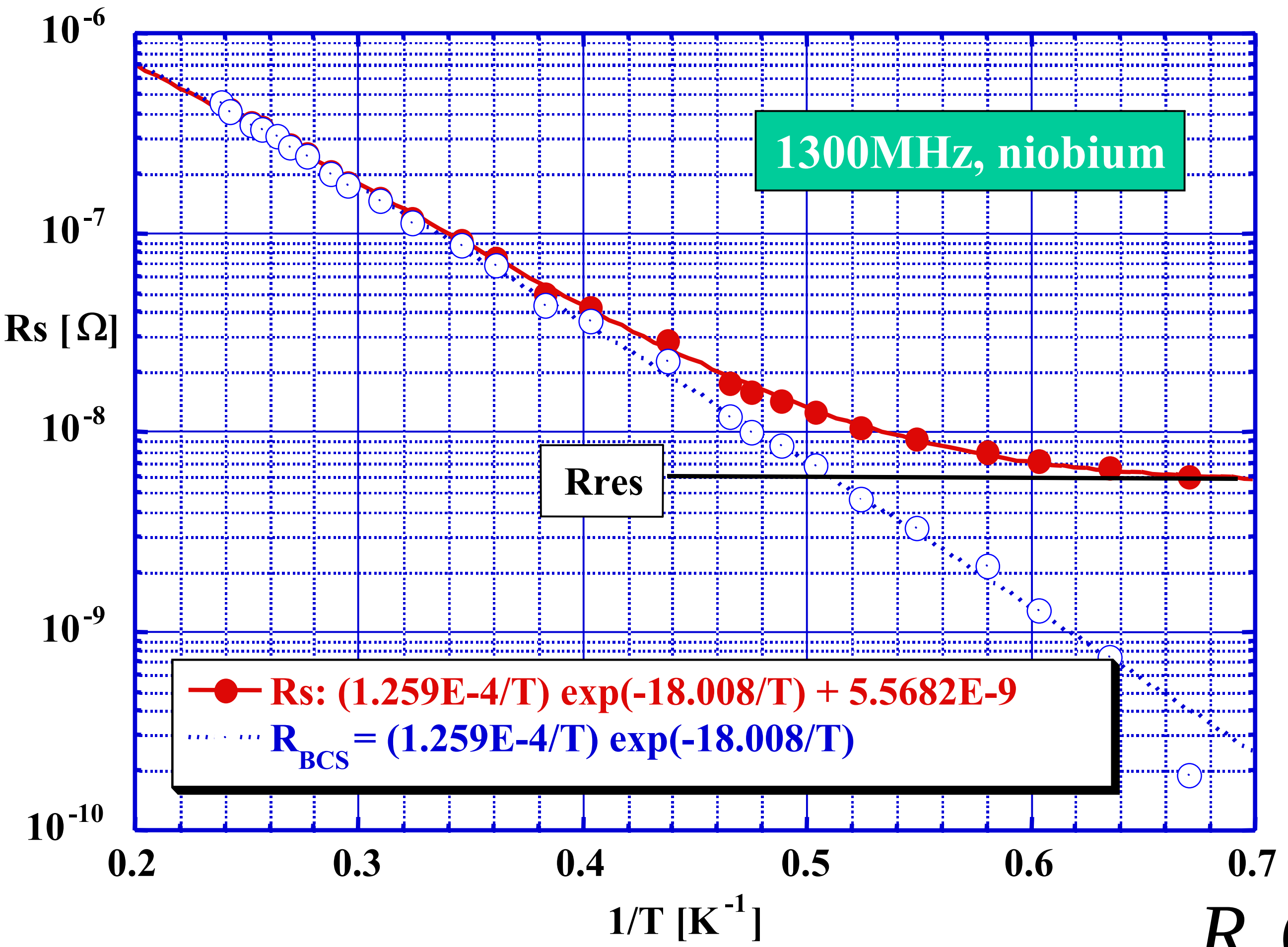

$$\frac{\Delta}{k_B} = 18.008 \Rightarrow \frac{2\Delta}{k_B T_c} = \frac{2 \cdot 18.008}{9.25} = 3.89$$

$$\frac{2\Delta}{k_B T_c} = 3.52 \ \textbf{(BCS theory)}$$

Residual surface resistance depends on residual magnetic field, surface contamination, and so on.

$$R_S(T) = R_S^{BCS}(T) + R_{res}$$

$R_{BCS} \sim 8\text{n}\Omega$,
which is smaller a factor of 10^{-6} than normal conducting!
The performance strongly depends on the surface!

BCS Surface Resistance Calculation for 1.3 GHz niobium cavity at 4.25 and 2K

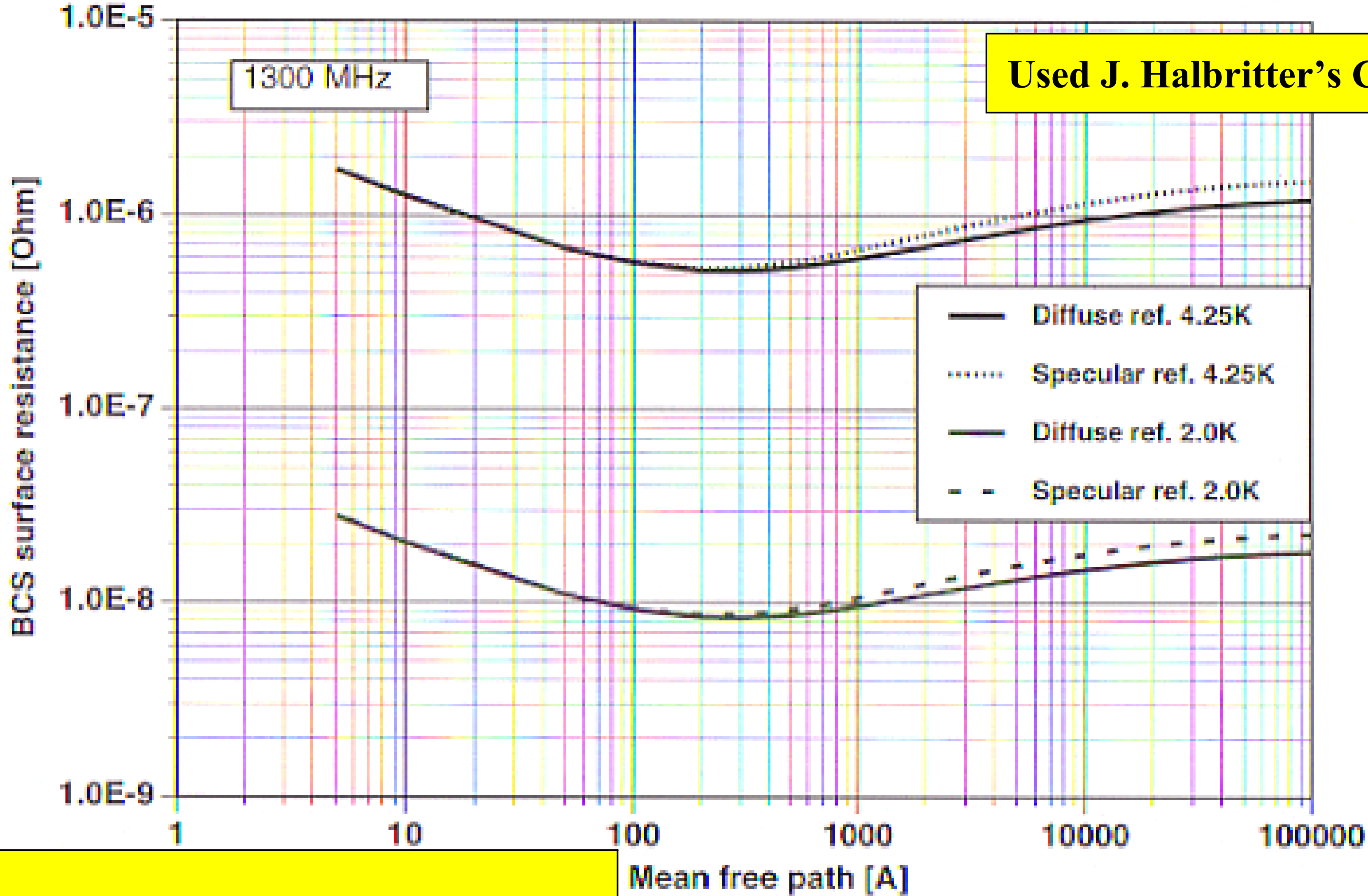

Used J. Halbritter's Code

$R_{BCS} \sim 8n\Omega$ @ 2K, 1300MHz

ℓ(mean free path) $\propto$ RRR

R_S minimum around mean free path $\ell \approx 300$ Å

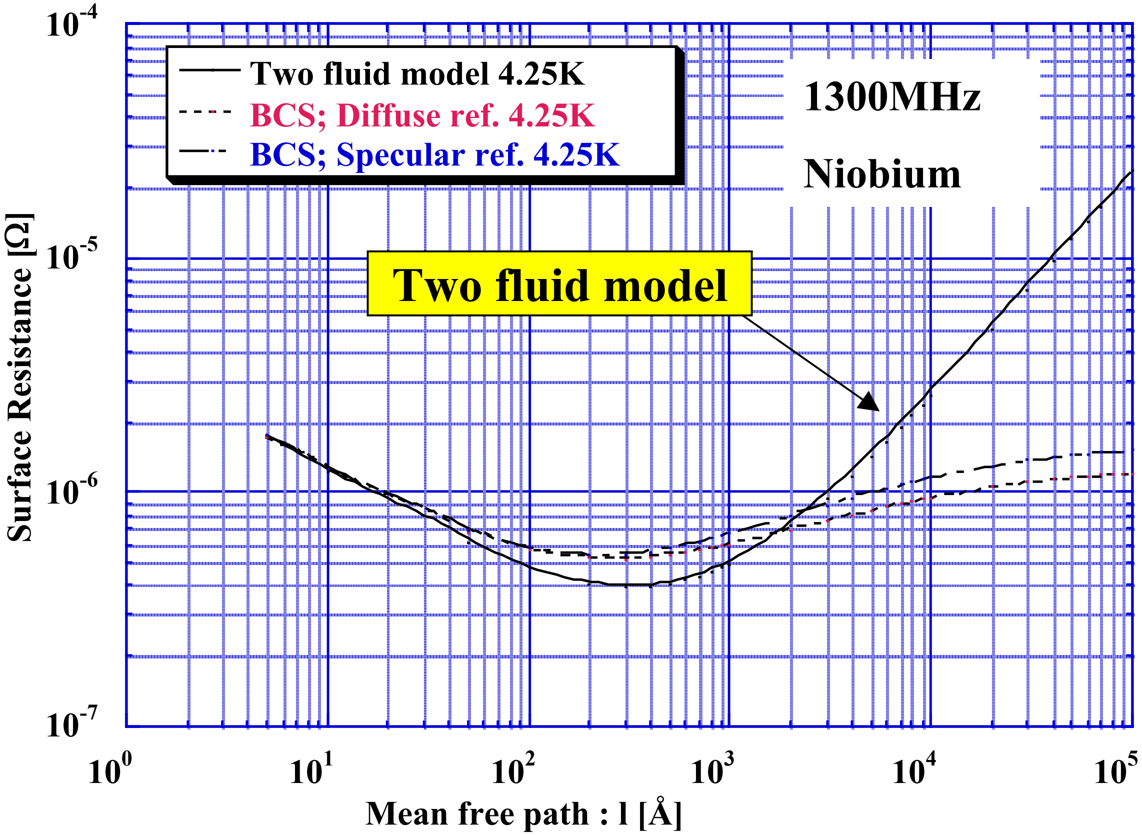

Strange behavior on mean free path(ℓ)

R_s minimum

@ ℓ~300 Å

London penetration depth λ : $\lambda(\ell) = \lambda_{\ell=\infty} \cdot \sqrt{1 + \frac{\xi_o}{\ell}}$,

$R_S(TF\ model) \propto (1 + \frac{\xi_o}{\ell})^{\frac{3}{2}} \cdot \ell$,

$\ell << 1,\ R_S \to \frac{\xi_o^{\frac{3}{2}}}{\sqrt{\ell}}$,

$\ell >> 1,\ R_s \to \ell$

Thermal conductivity

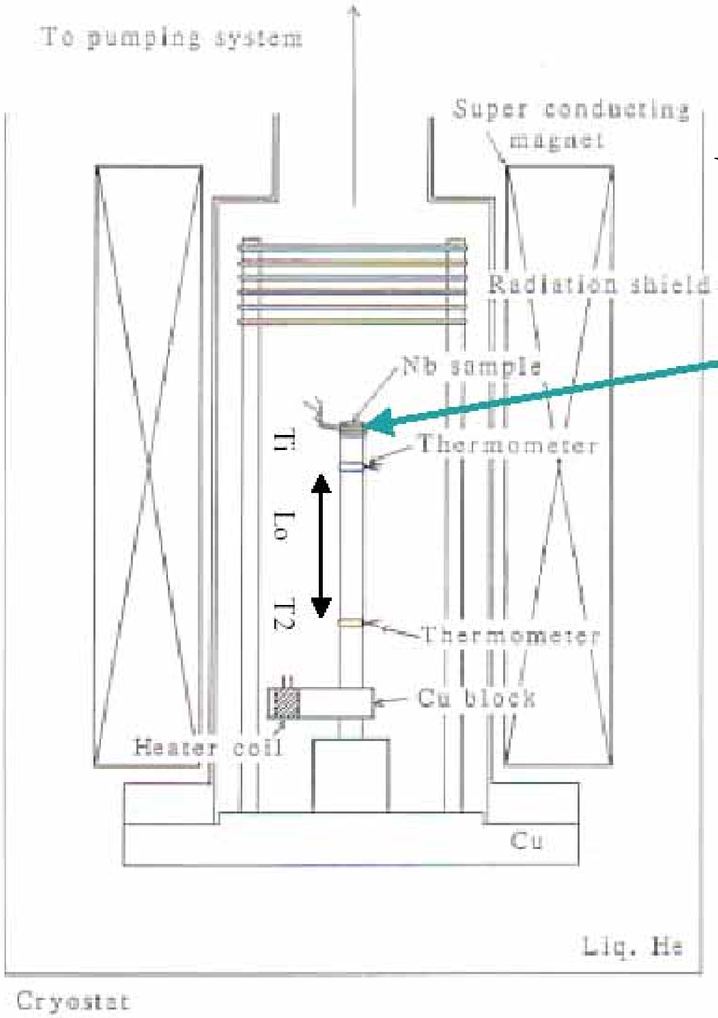

Normal conductor : $\kappa_{en} = \dfrac{1}{W_{en}} = \left[\dfrac{\rho}{L_O T} + a T^2 \right]^{-1}$

$\rho = \dfrac{\rho_{300K}}{RRR}$ e-impurities scatt.

e-lattices scatt.

Wiedemann-Franz low:

$$\kappa_e = \frac{\pi^2 n k_B^2 \tau}{3m} \cdot T, \quad \frac{\kappa_e}{\sigma} = \frac{\pi^2}{3}\left(\frac{k_B}{e}\right)^2 \cdot T = L_O T$$

$$P[w] = S(m^2) \cdot \kappa(T) \cdot \frac{T_1(K) - T_2(K)}{L_O(m)}$$

$$T \equiv \frac{T_1 + T_2}{2},\ S\text{: area of cross-section}$$

$$\kappa(T) = \frac{P}{S} \cdot \frac{L_O}{T_1 - T_2} \qquad \left[\frac{w}{m \cdot K}\right]$$

Thermal conductivity of Nb material at low temperature

Boltzmann statistics : Existing probability at energy Δ, and Temp. T

$$\exp\left(-\frac{\Delta}{k_B \cdot T}\right)$$

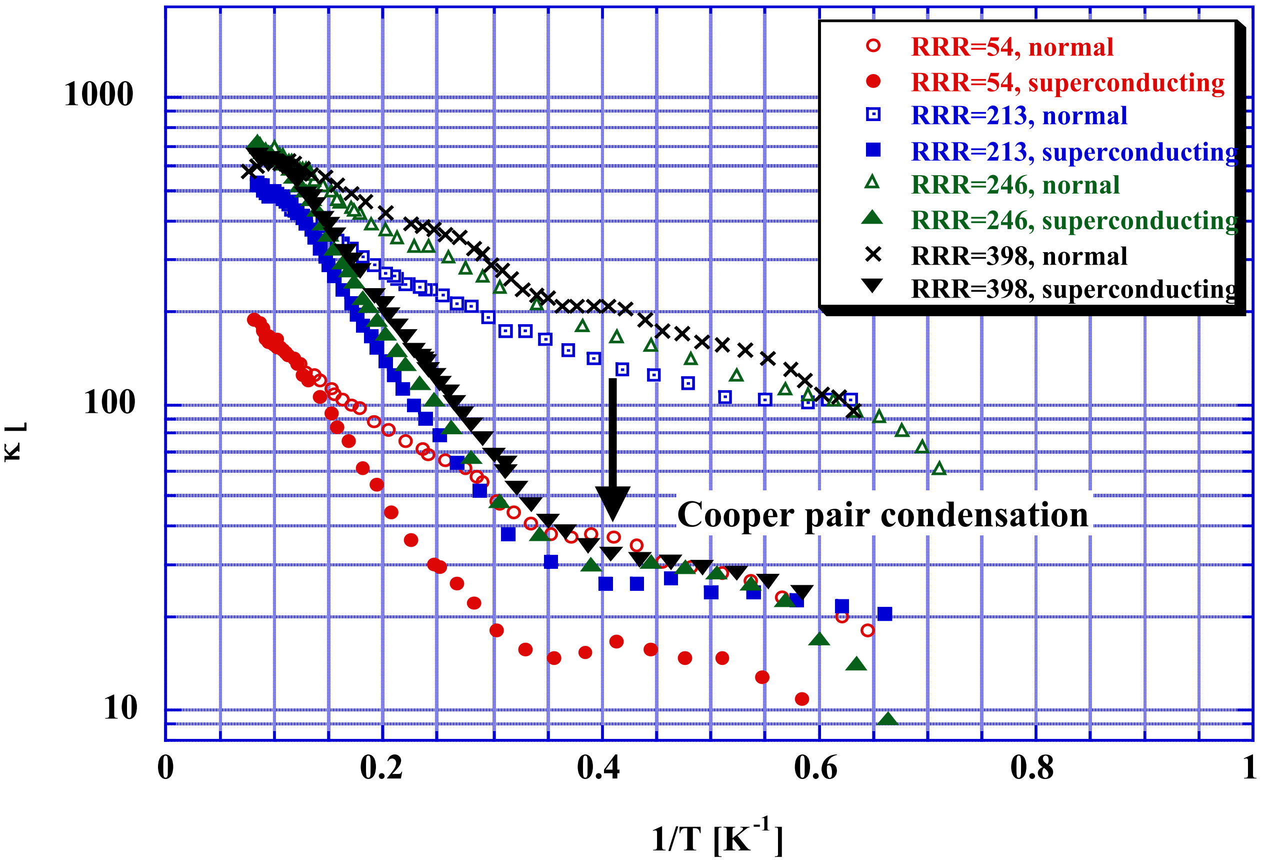

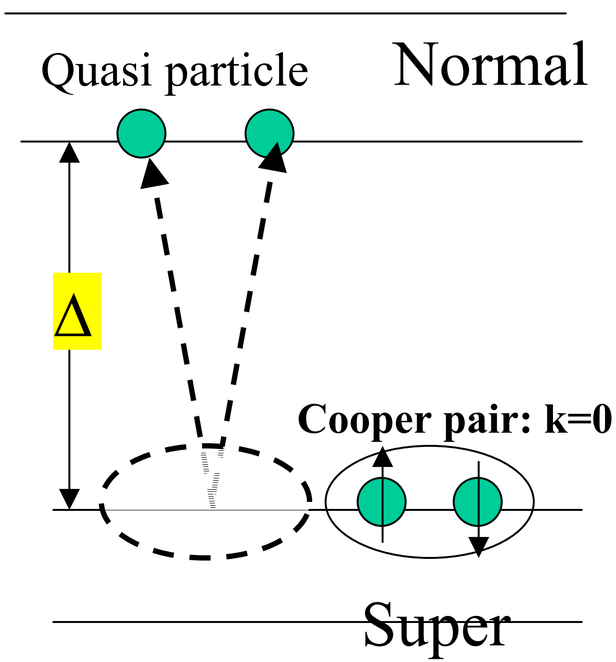

Thermal conductivity comparison with NC and SC

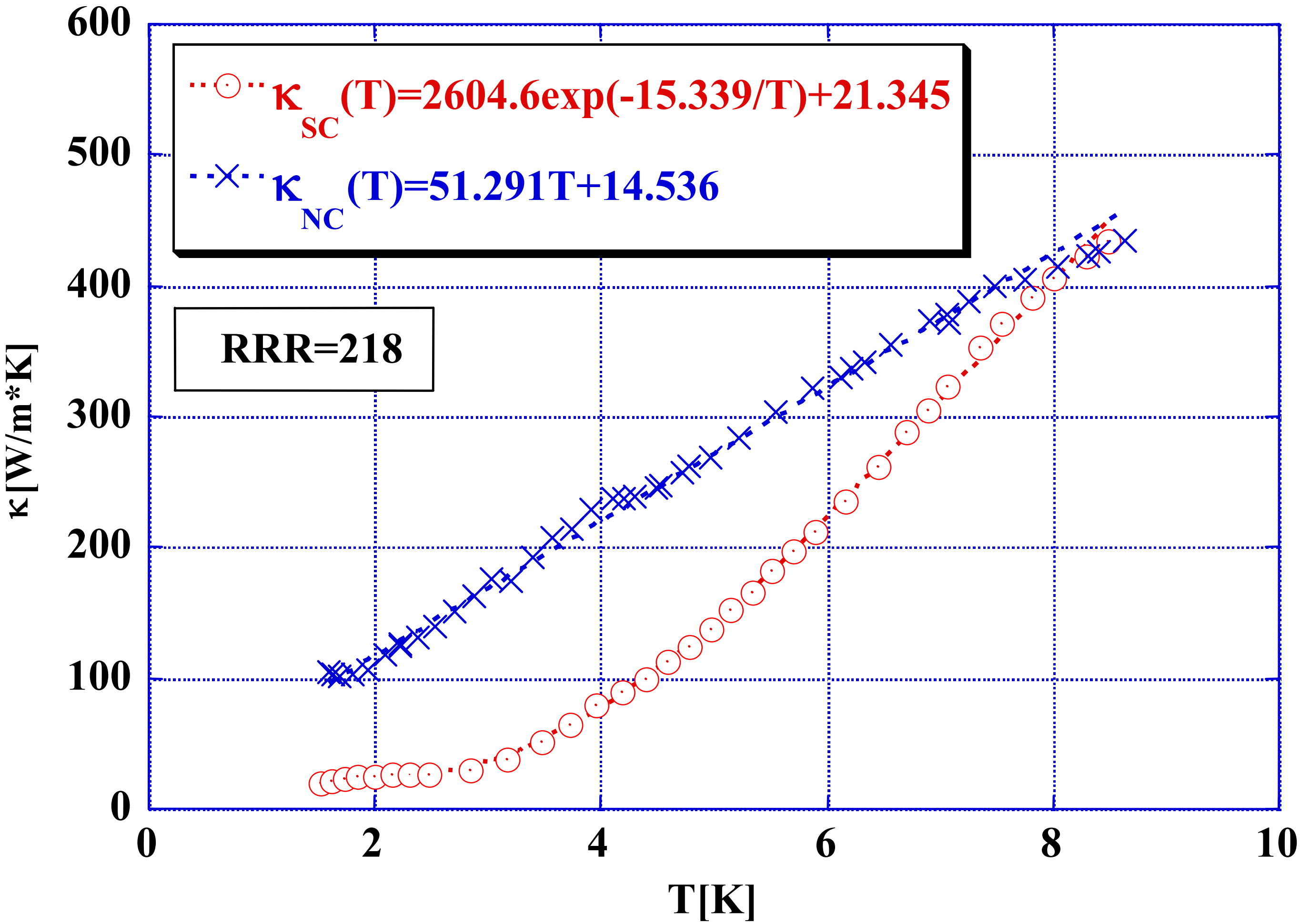

$$\frac{\Delta}{k_B} = 15.339$$

$$\Downarrow$$

$$\frac{2\Delta}{k_B T_c} = \frac{2 \times 15.339}{k_B\, 9.25}$$

$$2\Delta = 3.317 k_B T_c$$

BCS theory

$$2\Delta = 3.52 k_B T_c$$

Calculation of thermal conductivity based on Quantum mechanics

$$\kappa_s(T) = R(y)\cdot\left[\frac{\rho_{295K}}{L\cdot RRR\cdot T} + a\cdot T^2\right]^{-1} + \left[\frac{1}{D\cdot \exp(y)\cdot T^2} + \frac{1}{BlT^3}\right]^{-1}$$

e-impurities scatt. e-phonons scatt. lattice-phonnons scatt. lattice-grain boundaries scatt.

$L = 2.05E-8,\ RRR = 200,\ \rho_{295K} = 14.5E-8\ \Omega m,\ a = 7.52E-7$

$-y = \alpha\cdot\frac{T_c}{T},\ \alpha = 1.53,\ T_c = 9.25K,\ T \le 0.6\cdot T_c$

$D = 4.27E-3,\ B = 4.34E3,\ l = 50\mu m$

$$R(y) = \frac{\kappa_{es}}{\kappa_{en}} = \frac{2F_1(-y) + 2y\ln(1+e^{-y}) + \frac{y^2}{(1+e^y)}}{2F_1(0)},$$

$$F_n(-y) = \int_0^\infty \frac{z^n}{1+e^{z+y}}dz$$

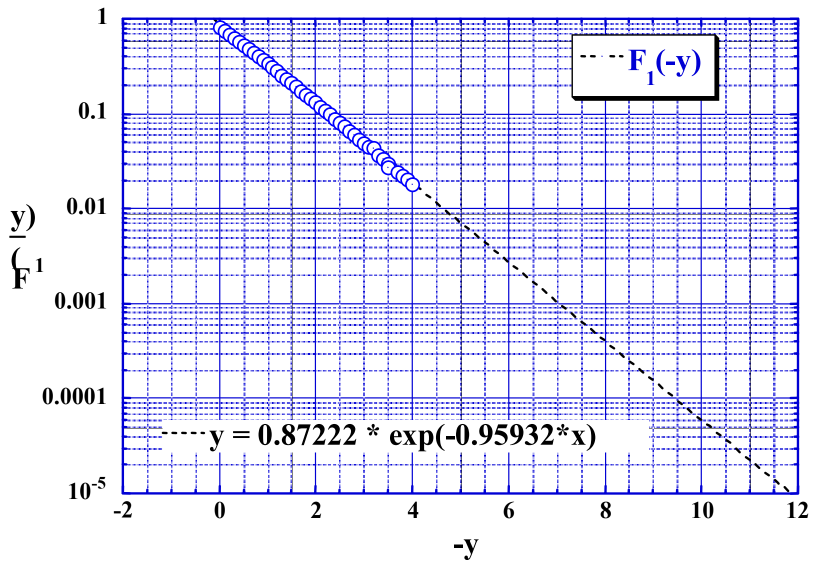

Calculated $\kappa_{sc}(T)$

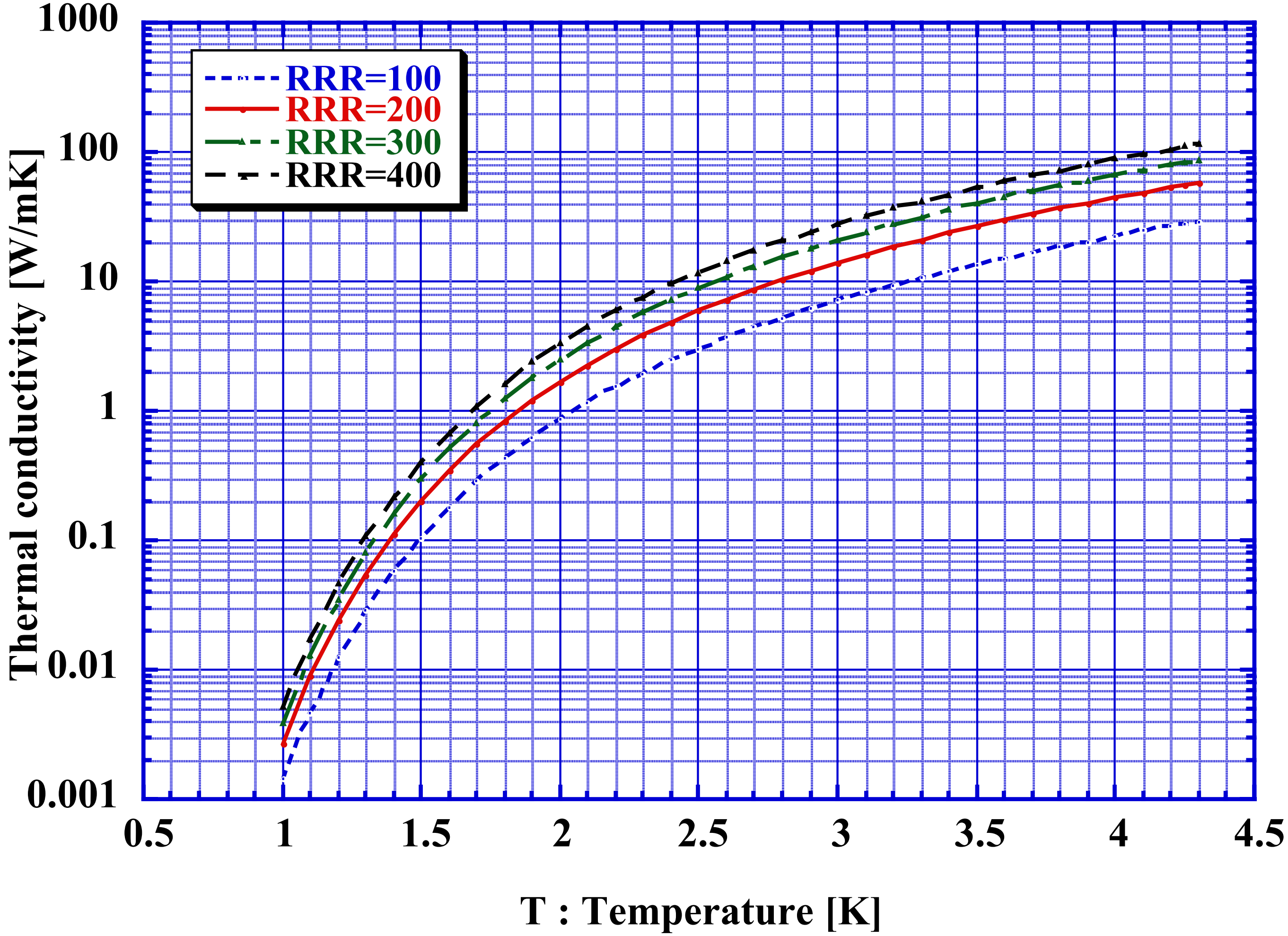

Thermal conductivity of niobium in superconductivity @ 2K is 1/15 that of stainless at R.T. (15W/(m•K)) and 1/6800 of pure cooper at 4.2K

Scattering mechanism limits both thermal conductivity and electric conductivity

Nb

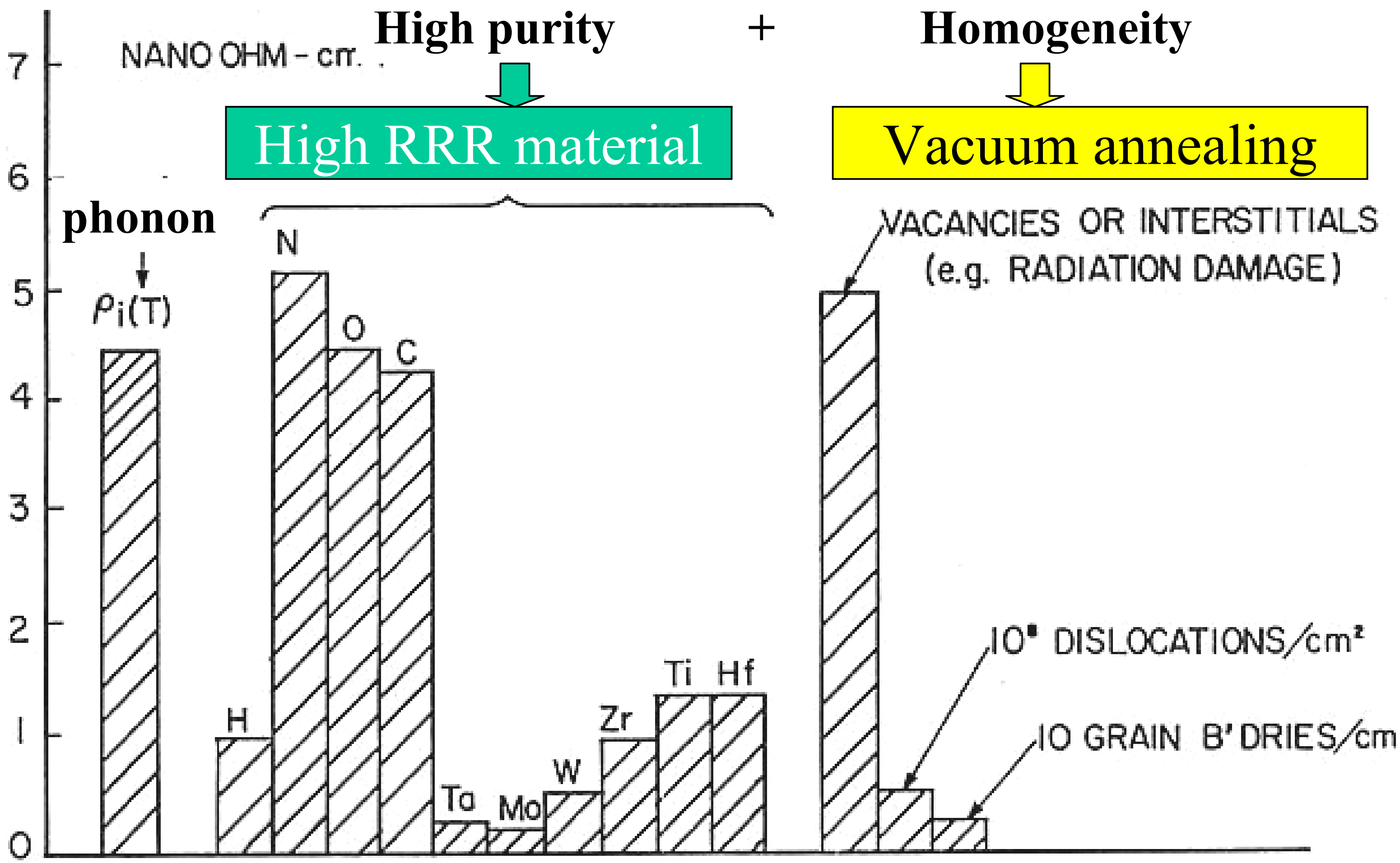

$$R = \text{e-phonon scat.} + \text{e-imprity scat.} + \text{e-inhomogenety scat.} + \cdots$$

$$\frac{1}{\kappa} = \text{e-phonon scat.} + \text{e-imprity scat.} + \text{e-inhomogenety scat.} + \cdots$$

RRR measurement

$$RRR \equiv \frac{R_{300K}}{R_{9.5K}}$$

Very simple measurement!!

RRR is linearly proportional to thermal conductivity.

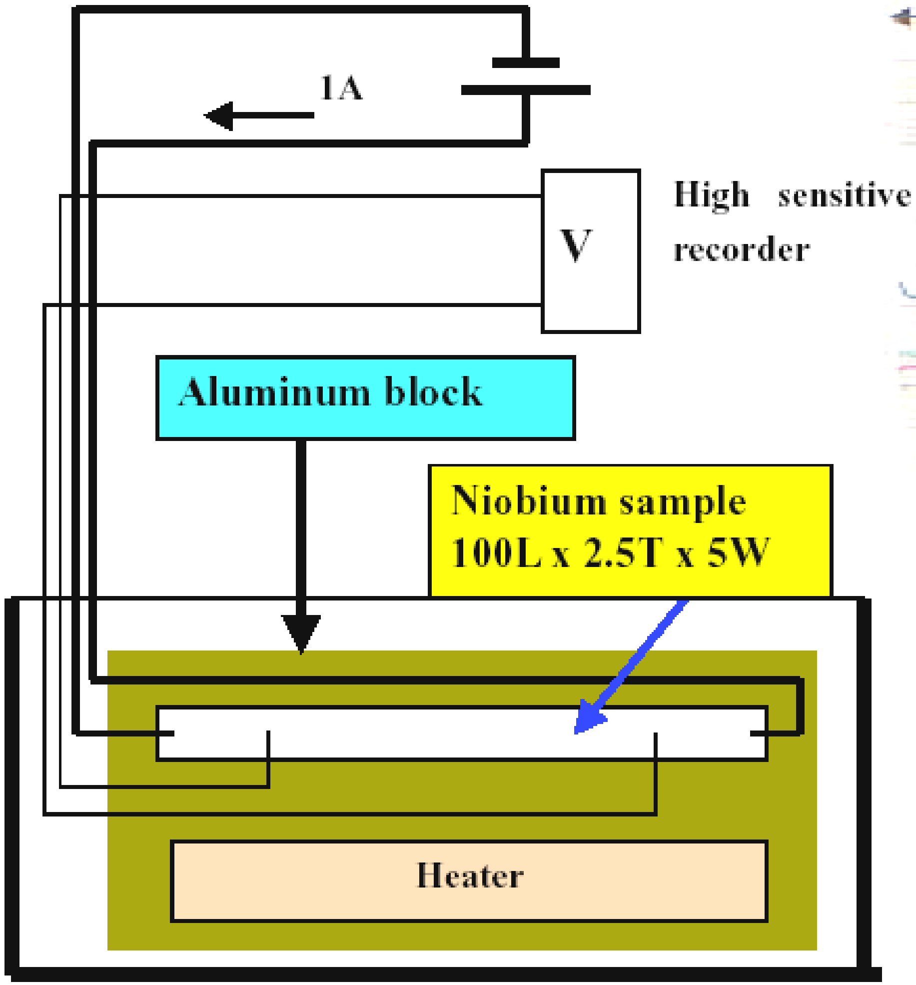

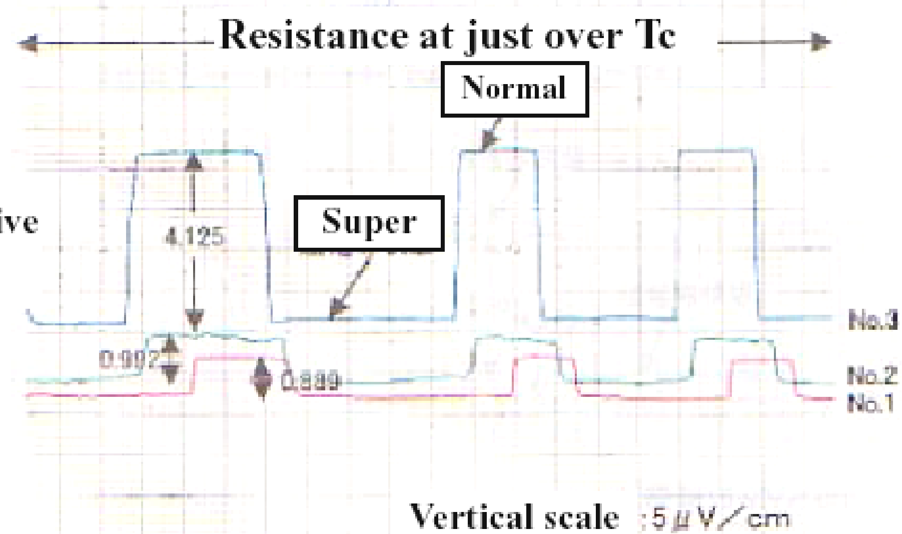

Linear relationship between κ_S(2, 4.25K) and RRR

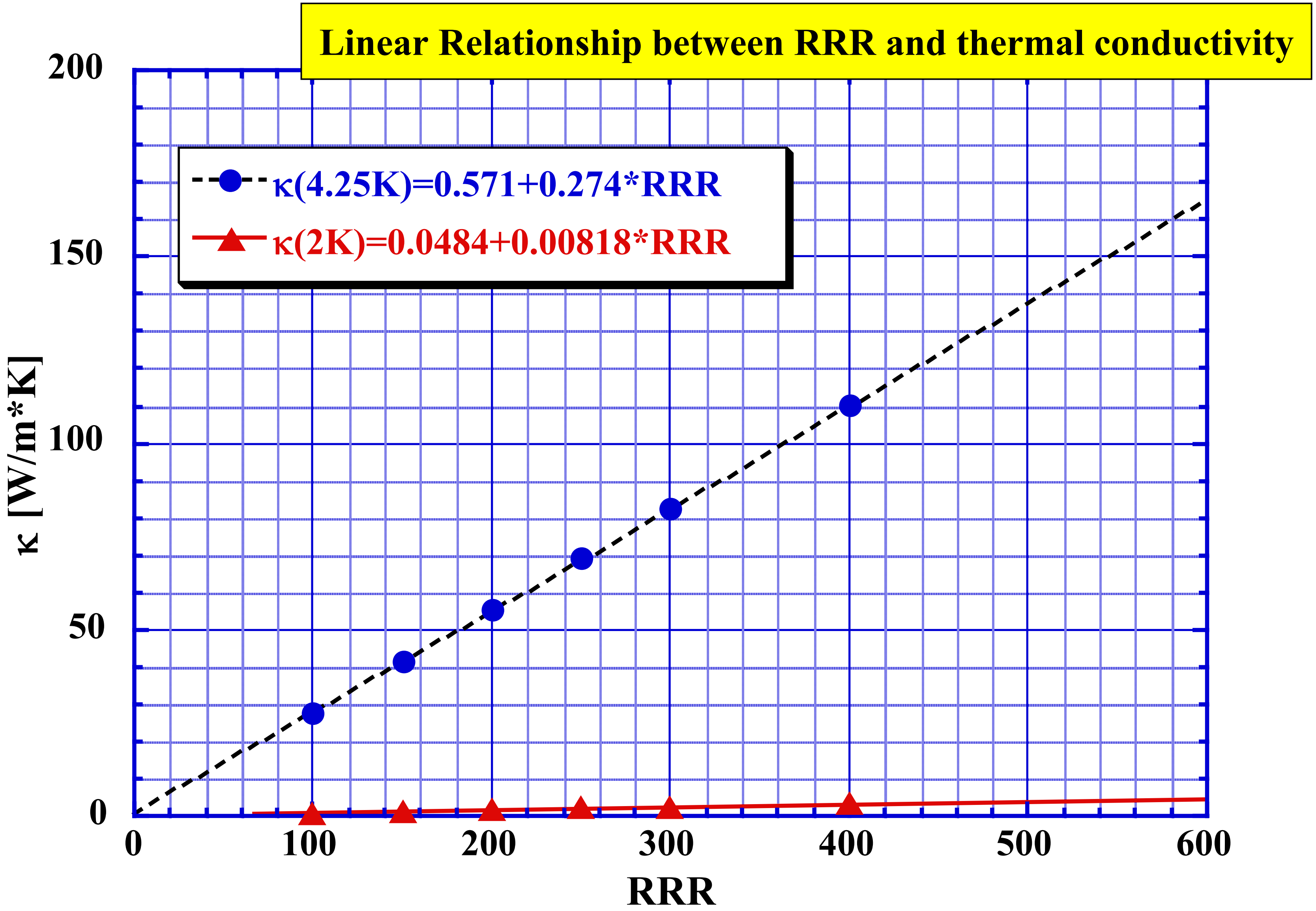

History of RRR improvement in a Nb production Company

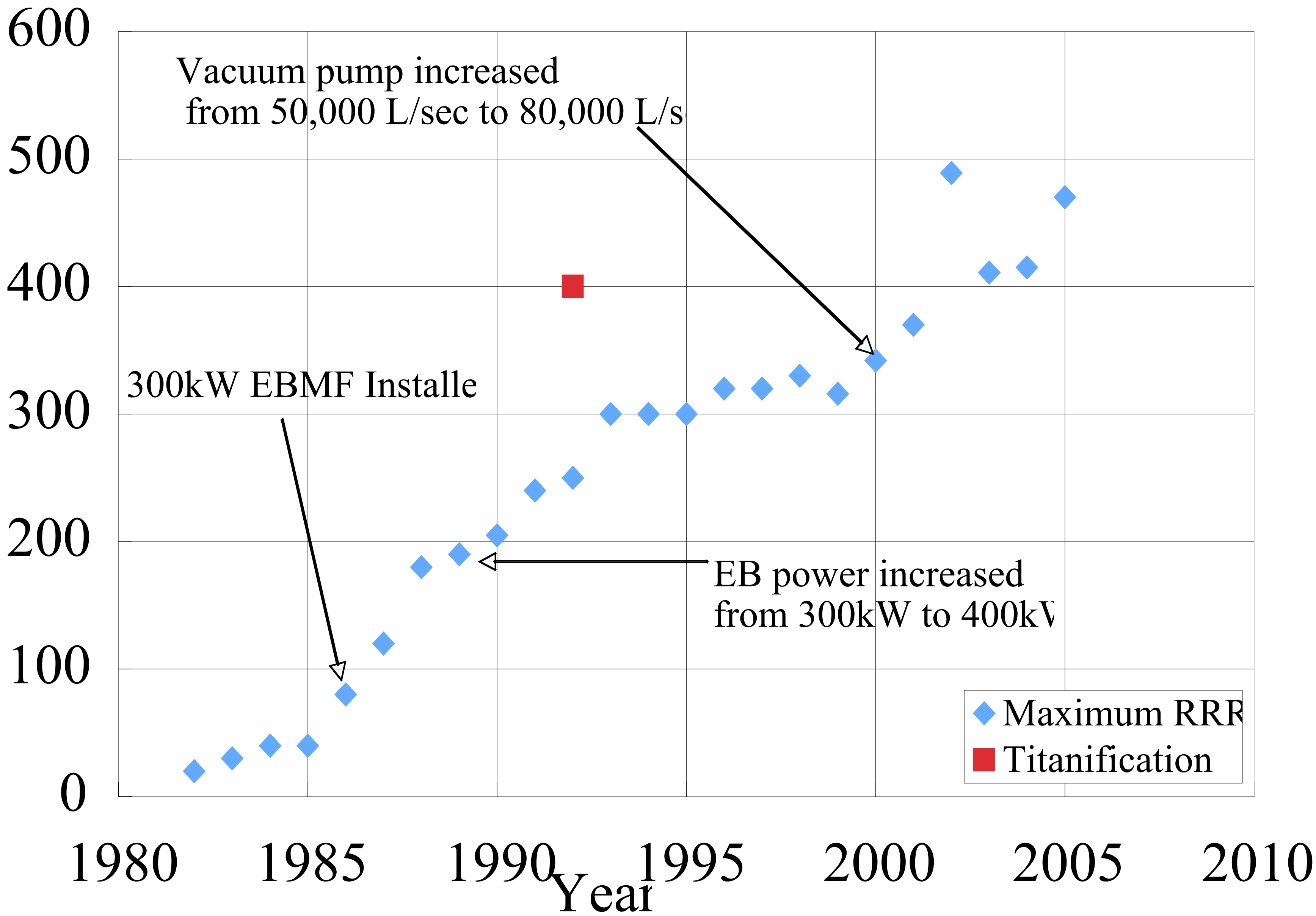

2. Niobium Material

2.1 Niobium Mien
2.2 High Purity Niobium Industrial Production

2.1 Niobium Miens

Niobium mine:Carbonatite

Big three mines in the world
Brazil：Araxa'(アラシャ)
Catalao（カタラウン)
Canada：St.Honore
（サン・オノレ)

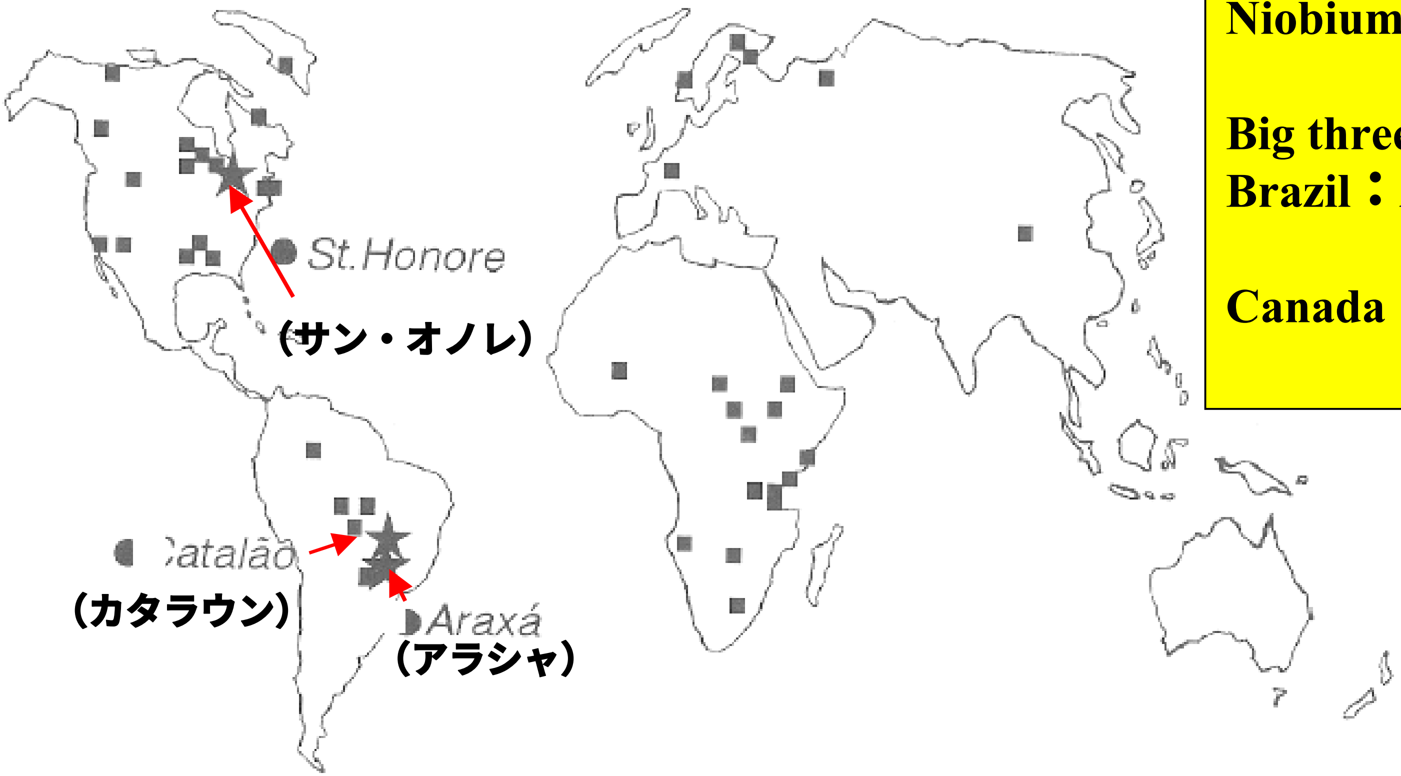

図１　世界のニオブ埋蔵地（■）とニオブ製品を生産する主要な鉱山（★）

金属 Vol.72 (2002) No.3

Niobium is 33rd abundant metal element in the earth.

A Niobium Mien

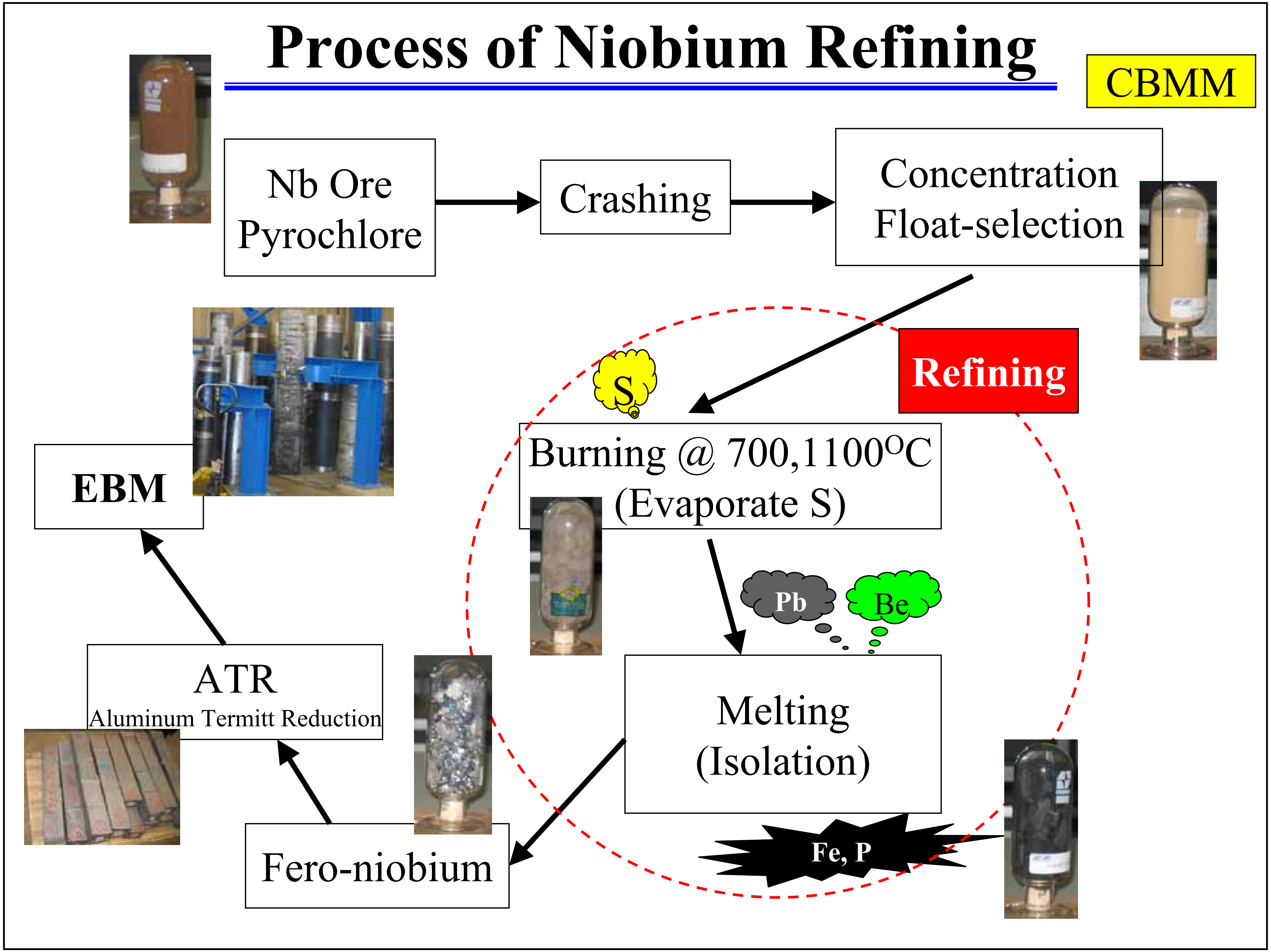

Process of Niobium Refining
CBMM
Nb Ore
Pyrochlore
Crashing
Concentration
Float-selection
Refining
S
Burning @ 700,1100^{O}C
(Evaporate S)
Pb
Be
Melting
(Isolation)
Fe, P
Fero-niobium
ATR
Aluminum Termitt Reduction
EBM

2.2 High Purity Nb Industrial Production

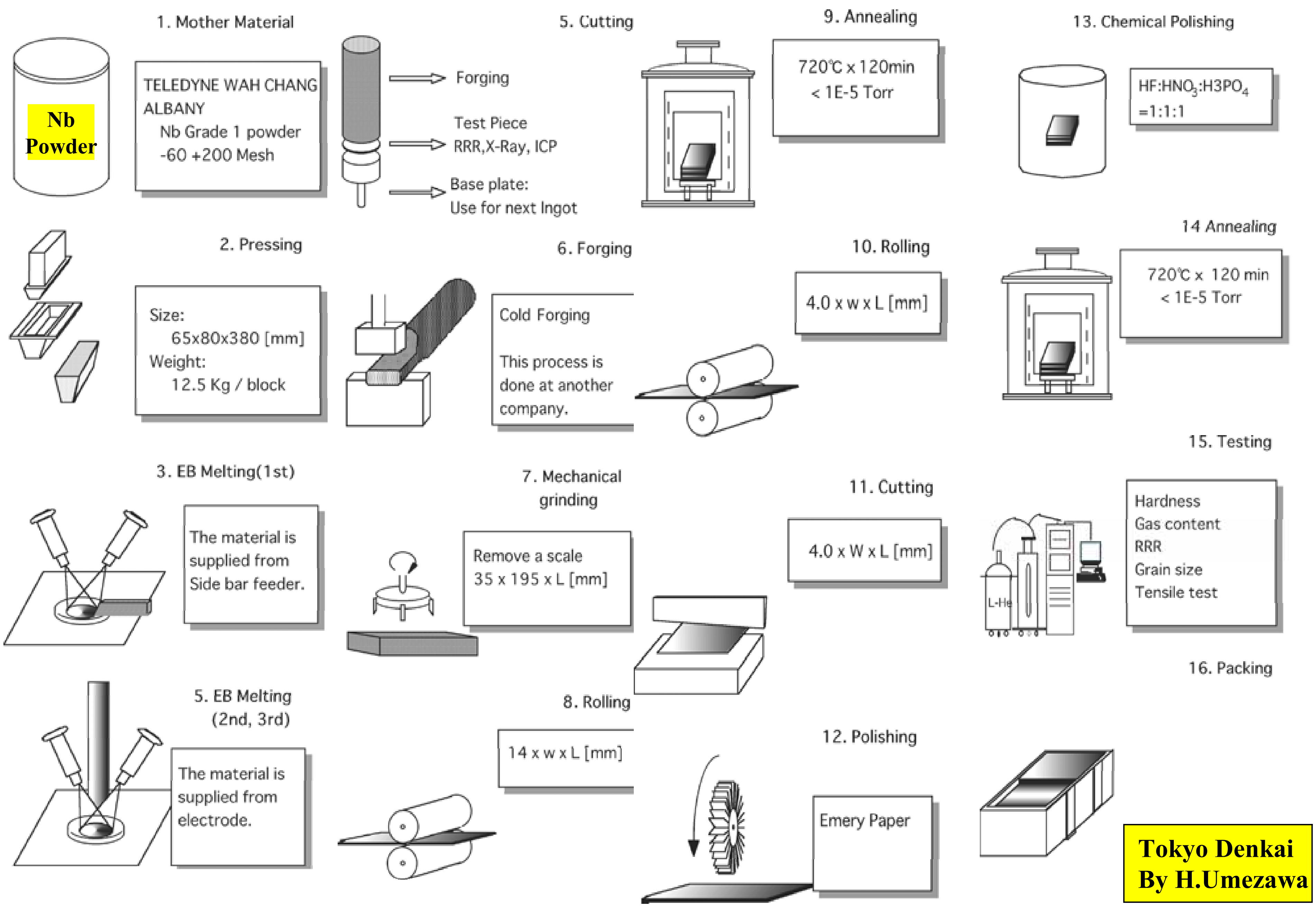

Original material for high pure niobium

Tokyo Denkai

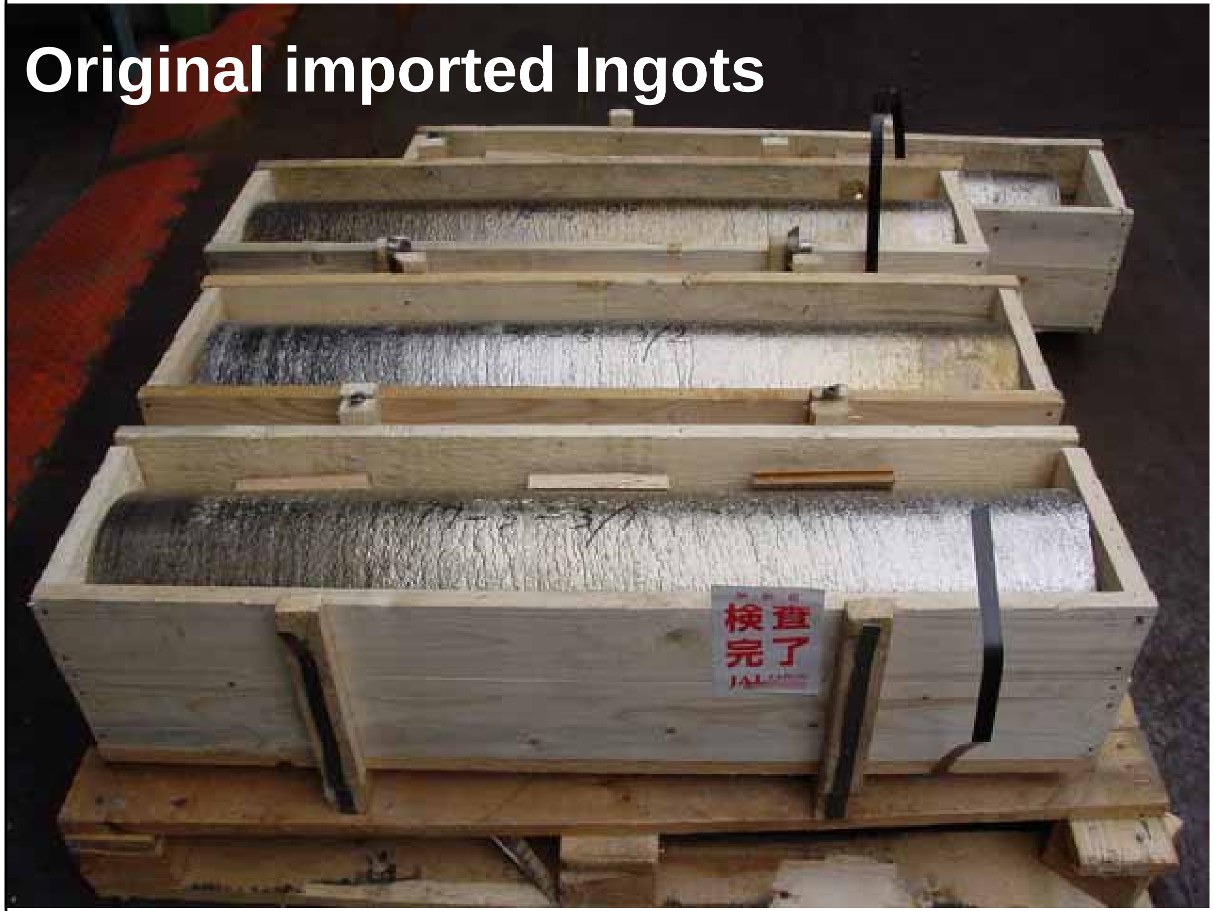

Vapor Presser for various metals

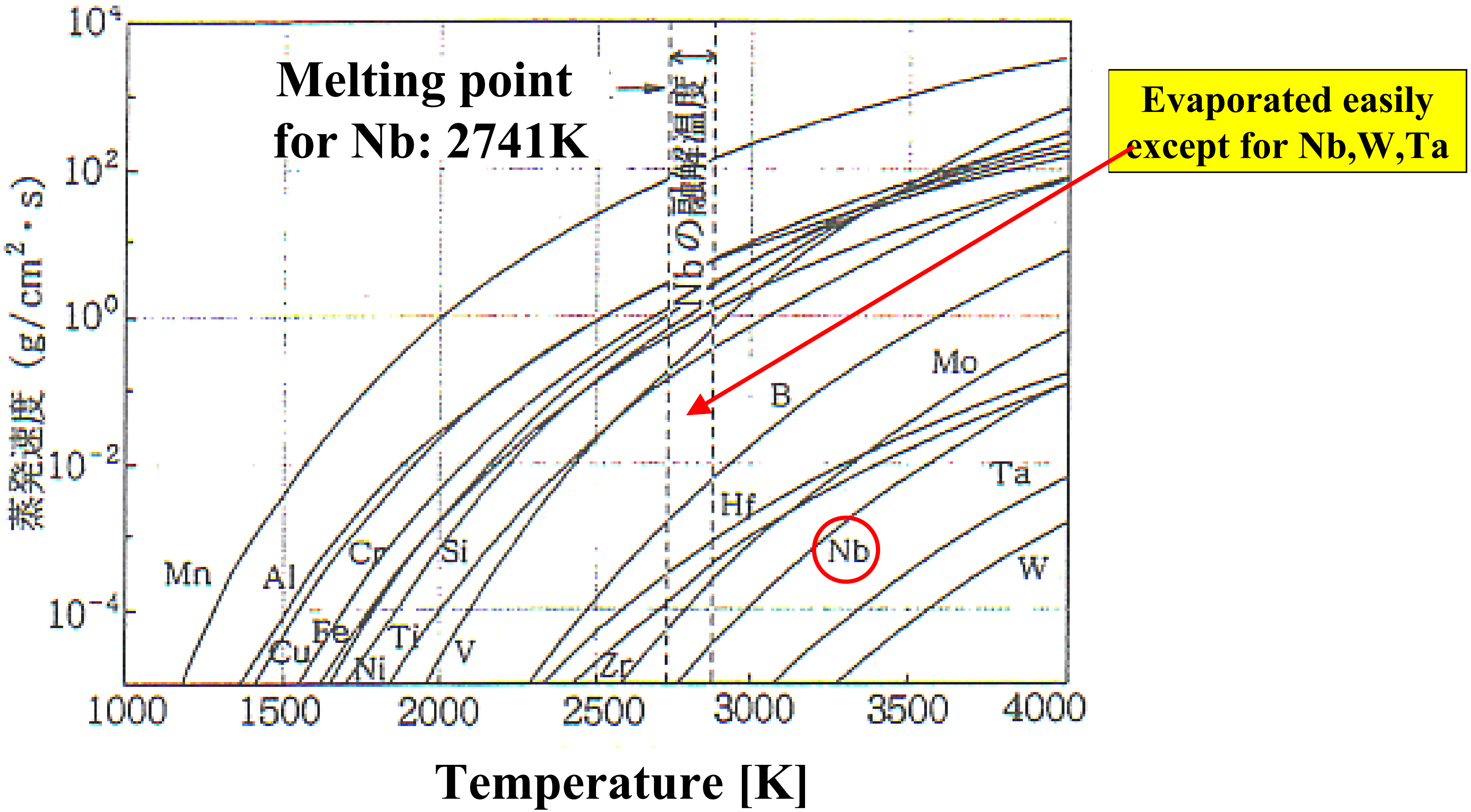

Electron Beam Melting

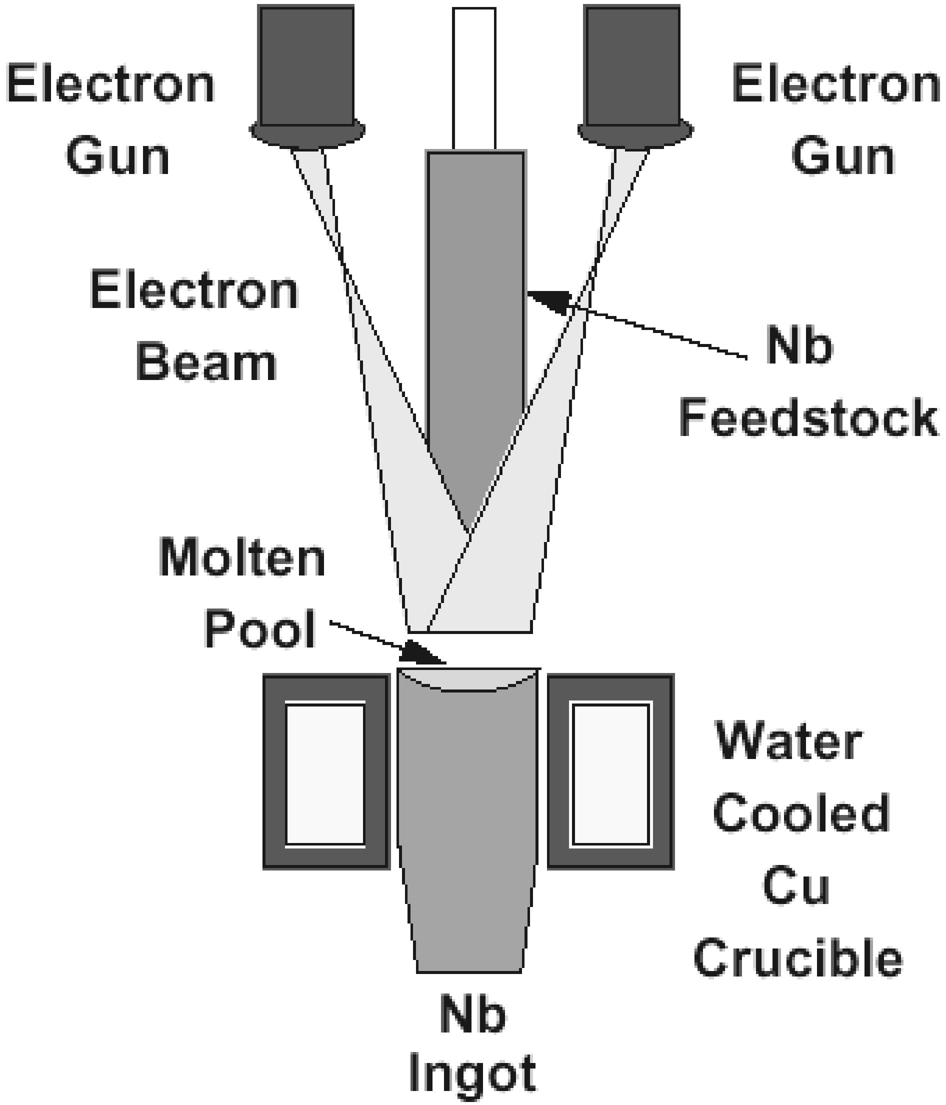

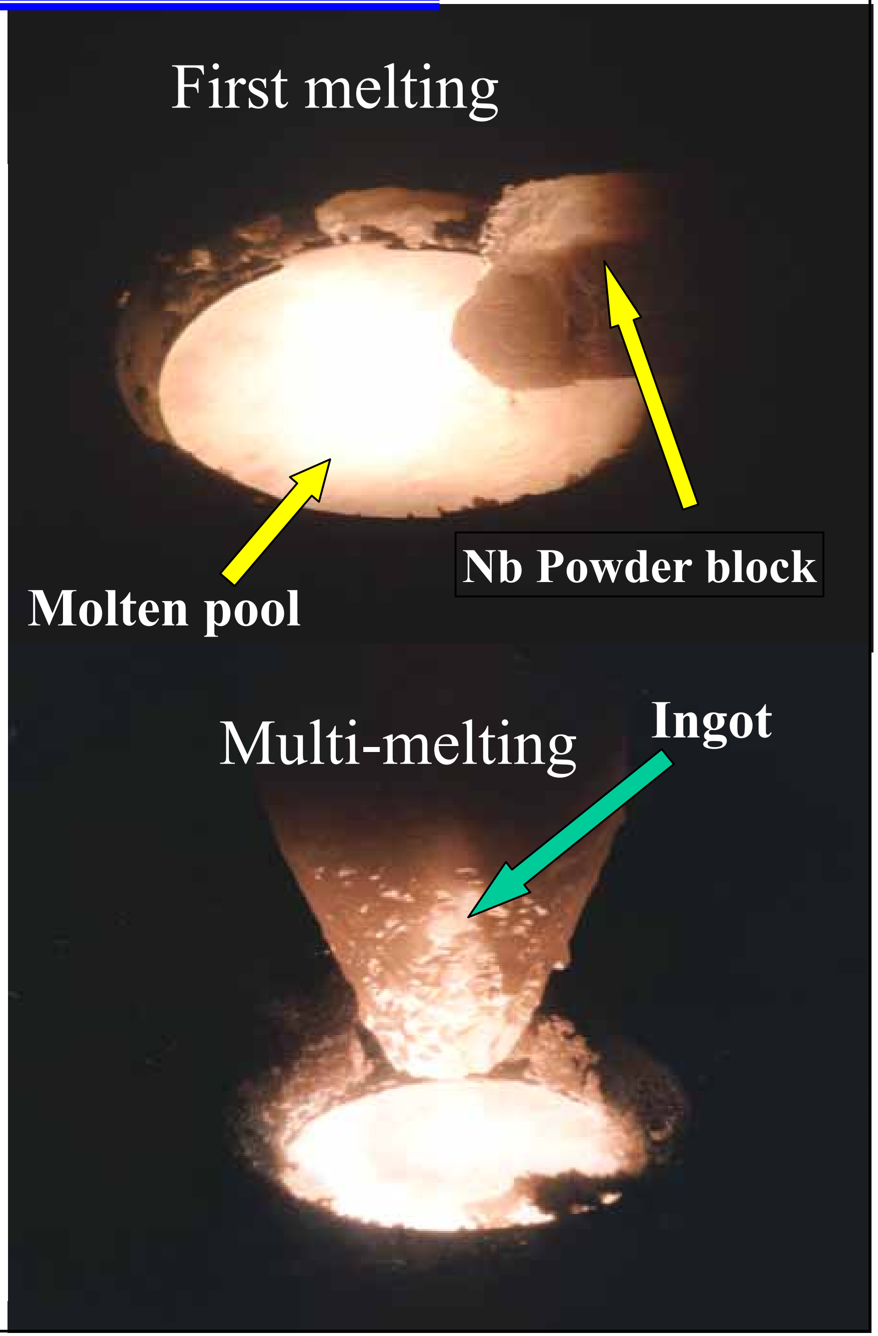

EBM furnace and Nb Ingots

Tokyo Denkai

Impurities

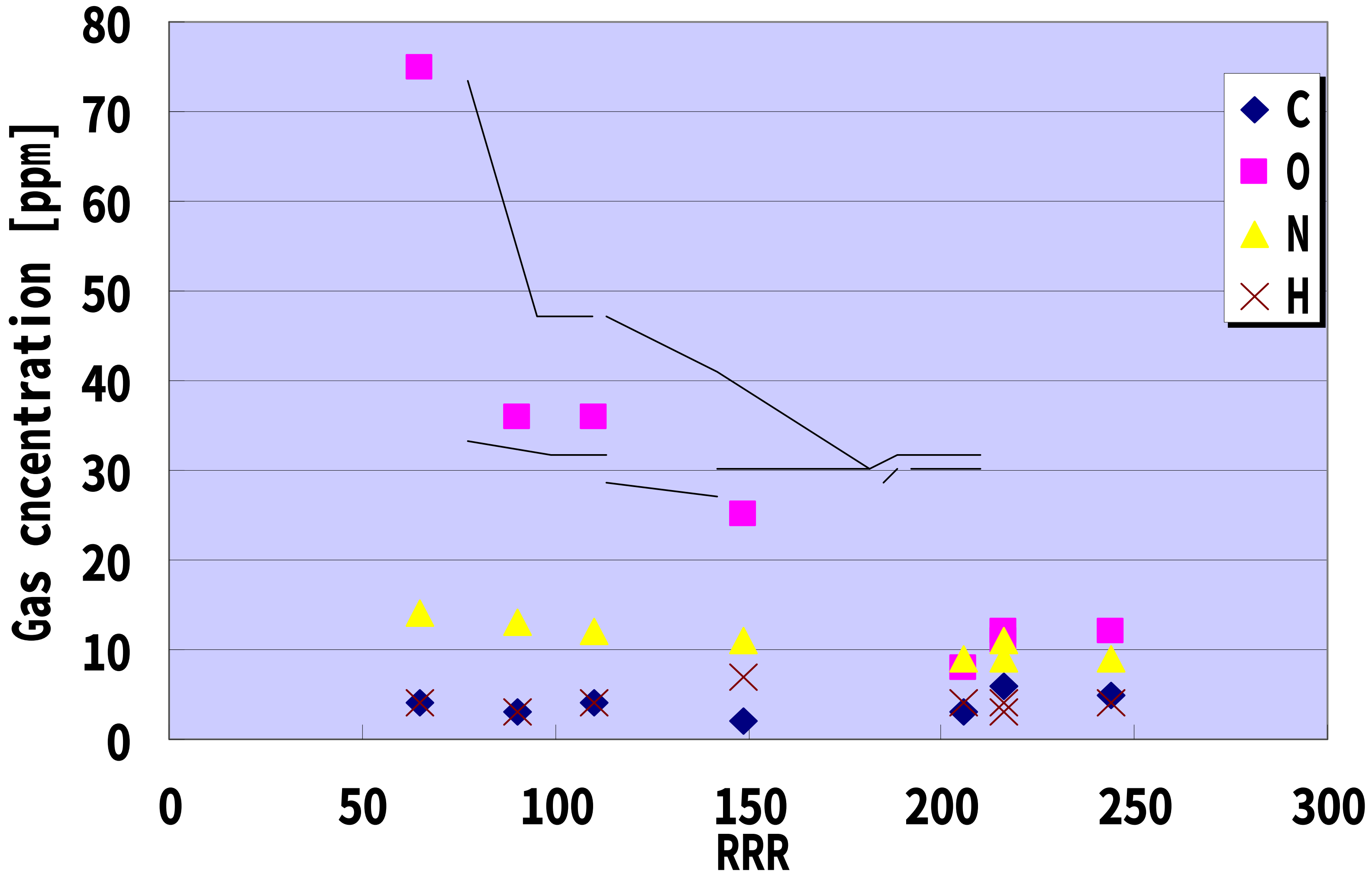

80
70
60
50
40
30
20
10
0
Gas cncentration [ppm]
0
50
100
150
200
250
300
RRR
C
O
N
H

Keys for High purity Nb Ingot production

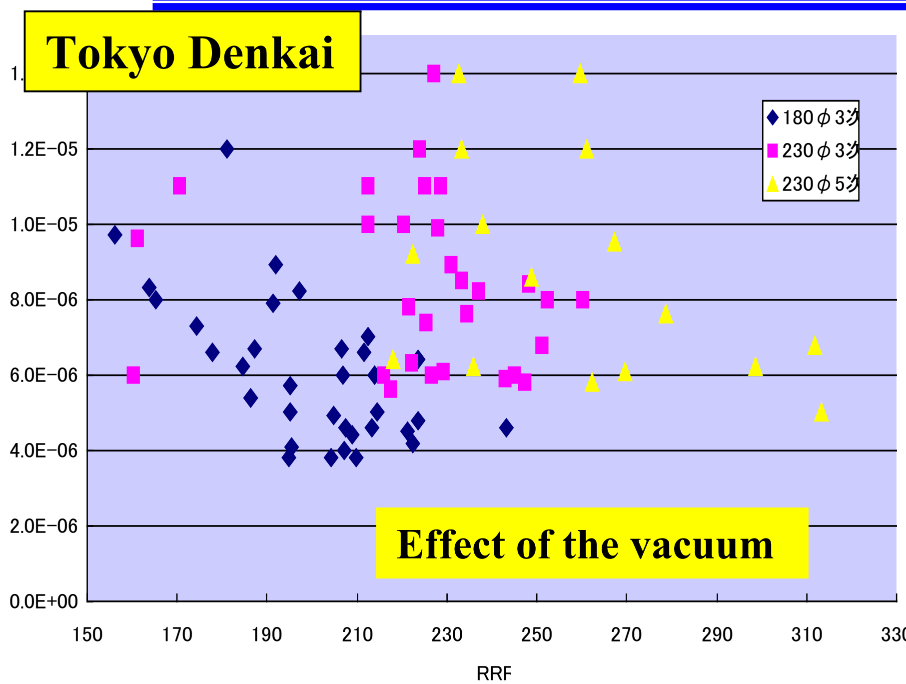

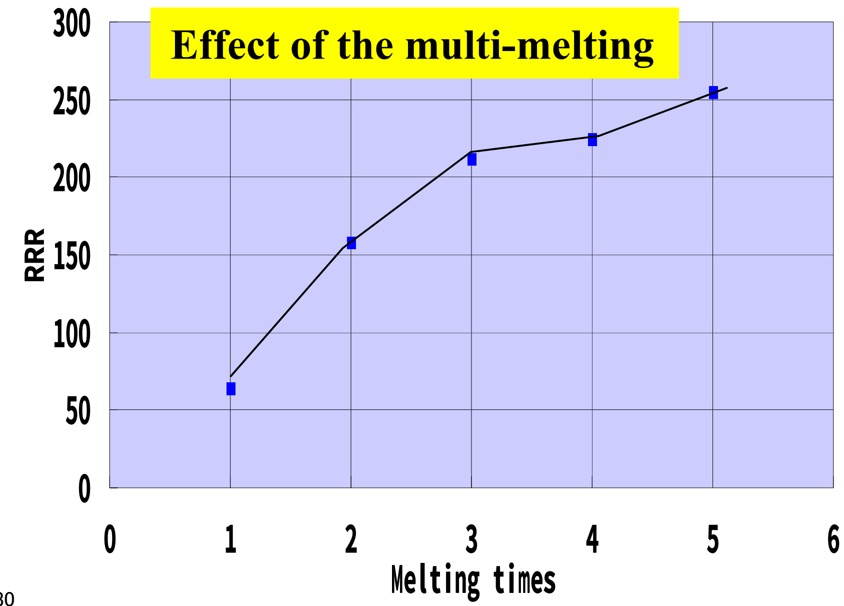

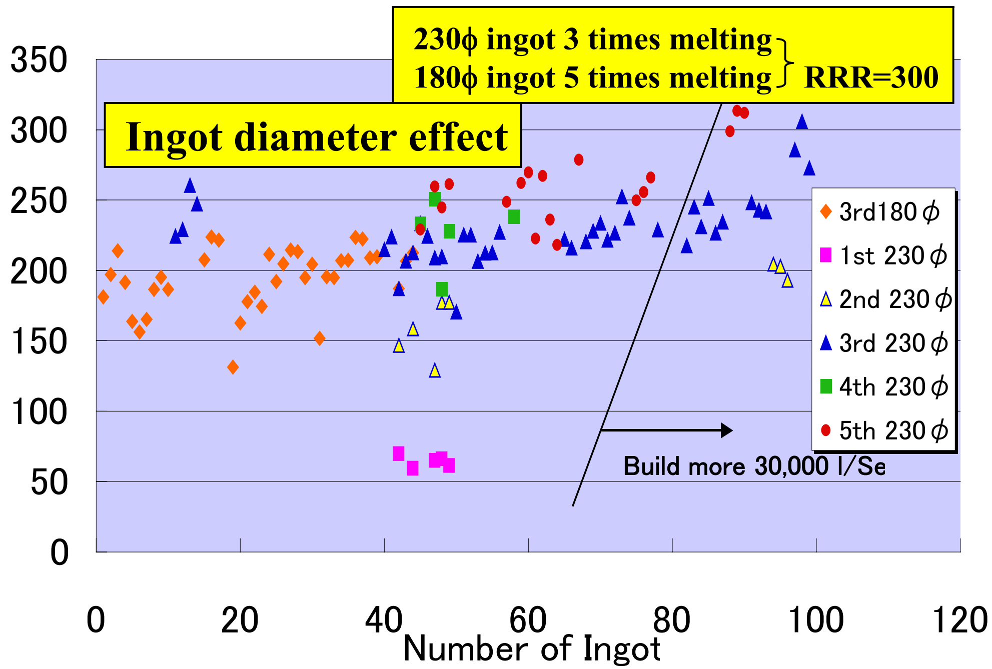

Three keys:

1) **High Vacuum,**
2) **2) Multi-melting,**
3) **Large molten pool surface (Large Ingot diameter)**

Gas analysis in niobium

Tokyo Denkai

Case of N

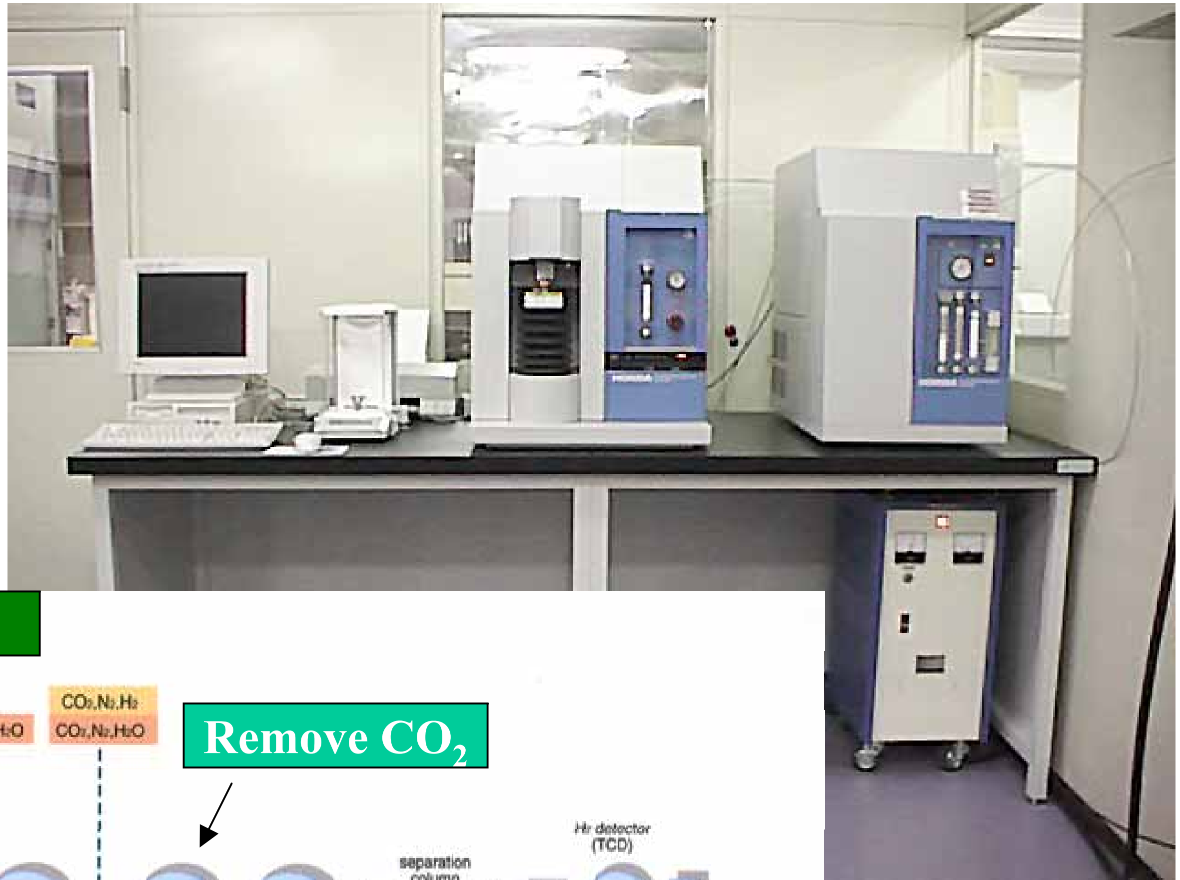

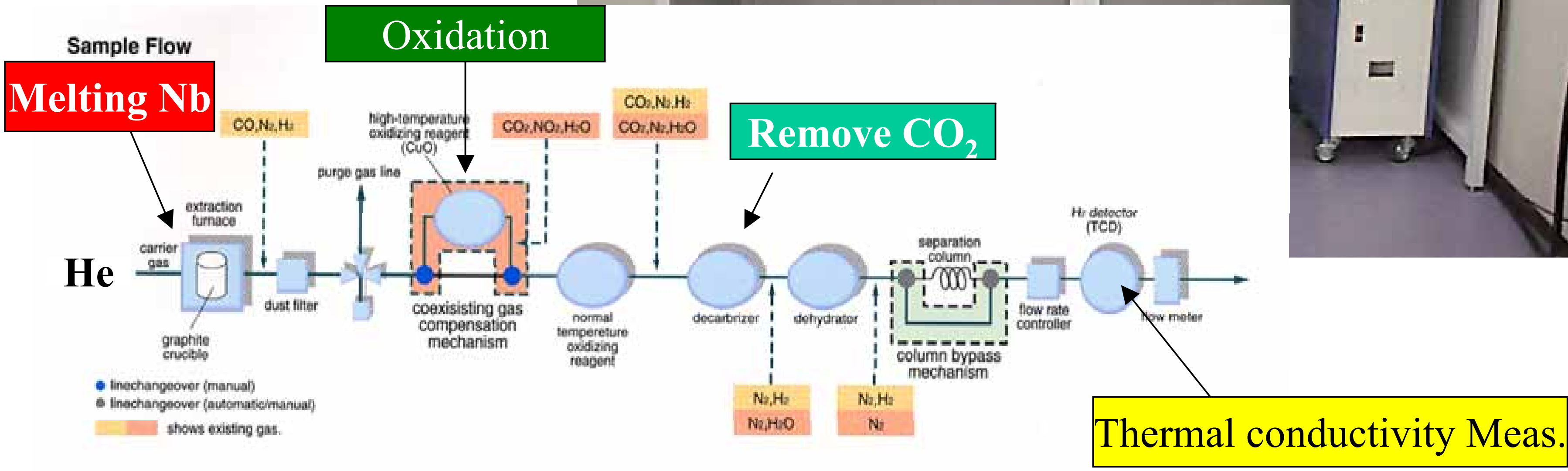

Gas analysis (Hydrogen, Oxygen, Nitrogen) ：HORIBA

Regression Analysis Result

K.K.Schulze: J. Metals, 33(1981), 33-41

$$\frac{1}{RRR}=\frac{O}{5000}+\frac{N}{3900}+\frac{H}{1550}+\frac{C}{4100}+\frac{Ta}{550000}+\ldots$$

Umezawa's (Tokyo Denkai) result.

$$\frac{1}{RRR}=\frac{O}{5800}+\frac{N}{2273}+\frac{H}{16322}+\frac{C}{8911}+\frac{Ta}{604690}+\frac{1}{1249}$$

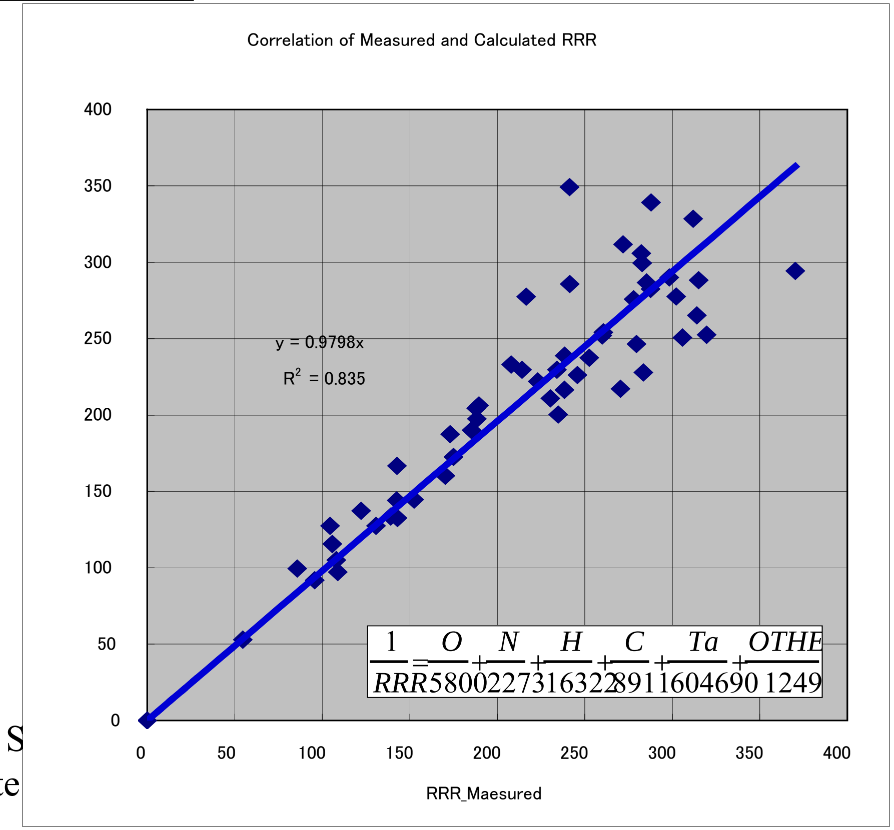

Rolling

Tokyo Denkai

Cleanroom

Intermediate rolling

Final rolling

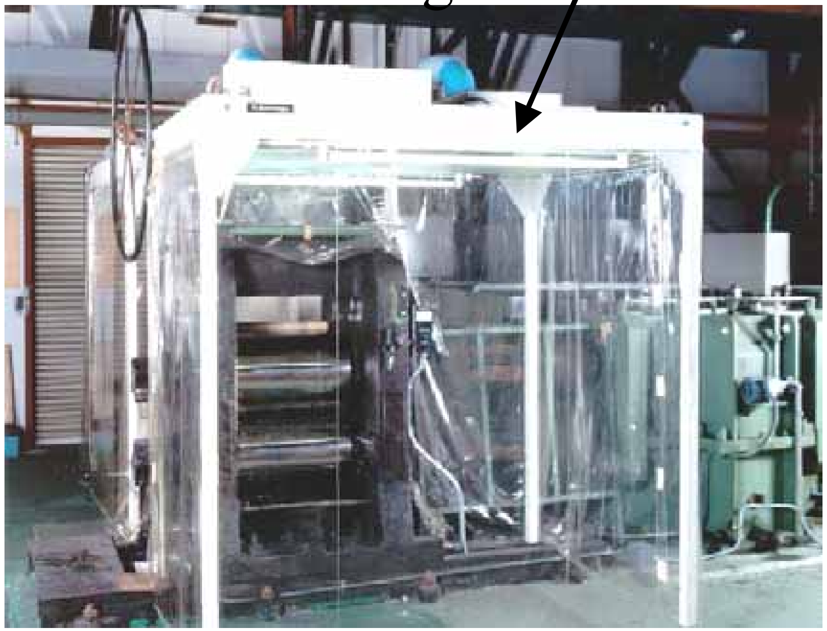

Careful control against dust

Vacuum annealing system

Tokyo Denkai
1400°C Max,
~1×10^{-6} Torr
Effective working zone
1000ϕ x 1800L
Ta heater

Metallurgy of Nb

Remained roll rolled structure

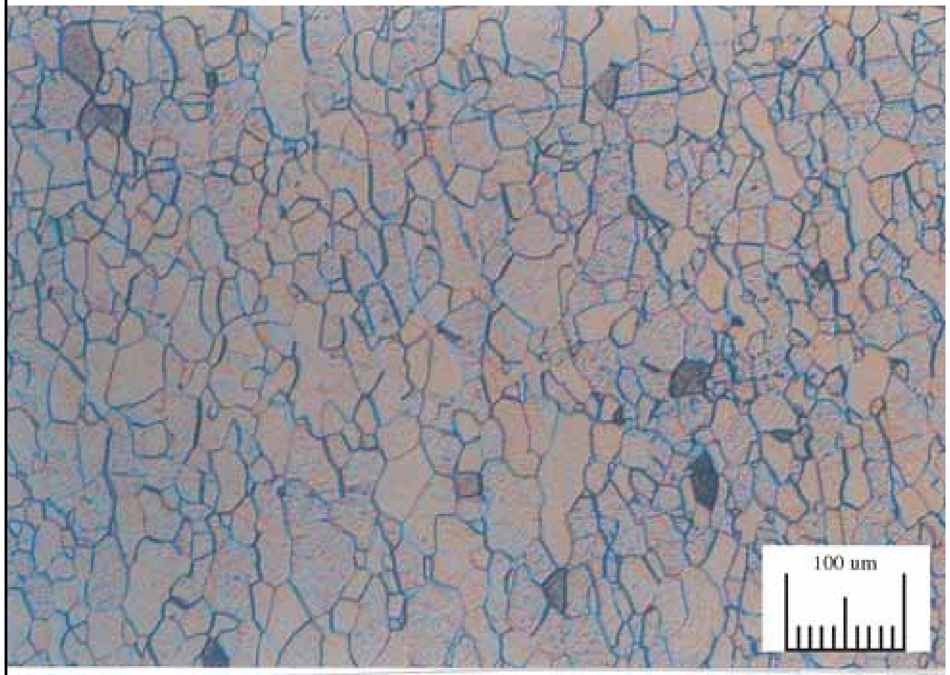

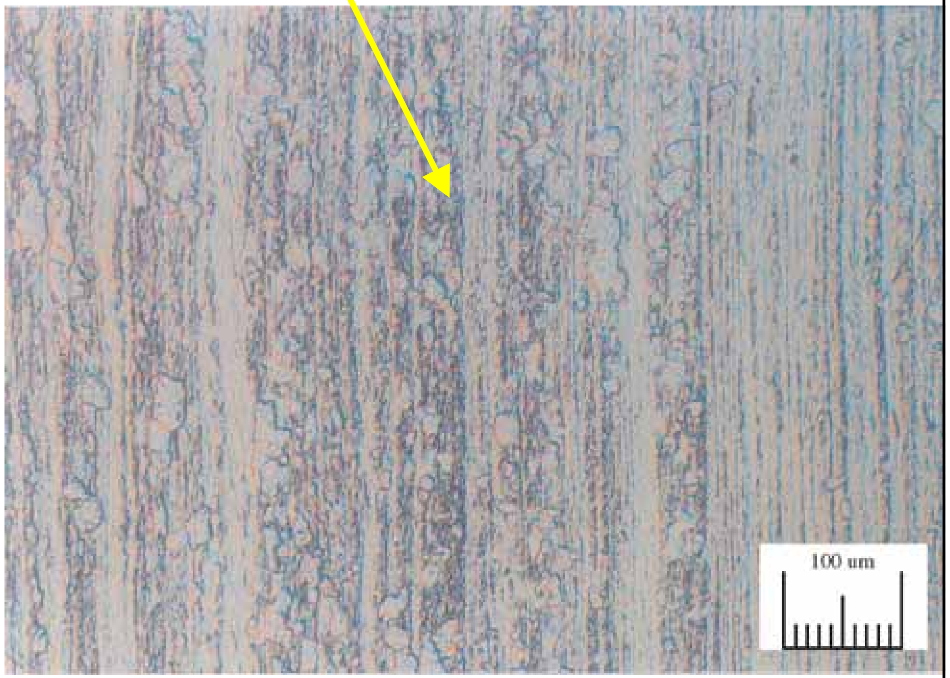

Well annealed

None annealed

Annealing Temp. and Mechanical Properties

TRISTAN

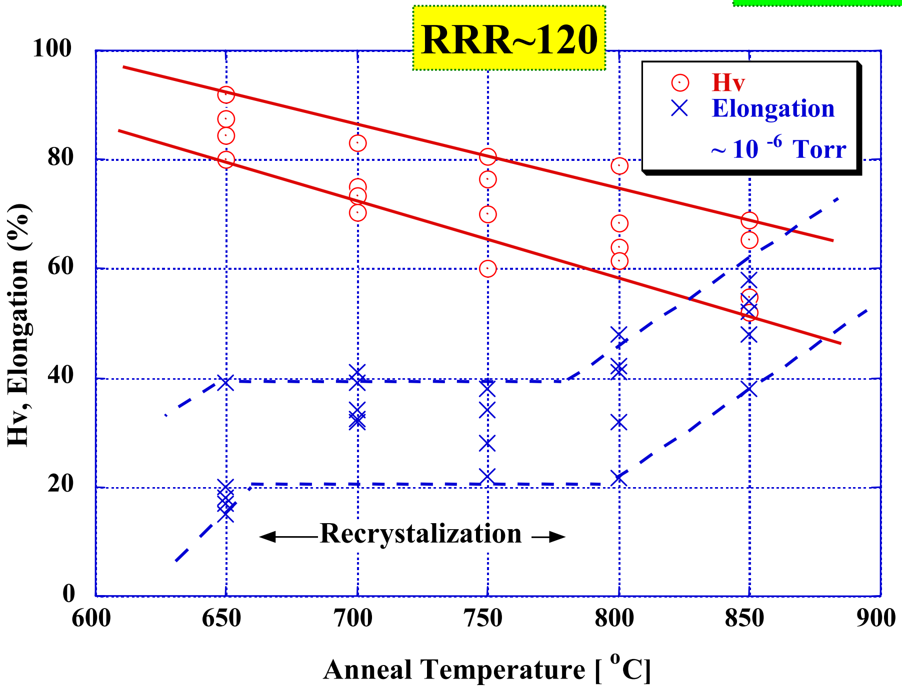

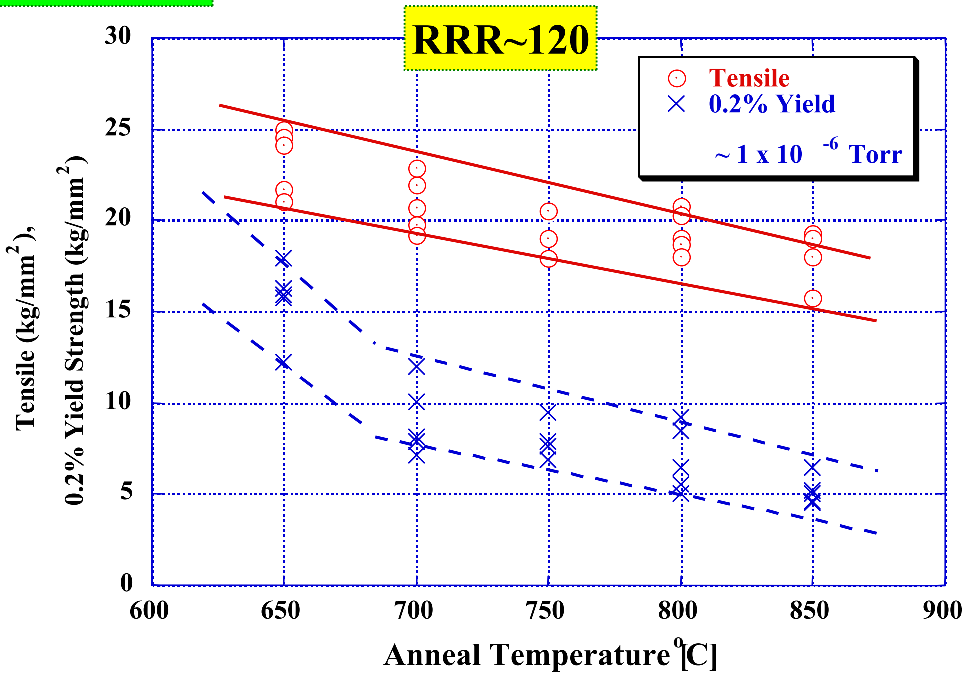

Re-crystallization Temperature : 680 ~ 780°C
Vacuum Pressure : ~10^{-6} Torr

High Pure Niobium Sheets

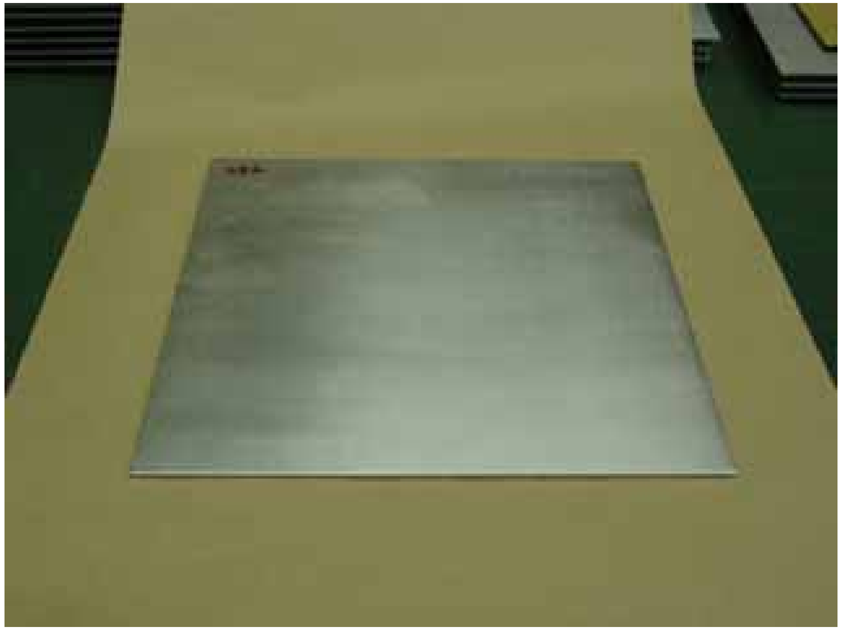

Tokyo Denkai

Improvement of RRR at Tokyo Denkai

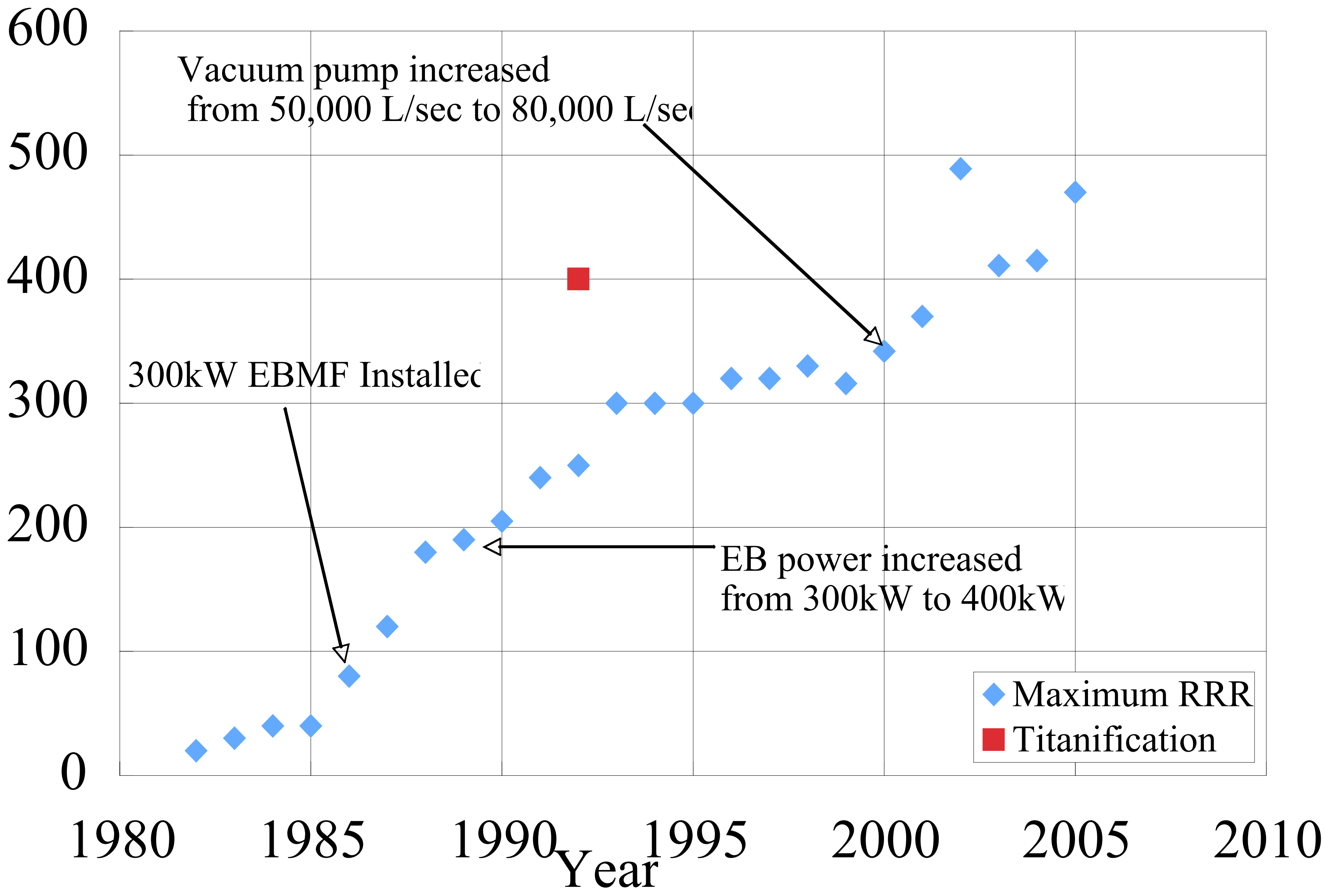

RRR measurement

Tokyo Denkai

K.Saito

Tensile Test

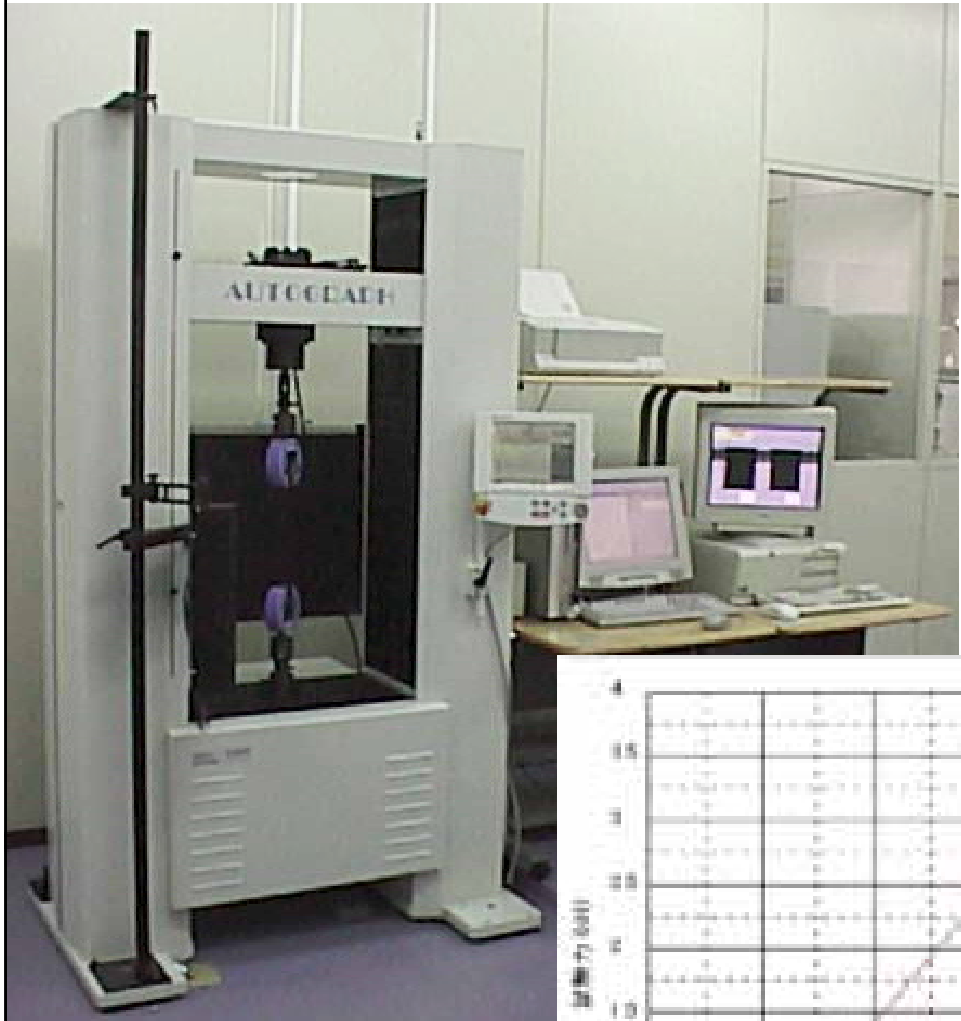

Tokyo Denkai

試験速度1 : 0.5 mm/min　　試験速度2 : 2.5 mm/min
切替点1 : 1 mm　　オペレータ : N.Nishida

形状: 平板

	厚さ	幅	標点距離
単位	mm	mm	mm
1 - 1	3.910	6.350	25.204

名前	耐力点 応力	最大点 応力	破断点 変位	弾性率 Standard	破断点ひずみ
パラメータ	0.2 %			0.4, 1 kN	
単位	N/mm2	N/mm2	mm	N/mm2	%
1 - 1	53.5389	144.129	13.9704	29151.2	48.5301

名前	最大点 試験力
単位	kN
1 - 1	3.63344

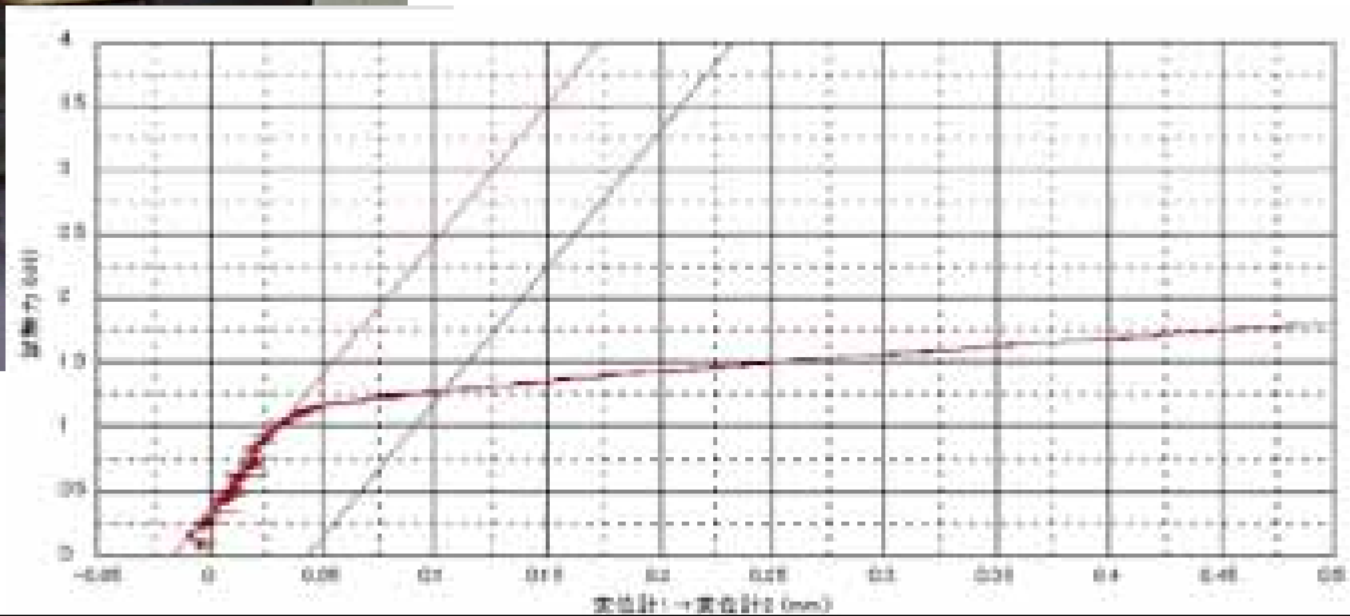

K.Saito

3. SRF RF Cavity Design

3.1 Single Cell Cavity Design
3.2 Criteria General for Cavity Shape
3.3 Criteria for Multi-cell Structures

What is RF cavity ?

Principle of RF acceleration
TM-mode : Ez≠0, Bz=0, frequency: f
TM_{010} - mode, π -mode, Standing Wave
V(electron velocity)～C(light velocity)
L(cell length) = λ/2 ; λ(wave length)=C/f
If the velocity is low like protons,
β=V/C < 1, then L=βλ/2

RF Cavity: accelerates charged particles by the electric field synchronized with RF frequency.

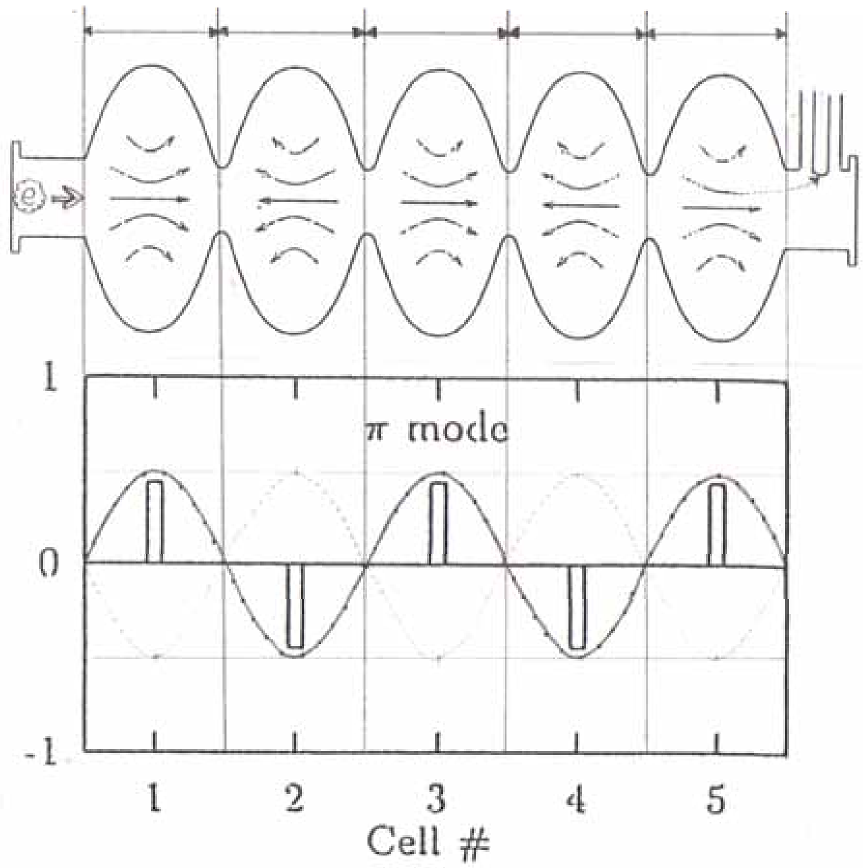

Equivalent circuit

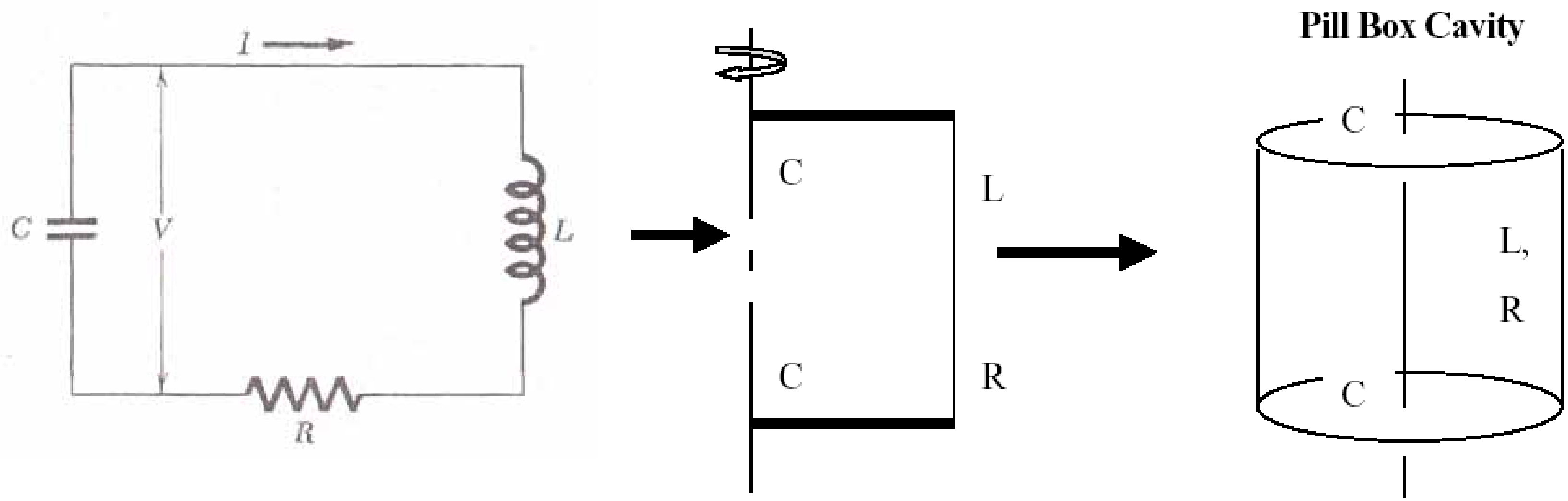

$$I = -\frac{dQ}{dt}, \quad Q = CV, \quad V = L\frac{dI}{dt} + RI$$

$$\frac{d^2V}{dt} + \left(\frac{R}{L}\right)\frac{dV}{dt} + \left(\frac{1}{LC}\right) = 0, \quad V(t) = V_O \exp(-\alpha + i\omega)t$$

$$(-\alpha + i\omega)^2 + (-\alpha + i\omega)\left(\frac{R}{L}\right) + \left(\frac{1}{LC}\right) = 0,$$

$$\alpha = \frac{R}{2L}, \quad \omega^2 = \frac{1}{LC} - \frac{R^2}{4L^2}$$

$$R << L, \quad \omega_O^2 = \frac{1}{LC} \Rightarrow f = \frac{1}{2\pi\sqrt{LC}}$$

Q-value of the circuit

$$Q \equiv \omega \cdot \frac{stored\,energy}{power\,loss/\sec} = \omega \cdot \frac{P}{dP/dt} = \omega \cdot \frac{L}{R}$$

$$= \frac{\omega}{2\alpha}$$

Q : proportional to 1/R

Simple Circuit Model of RF Cavity
- Oscillation in the LCR Circuit -

$$\propto \exp\left(-\frac{\omega}{2Q}t\right)$$

Q : Damping factor of the stored energy

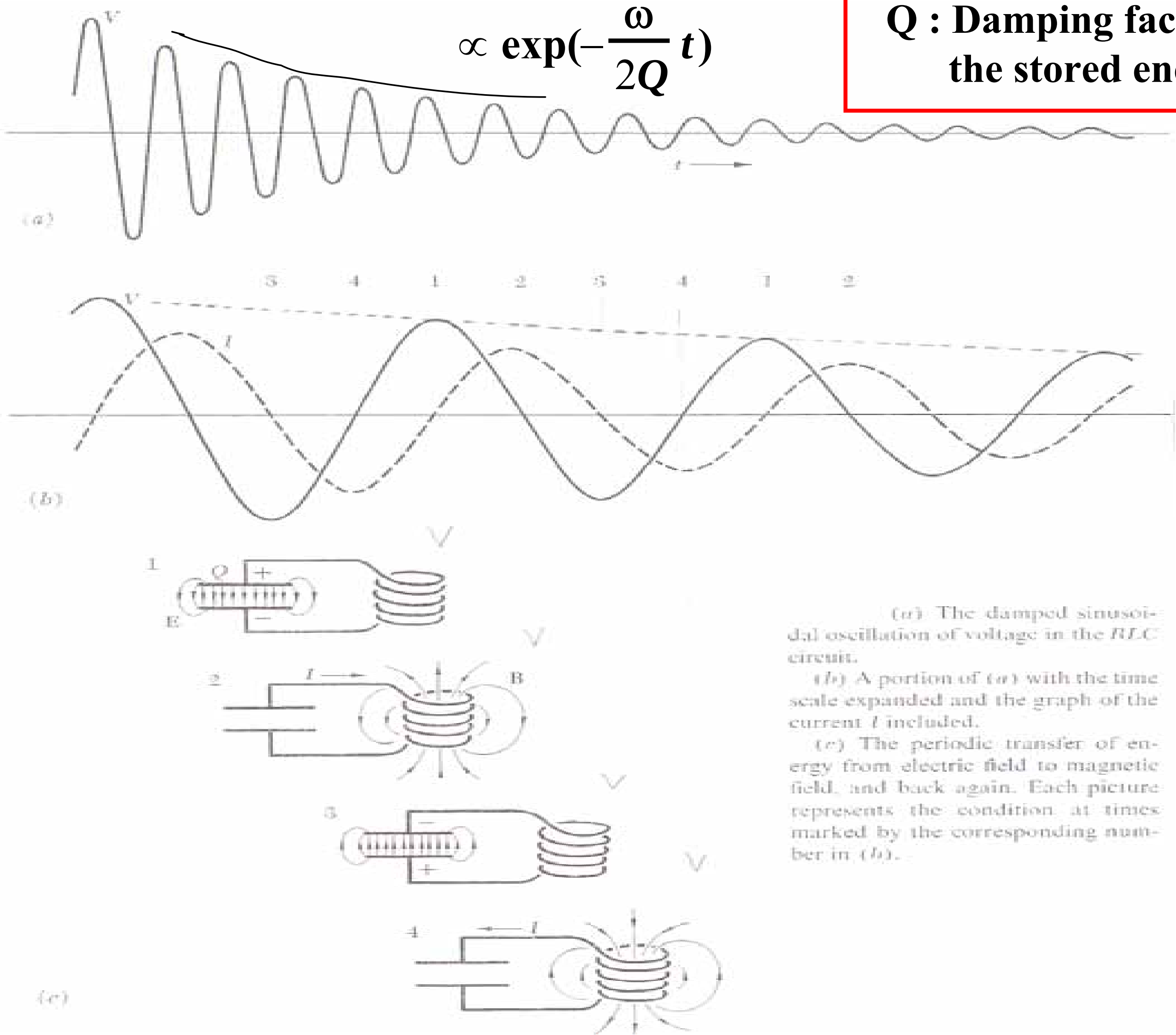

(a) The damped sinusoidal oscillation of voltage in the *RLC* circuit.
(b) A portion of (a) with the time scale expanded and the graph of the current *I* included.
(c) The periodic transfer of energy from electric field to magnetic field, and back again. Each picture represents the condition at times marked by the corresponding number in (b).

Electro-magnetic field in a waveguide

Maxwell equations in a waveguide

$$\nabla\times\mathbf{E}=i\frac{\omega}{c}\mathbf{B},\ \nabla\cdot\mathbf{B}=0,\ \nabla\times\mathbf{B}=-i\mu\varepsilon\frac{\omega}{c}\mathbf{E},\ \nabla\cdot\mathbf{E}=0,\ \rho=0,\ \mathbf{j}=0$$

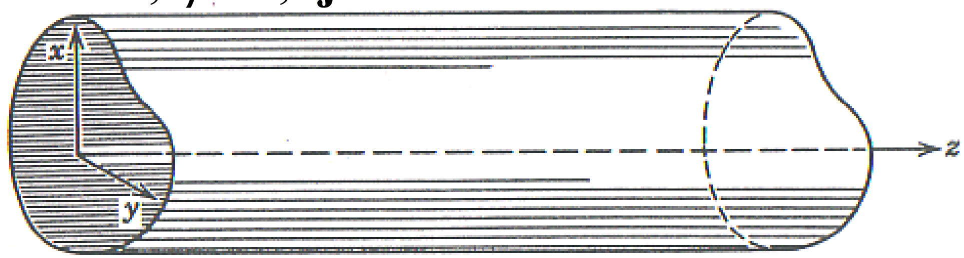

$$\left(\nabla^2+\mu\varepsilon\frac{\omega^2}{c^2}\right)\left\{\frac{\mathbf{E}}{\mathbf{B}}\right\}=0,$$

$\mathbf{E}(x,y,z,t)=\mathbf{E}(x,y)\exp(\pm ikz-i\omega t)$, k: wavevector,

$\mathbf{B}(x,y,x,t)=\mathbf{B}(x,y)\exp(\pm ikz-i\omega t)$,

$$\left[\nabla_t^2+(\varepsilon\mu\frac{\omega^2}{c^2}-k^2\right]\left\{\frac{\mathbf{E}}{\mathbf{B}}\right\}=0,\quad \nabla_t^2\equiv\nabla^2-\frac{\partial^2}{\partial^2 z},\quad \mathbf{E}=E_z\mathbf{e}_z+\mathbf{E}_t,\quad \mathbf{B}=B_z\mathbf{e}_z+\mathbf{B}_t$$

$$\mathbf{B}_t=\frac{1}{\left(\varepsilon\mu\frac{\omega^2}{c^2}-k^2\right)}\left[\nabla_t\left(\frac{\partial B_z}{\partial z}\right)+i\varepsilon\mu\frac{\omega}{c}\mathbf{e}_z\times\nabla_t E_z\right],$$

$$\mathbf{E}_t=\frac{1}{\left(\varepsilon\mu\frac{\omega^2}{c^2}-k^2\right)}\left[\nabla_t\left(\frac{\partial E_z}{\partial z}\right)-i\frac{\omega}{c}\mathbf{e}_z\times\nabla_t B_z\right]$$

Exercise IV.
Get this formula.

TM- mode Assign

TM-mode : $\boldsymbol{B_z} = 0,\ \boldsymbol{E_z} \neq 0$ → Can accelerate beam Beam

$$\mathbf{B}_t = \frac{i\varepsilon\mu\frac{\omega}{c}}{\left(\varepsilon\mu\frac{\omega^2}{c^2} - k^2\right)}\left[\mathbf{e}_z \times \nabla_t E_z\right],$$

$$\mathbf{E}_t = \frac{1}{\left(\varepsilon\mu\frac{\omega^2}{c^2} - k^2\right)}\nabla_t\left(\frac{\partial E_z}{\partial z}\right),$$

$$\left[\nabla_t^2 E_z + \left(\varepsilon\mu\frac{\omega^2}{c^2} - k^2\right)\right]E_z = 0,$$

→ **Solve the eigenvalue problem, get k and Ez**

Boundary condition $E_z|_S = 0$ ($\because$ $\mathbf{n} \times \mathbf{E} = 0$ **on the surface of perfect conductor)**

$\frac{\partial B_z}{\partial n}|_S = 0$ ($\because$ $\mathbf{n} \cdot \mathbf{B} = 0$ **on the surface,**

but automatically satisfied by the TM - mode condition)

TE-mode Assign

TE-mode : $\boldsymbol{E_z} = 0$, $\boldsymbol{B_z} \neq 0$ ⇨ **Can not accelerate beam**

$$\mathbf{B}_t = \frac{i\varepsilon\mu \frac{\omega}{c}}{(\varepsilon\mu \frac{\omega^2}{c^2} - k^2)} \nabla_t \left(\frac{\partial B_z}{\partial z} \right),$$

$$\mathbf{E}_t = \frac{-i \frac{\omega}{c}}{\left(\varepsilon\mu \frac{\omega^2}{c^2} - k^2 \right)} \mathbf{e}_z \times \nabla_t B_z,$$

$$\left[\nabla_t^2 B_z + (\varepsilon\mu \frac{\omega^2}{c^2} - k^2) \right] B_z = 0,$$

Boundary condition $E_z|_S = 0$ ($\because$ $\mathbf{n} \times \mathbf{E} = 0$ **on the surface of perfect conductor**
but automatically satisfied by the TE- mode condition)

$$\frac{\partial B_z}{\partial n}\Big|_S = 0 \ (\because \ \ \mathbf{n} \cdot \mathbf{B} = 0 \ \text{ on the surface)}$$

Eigevalue problem

$$\psi(x,y) = E_z(x,y) \text{ for TM- mode or } B_z(x,y) \text{ for TE- mode}$$

$$\left(\vec{\nabla}_t^2 + \gamma^2\right)\psi = 0, \quad \psi\big|_S = 0 \text{ (for TM - mode) or } \frac{\partial}{\partial n}\psi\big|_S = 0 \text{ (for TE - mode)}$$

$$\gamma^2 = \varepsilon\mu\frac{\omega^2}{c^2} - k^2 \geq 0$$

From the boundary condition,

$$\gamma^2 = \gamma_\lambda^2, \; \psi = \psi_\lambda \quad (\lambda = 1, 2, \cdots)$$

$$\Rightarrow \quad k_\lambda^2 = \varepsilon\mu\frac{\omega^2}{c^2} - \gamma_\lambda^2$$

If $\omega < c\dfrac{\gamma_\lambda}{\sqrt{\varepsilon\mu}}$, then k_λ is an imaginal number. The wave is damped in the waveguide.

$\omega_\lambda = c\dfrac{\gamma_\lambda}{\sqrt{\varepsilon\mu}} \cdots$cutoff frequency

When $\omega \geq \omega_\lambda$, wave number k_λ is a real number,

then the wave can propagate into the waveguide.

TM-mode in a Pill Box Cavity

TM-modes

$\mathbf{E}(x,y,z,t) = \mathbf{E}(x,y)\exp(ikz - i\omega t)$

When shorted at $z = 0$ and $z = d$, then the wave makes a standing wave.

$\therefore\ \mathbf{E}(x,y,z,t) = \left[\mathbf{A}(x,y)\cos(kz) + \mathbf{B}(x,y)\sin(kz)\right]\exp(-i\omega t)$

If the cavity is made from perfect conductor, $\mathrm{E_t} = 0\ at\ z = 0$ and d.

$\therefore\ \mathbf{E}(x,y,z) = \mathbf{B}(x,y)\sin(kz)$ and $\sin(kd) = 0 \Rightarrow kd = p\pi (p = 0,1,2,\cdots) \Rightarrow k = \dfrac{p\pi}{d}$

$\mathbf{E}_z(x,y,z) = \Psi(x,y,z)\mathbf{e}_z = \left[\mathbf{A}_z(x,y)\cos(kz) + \mathbf{B}_z(x,y)\sin(kz)\right]\mathbf{e}_z$

$\mathbf{E}_t(x,y,z,) = \dfrac{1}{\gamma^2}\nabla_t\left(\dfrac{\partial\Psi}{\partial z}\right)$, and the boundary condition: $\mathrm{E_t} = 0$ at $z = 0$.

$\Rightarrow \Psi = B_z(x,y)\cos(kz) = B_z(x,y)\cos(\dfrac{p\pi}{d}z)$

Now one can solve the eigenvalue problem.

$\left(\nabla_t^2 + \gamma^2\right)\Psi = 0,\ \gamma^2 = \varepsilon\mu\dfrac{\omega^2}{c^2} - k^2 = \varepsilon\mu\dfrac{\omega^2}{c^2} - \left(\dfrac{p\pi}{d}\right)^2$

Cylindorical cordinate (r,θ,z), $\Psi \rightarrow \Psi = B_z(r,\theta)$

$\left(\nabla_t^2 + \gamma^2\right)\Psi = \left(\dfrac{\partial^2}{\partial^2 r} + \dfrac{1}{r}\dfrac{\partial}{\partial r} + \dfrac{1}{r^2}\dfrac{\partial^2}{\partial^2\theta}\right)\Psi + \gamma^2\Psi = 0$

$\Psi(r,\theta) = R(r)\cdot\Theta(\theta)$

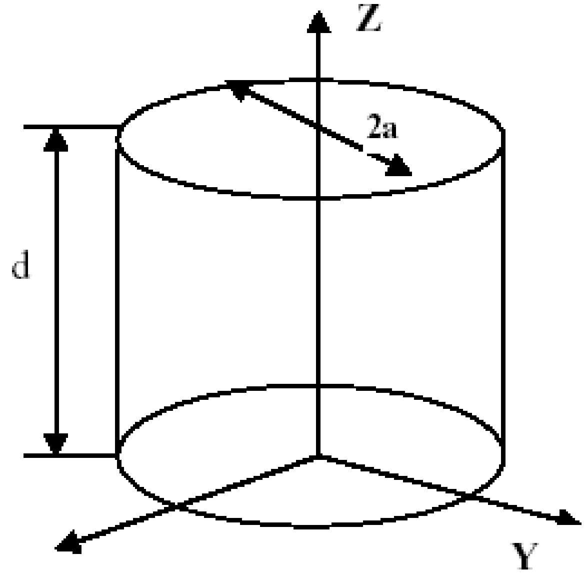

$$r^2 \frac{\partial^2 R(r)}{\partial^2 r} + \frac{r}{R(r)} \frac{\partial R(r)}{\partial r} + \gamma^2 r^2 = -\frac{1}{\Theta(\theta)} \frac{\partial^2 \Theta(\theta)}{\partial^2 \theta}$$

$$-\frac{1}{\Theta(\theta)} \frac{\partial^2 \Theta(\theta)}{\partial^2 \theta} = m^2 \Rightarrow \Theta(\theta) = \Theta_0 \exp(\pm im\theta), m = 0,1,2,\cdots$$

Θ is for a single-value function at θ=0 ~ 2π.

$\rho=\gamma r$,

$$\frac{\partial^2 R}{\partial^2 \rho} + \frac{1}{\rho} \frac{\partial R}{\partial \rho} + (1 - \frac{m^2}{\rho^2}) R = 0 \Rightarrow R : mthBesselfunction(J_m)$$

For no divergence at ρ=0 $\Rightarrow R(\rho) = J_m(\rho)$

Boundary condition: $E_z(r,\theta) = 0$ at $r = a \Rightarrow J_m(\gamma a) = 0 \Rightarrow \gamma a = \rho_{m,n}$: nth solution of J_m

$\rho_{m,n}$	n=1	n=2	n=3
m=0	$\rho_{0,1} = 2.405$	$\rho_{0,2} = 5.520$	$\rho_{0,3} = 8.654$
m=1	$\rho_{1,1} = 3.832$	$\rho_{1,2} = 7.016$	$\rho_{1,3} = 10.173$
m=2	$\rho_{2,1} = 5.136$	$\rho_{2,2} = 8.417$	$\rho_{2,3} = 11.620$

$$\gamma_{m,n} = \frac{\rho_{m,n}}{a}, \quad \text{thus } \Psi(r,\theta) = J_m(\frac{\rho_{m,n}}{a} \cdot r) \cdot \exp(\pm im\theta),$$

Resonance frequency ($\mathrm{TM}_{m,n,p}$ – mode)

$$\omega_{m,n,p} = \frac{c}{\sqrt{\varepsilon\mu}} \sqrt{\frac{\rho_{m,n}}{a^2} + \frac{p^2 \pi^2}{d^2}}$$

For E_t and B_t, calculate

$$\mathbf{B}_t = \frac{i\varepsilon\mu\frac{\omega}{c}}{\left(\varepsilon\mu\frac{\omega^2}{c^2} - k^2\right)}\left[\mathbf{e}_z \times \nabla_t E_z\right],$$

$$\mathbf{E}_t = \frac{1}{\left(\varepsilon\mu\frac{\omega^2}{c^2} - k^2\right)}\nabla_t\left(\frac{\partial E_z}{\partial z}\right),$$

$TM_{m,n,p}$ − mode

$$E_z = E_o \cos(kz) J_m\left(\frac{\rho_{m,n}}{a} r\right)\exp(-im\theta), \qquad B_z = 0$$

$$E_r = \frac{iE_0 p\pi}{\gamma_{m,n,p}}\cos\left(\frac{p\pi}{d}z\right)\frac{\partial J_m(\rho)}{\partial \rho}\exp(-im\theta), \qquad B_r = -\frac{E_0 m\varepsilon\mu\omega_{m,n,p}}{}\cos(kz) J_m\left(\frac{\rho_{m,n}}{a} r\right)\exp(-im\theta)$$

$$E_\theta = \frac{E_0 m p\pi}{\gamma_{m,n,p}^2 dc}\cos\left(\frac{p\pi}{d}z\right) J_m\left(\frac{\rho_{m,n}}{a} r\right)\exp(-im\theta), \quad B_\theta = \frac{iE_0\varepsilon\mu\omega_{m,n,p}}{\gamma_{m,n,p} c}\cos(kz)\exp(-im\theta)\frac{\partial J_m(\rho)}{\partial \rho}$$

Design of TM_{010}-mode single cell cavity

Exercise V.
Make design a 1300MHz single cell Pill Box cavity
1.What is the diameter of the cell?
2. What is the cell length?

Transit time factor

$$E_z(r=0,z,t) = E_0 J_0\left(\frac{\rho_{0,1}}{a} r\right)\cdot \exp(-i\omega t)$$

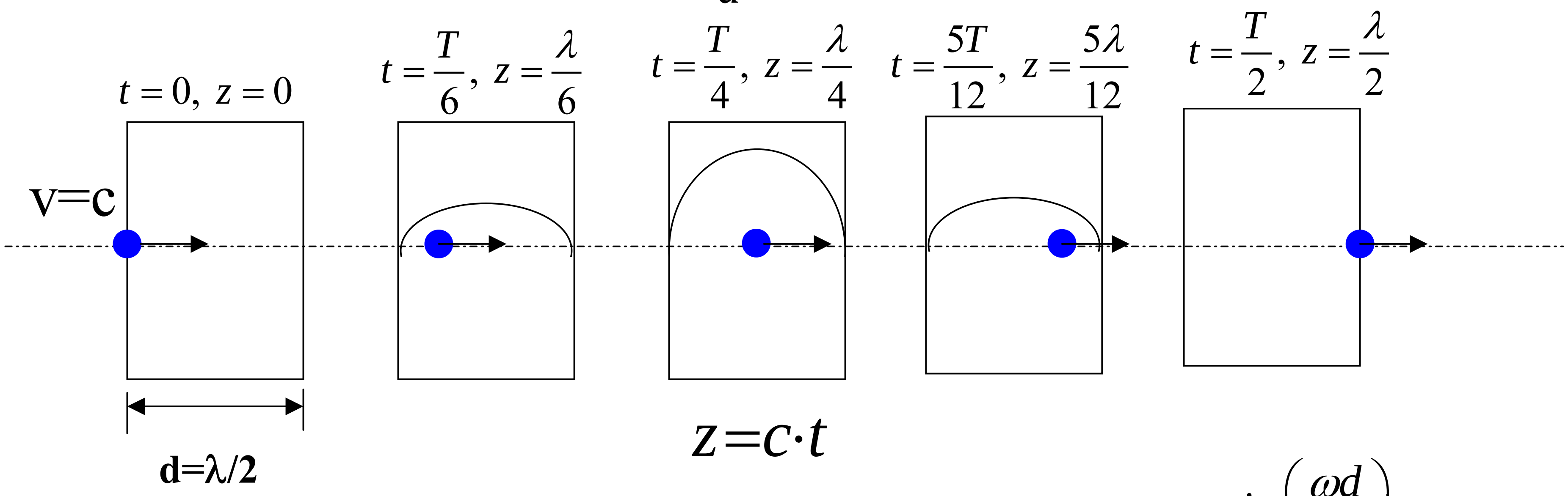

$$V = \left|\int_0^d E_z(r=0,z)e^{i\omega t}dz\right| = \left|\int_0^d E_z(r=0,z)e^{i\omega\frac{z}{c}}dz\right| = E_0\left|\int_0^d e^{i\omega\frac{z}{c}}dz\right| = E_0 d\,\frac{\sin\left(\frac{\omega d}{2c}\right)}{\frac{\omega d}{2c}} = E_0 d\cdot T$$

T : Transit time factor

$$T = \frac{2}{\pi} = 0.637 \quad \text{(for Pill Box Cavity)}$$

$$Eacc \equiv \frac{V}{d} = E_0 T$$

Characteristic parameters of RF cavity

Surface Impedance Z[Ω]: $\boldsymbol{Z} \equiv \frac{\mathbf{E}_{//}}{\mathbf{H}_{//}} = \mathbf{R_S} + i\boldsymbol{X}$, $\mathbf{R_S} = \frac{1}{\sigma\delta} = \sqrt{\frac{\mu\omega}{2\sigma}}$,

Skin depth δ [m] : $\delta = \sqrt{\frac{2}{\mu\omega\sigma}}$

Wall loss P_{loss} [W]: $P_{loss} = \frac{1}{2} R_S \int_S H_s^2 ds$ $\left(= \frac{\pi R_S E_o^2}{(\mu/\varepsilon)} J_1^2(2.405) \cdot a \cdot (a+d)\right.$ for pill box cavity)

Transit time factor T : $T = \frac{\int_0^d E_z e^{i(\omega \times \frac{z}{c})} dz}{\int_0^d E_z dz}$ $\left(= \frac{2}{\pi}\right.$ for pill box cavity)

Accelerating Voltage V : $V = \int_0^d E_o(\rho = 0, z)\, e^{i(\omega \frac{z}{c})} dz$ $(= dE_o T$ for pill box)

Accelerating gradient E_{acc} : $E_{acc} = \frac{V}{d}$ $\left(= E_o T = 2\frac{E_o}{\pi}\right.$ for pill box cavity)

Stored energy U: $U = \frac{1}{2}\mu \int_V H^2 dv = \frac{1}{2}\varepsilon \int_V E^2 dv$ $\left(= \frac{\pi\varepsilon E_0^2}{2} \cdot J_1^2(2.405) \cdot d \cdot a^2\right.$ for pill box cavity

Unloaded Q-value Q_O: $Q_O = \frac{\omega \cdot U}{P_{loss}}$ $\left(= \omega \cdot \frac{\mu \cdot a^2 d}{2 \cdot a(a+d)} \cdot \frac{1}{R_S}\right.$ for pill box cavity)

Characteristic parameters of RF cavity

Shunt impedance R_{sh} [Ω]: $R_{sh} = \dfrac{V^2}{P_{loss}}$ $\left(= \dfrac{4(\varepsilon/\mu)d^2}{\pi^3 R_S J_1^2(2.405)a(a+d)} \right.$ **for pill box cavity**

Geometrical factor Γ: $\Gamma = Q_O \cdot R_S = \dfrac{\omega\mu\int_V H^2 dv}{\int_S H_S^2 ds}$ $\left(= \dfrac{\omega\mu d a^2}{2(a^2+ad)} \right.$ for pill box cavity$)$ $\Rightarrow R_S = \dfrac{\Gamma}{Q_O}$

R/Q : $\left(R/Q\right) = \dfrac{R_{sh}}{Q_O} = \dfrac{V^2}{\omega U}$ Goodness of the cavity shape, No dependent on material

E_{SP}/E_{acc} $\left(= \dfrac{\pi}{2} = 1.57\right.$ for pill box cavity), H_{SP}/E_{acc} $\left(= 30.5 \dfrac{Oe}{MV/m}\right.$ for pill box cavity)

Smaller value is better from field emission problem point of view

Smaller value is better from high gradient point of view

Pill-box cavity maximum Eacc = 1750/30.5 =57.4MV/m

Frequency dependence of the cavity parameters

Characteristic Parameter	ω dependence Normal conducting	ω dependence Super conducting
R_S	$\omega^{\frac{1}{2}}$	ω^{2}
P_{loss}	$\omega^{-\frac{3}{2}}$	No dependence
U	ω^{-3}	ω^{-3}
Q_O	$\omega^{-\frac{1}{2}}$	ω^{-2}
R_{sh}	$\omega^{-\frac{1}{2}}$	ω^{-2}
R_{sh}/L	$\omega^{\frac{1}{2}}$	ω^{-1}
Γ	No dependence	No dependence
R/Q	No dependence	No dependence

Rsh per length linearly increases to $\sqrt{\omega}$, so normal conducting choose higher frequency, for example 11.4GHz @ warm LC.

3.2 Criteria General for Cavity Shape

- Suppressed Multipacting
- Lower Surface Electric field

- Lower Surface Magnetic field
- High Efficient
- High Gradient

} incorporate

2001-2004

Real Cavity Design

Diameter of BP	➡	bigger
Ep/Eacc	→	larger
Hp/Eacc	→	larger
R/Q	→	larger
Cell to cell coupling	→	smaller
HOM issue	→	more serious

1) Need a hole on the cavity for electron to pass the cavity
2) Need RF input port
3) HOM coupler port

→ Need Beam pipes on both Ends

4) High efficient cavity
5) Better performance
   Smaller Ep/Eacc : Field emission
   Smaller Hp/Eacc : Multipaction

→ Optimization of cell shape
Multi-cell cavity

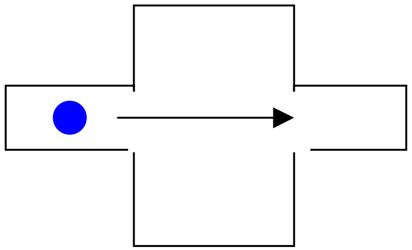

Choose spherical shape to reduce multipacting

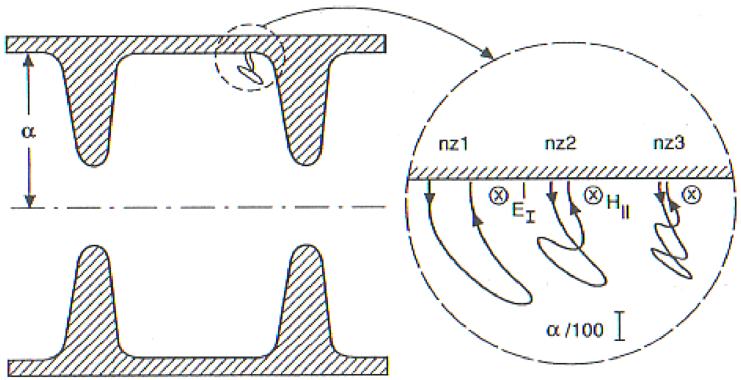

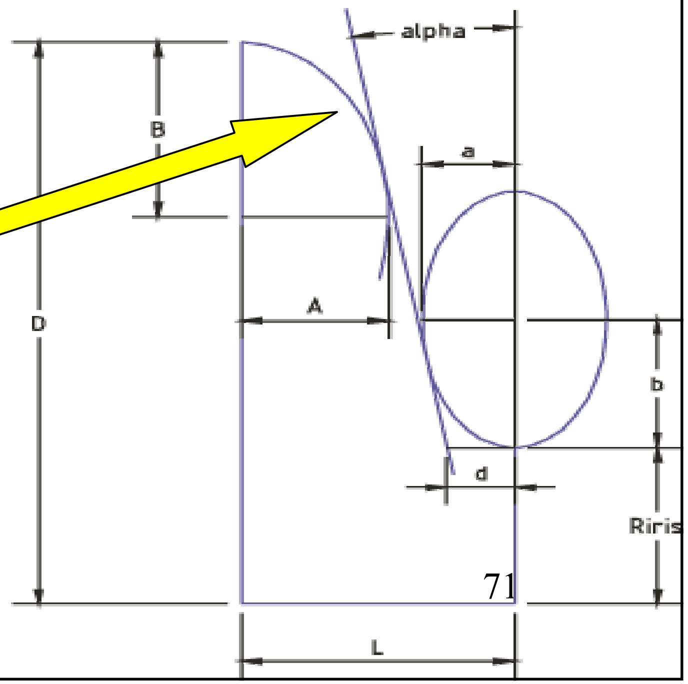

Cavity Design (single cell cavity)

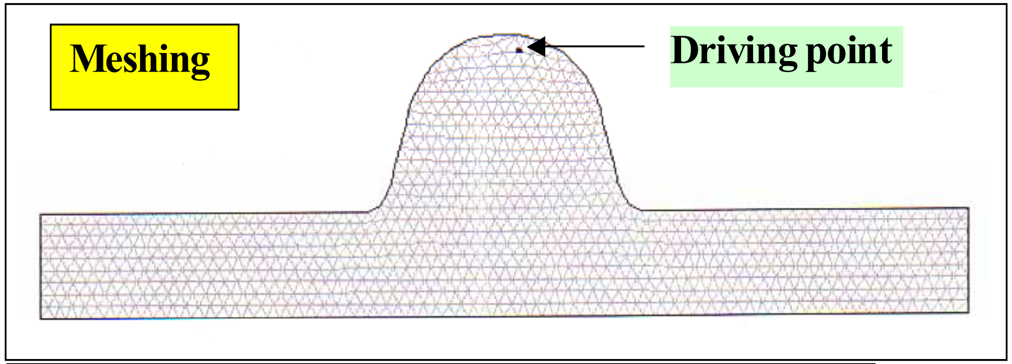

All calculated values below refer to the mesh geometry only.
Field normalization (NORM = 0): EZERO = 1.00000 MV/m
Length used for E0 normalization = 10.76000 cm
Frequency (starting value = 1300.000) = 1293.77430 MHz
Particle rest mass energy = 0.510999 MeV
Beta = 1.0000000
Normalization factor for E0 = 1.000 MV/m = 7048.913
Transit-time factor Abs(T+iS) = 0.5454664
Stored energy = 0.0038869 Joules
Using standard room-temperature copper.
Surface resistance = 9.38405 milliOhm
Normal-conductor resistivity = 1.72410 microOhm-cm
Operating temperature = 20.0000 C
Power dissipation = 1118.1551 W
Q = 28257.6 Shunt impedance = 96.230 MOhm/m
Rs*Q = 265.171 Ohm Z*T*T = 28.632 MOhm/m
r/Q = 109.024 Ohm Wake loss parameter = 0.22157 V/pC
Average magnetic field on the outer wall = 1729.9 A/m, 1.40411 W/cm^2
Maximum H (at Z,R = 3.32643,8.55466) = 1753.44 A/m, 1.44258 W/cm^2
Maximum E (at Z,R = 4.75232,4.24425) = 0.946176 MV/m, 0.02953 Kilp.
Ratio of peak fields Bmax/Emax = 2.3288 mT/(MV/m)
Peak-to-average ratio Emax/E0 = 0.9462

Superfish

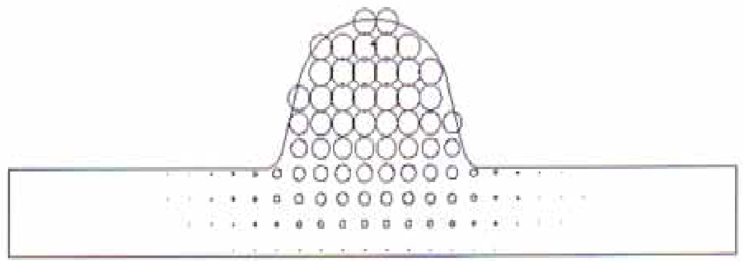

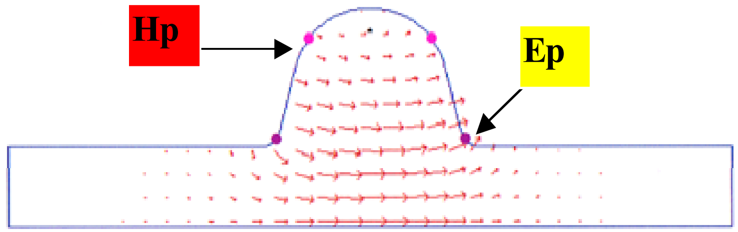

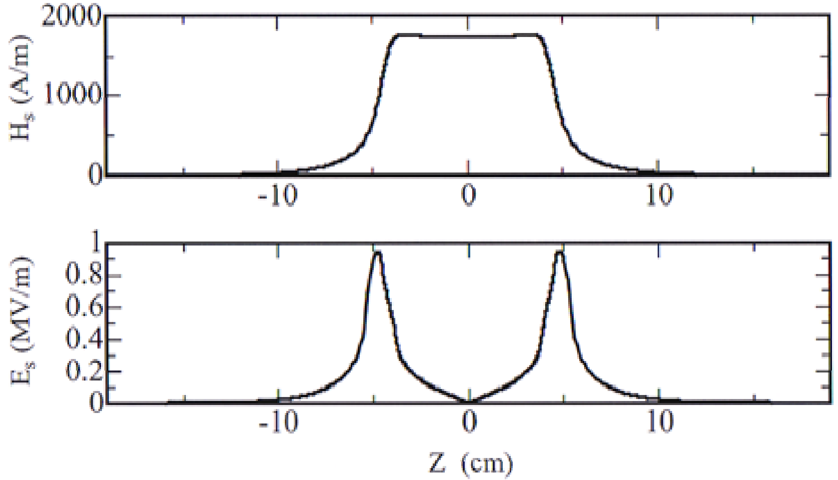

Exercise VI.

Superfish outputs

f_0=1293.77430MHz
Ploss=118.1551W
RsQ=265.171 Ω
Qo=28257.6
(Rsh/Q)=109.24 Ω
Hp=1753.44 A/m
Ep=0.946176 MV/m

Calculate the following cavity RF parameters from the Superfish outputs.

Rsh [Ω] =

Accelerating Voltage V [MV]=

RF wave length λ[m] =

Gradient Eacc = V/L_{eff}[MV/m]= ,defined as $L_{eff} = \lambda/2$

Hp/Eacc[Oe/(MV/m)] = , use 1A/m= $4\pi 10^{-3}$ Oe

Ep/Eacc =

Eacc [MV/m] = $Z \cdot \sqrt{P_{loss} \cdot Q_O}$, Z=

Geometrical factor Γ [Ω] =

High Gradient Shapes

Cavity shape designs with low Hp/Eacc

from J.Sekutowicz lecture Note

TTF: TESLA shape
Reentrant (RE): Cornell Univ.
Low Loss(LL): JLAB/DESY
Ichiro-Single(IS): KEK

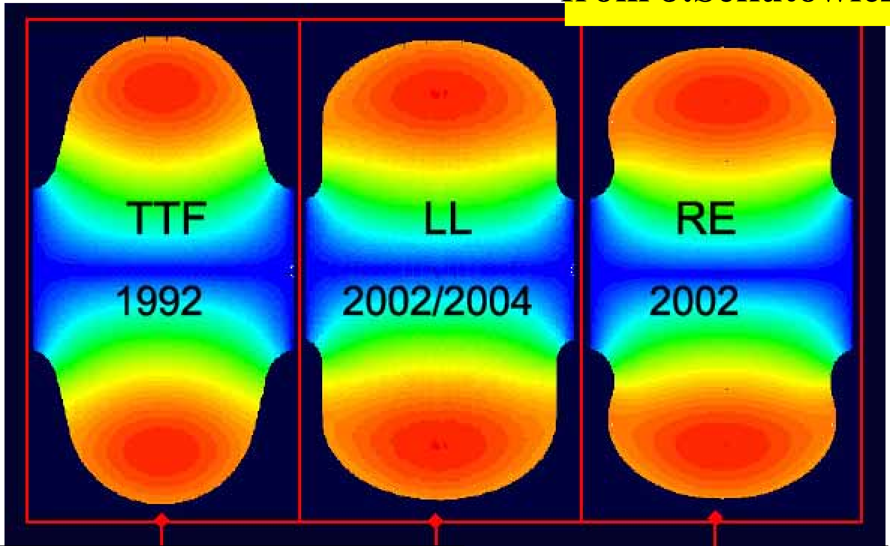

	TESLA	LL	RE	IS
Diameter [mm]	**70**	**60**	**66**	**61**
Ep/Eacc	**2.0**	**2.36**	**2.21**	**2.02**
Hp/Eacc [Oe/MV/m]	**42.6**	**36.1**	**37.6**	**35.6**
R/Q [W]	**113.8**	**133.7**	**126.8**	**138**
G[W]	**271**	**284**	**277**	**285**
Eacc max	**41.1**	**48.5**	**46.5**	**49.2**

Eacc vs. Year

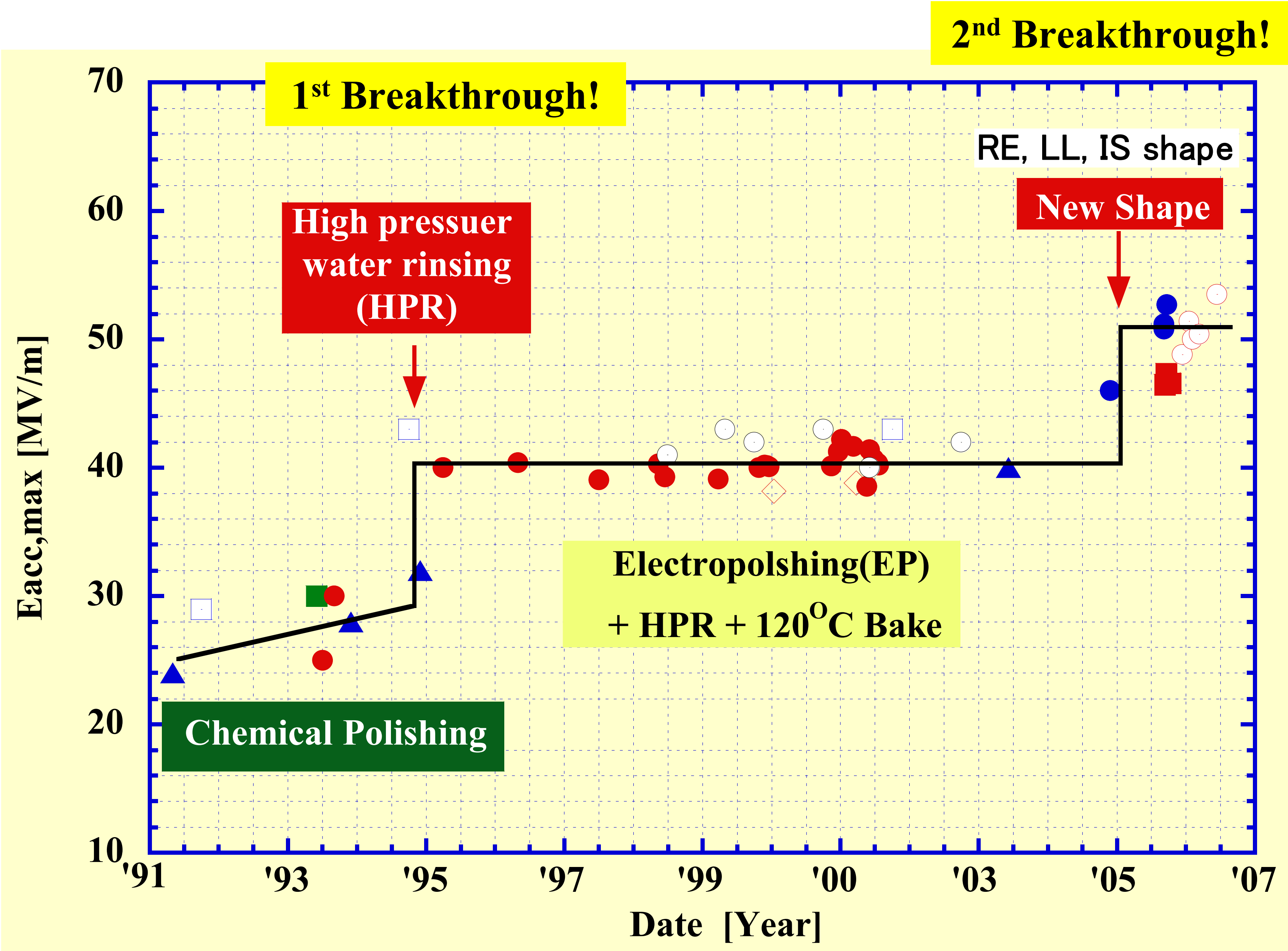

2nd Breakthrough!
1st Breakthrough!
RE, LL, IS shape
New Shape
High pressuer water rinsing (HPR)
Electropolshing(EP) + HPR + 120OC Bake
Chemical Polishing
70
60
50
40
30
20
10
'91
'93
'95
'97
'99
'00
'03
'05
'07
Eacc,max [MV/m]
Date [Year]

3.3 Criteria for Multi-cell Structures

Pros and cons for a multi-cell structure

- *Cost of accelerators is lower (less auxiliaries: LHe vessels, tuners, fundamental power couplers, control electronics)*
- *Higher real-estate gradient (better fill factor)*

- *Field flatness vs. N*
- *HOM trapping vs. N*
- *Power capability of fundamental power couplers vs. N*
- *Chemical treatment and final preparation become more complicated*
- *The worst performing cell limits whole multi-cell structure*

How to decide the number of cells

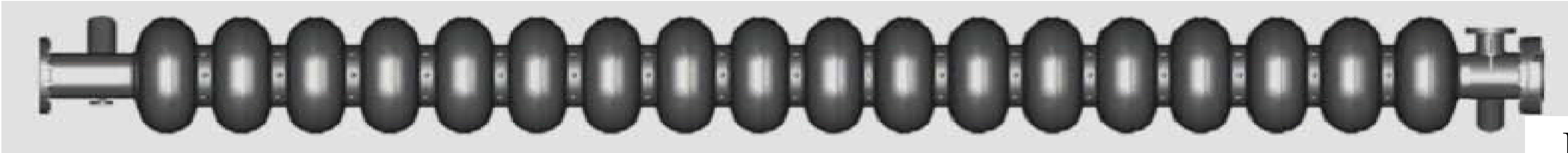

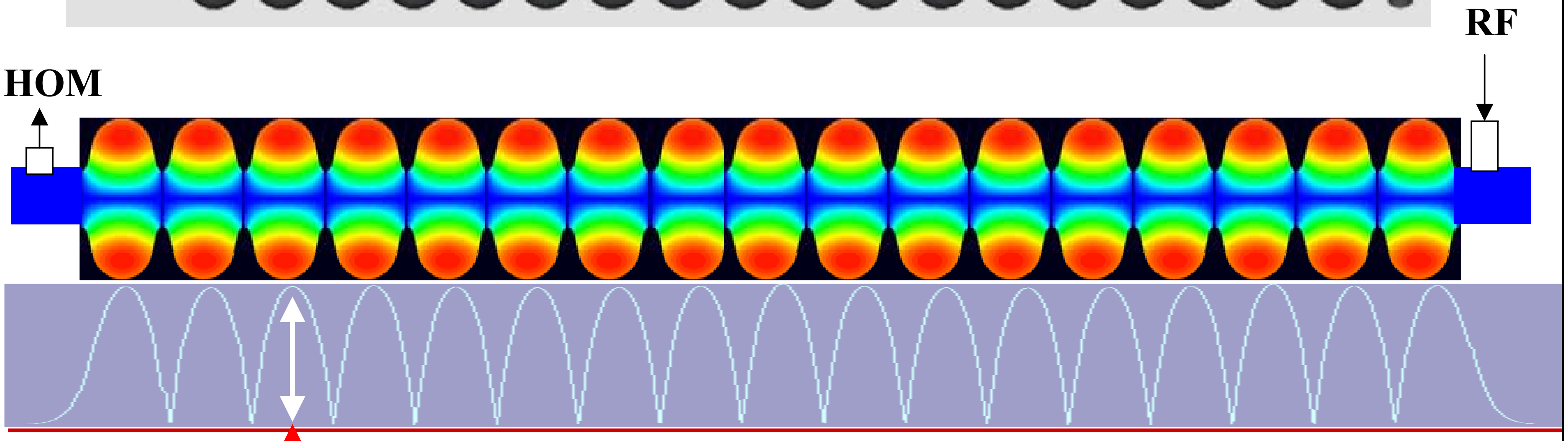

$$\frac{\Delta A_i}{A_i} = a_{ff}\,\frac{\Delta f_i}{f_i} = \frac{N^2}{k_{cc}}\cdot\frac{\Delta f_i}{f_i}$$

Beam pipe has no acceleration beam.
BP reduce the efficiency.
Multi-cell is more efficient.

N: number of cells

Field flatness factor : $a_{ff} = \dfrac{N^2}{k_{cc}}$

Cell to cell coupling : $k_{cc} = 2\cdot\dfrac{f_\pi - f_0}{f_\pi + f_0}$

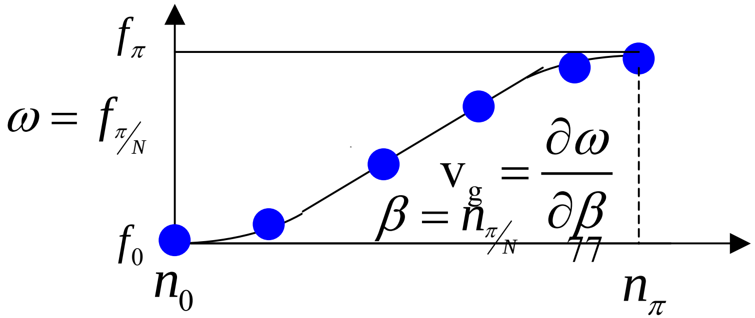

HOM trapping vs. N

No fields at HOM couplers positions, which are always placed at end beam tubes

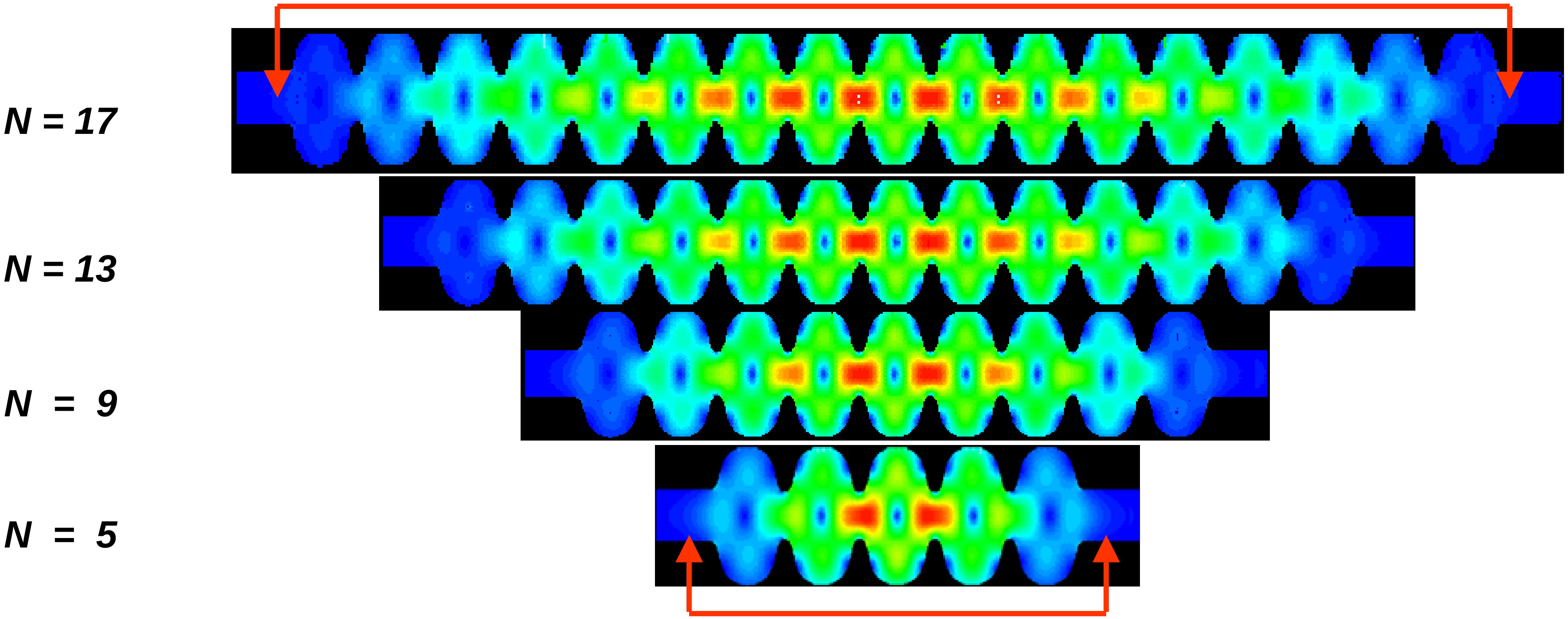

e-m fields at HOM couplers positions

Smaller number of cells is easy to take out HOMs.

RF Structure Simulation

Currently full 3D analysis is possible using cords Omega or ANALIS, example SLAC, KEK

Element Model (Mesh)

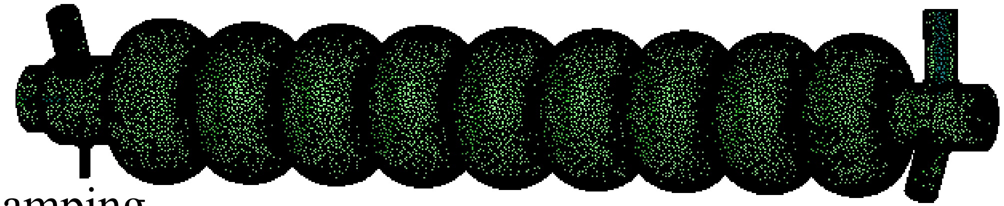

Simulation of Higher Order Mode Damping

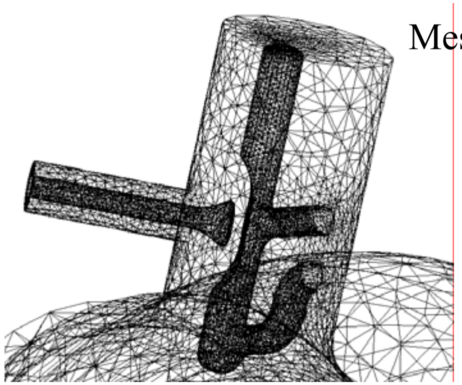

Mesh of HOM Damper

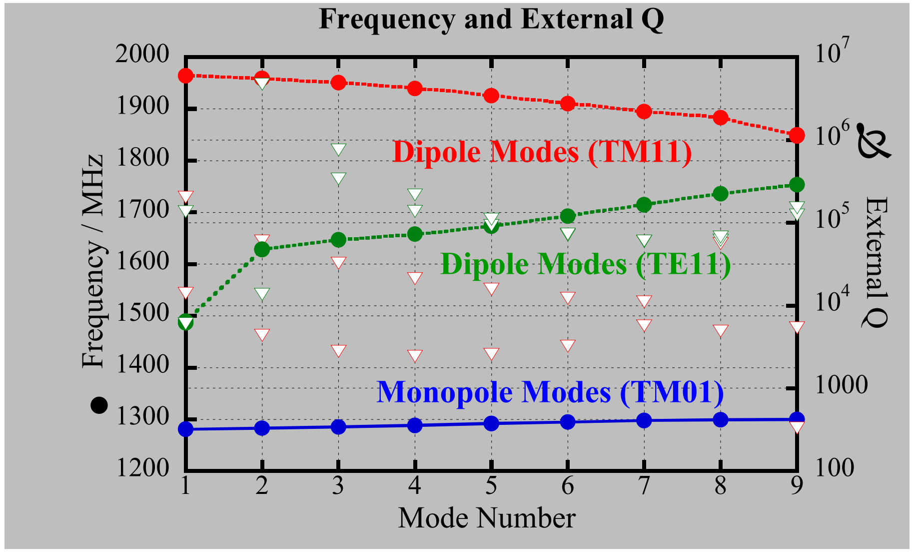

Analysis of Wall Loss in Vertical Testing

Measured Low Q of 1.1×10^{10} at 21 MV/m for 38 W ----- Reproduced by Simulation

Magnetic Field Contour

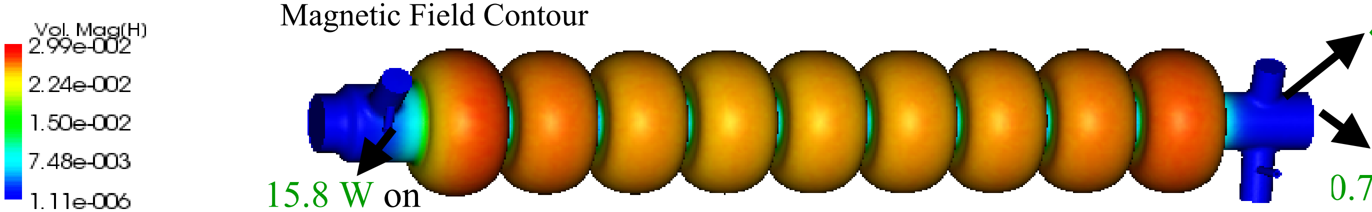

«1 W

15.8 W on SUS 316 Wall

0.7 W on SUS 316L Wall

21.8 W on Niobium Walls

Note

Pass-band modes of TM010 in a 9-cell cavity

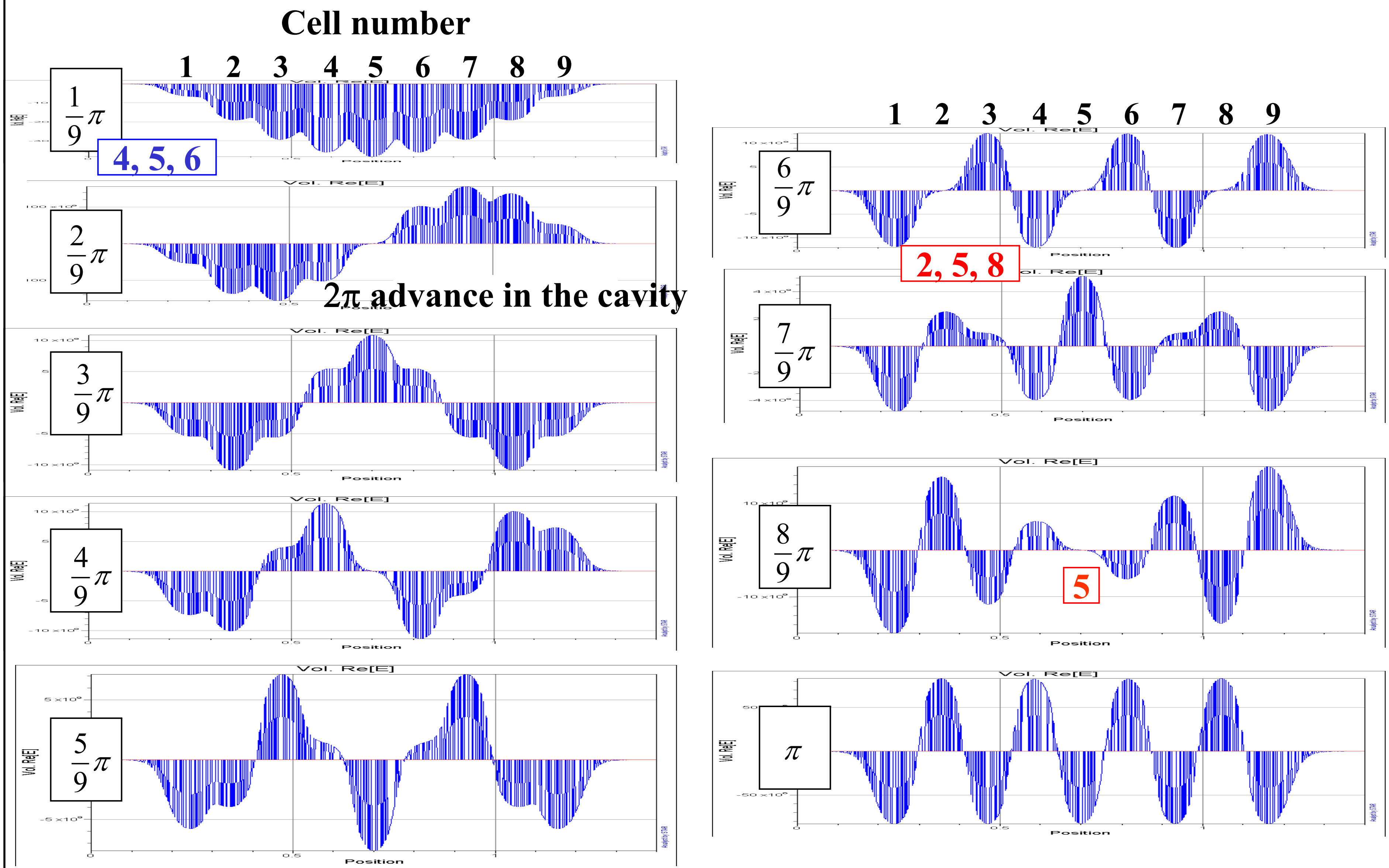

ILC Cavity

17000 cavities

BCD Cavity shape : TESLA

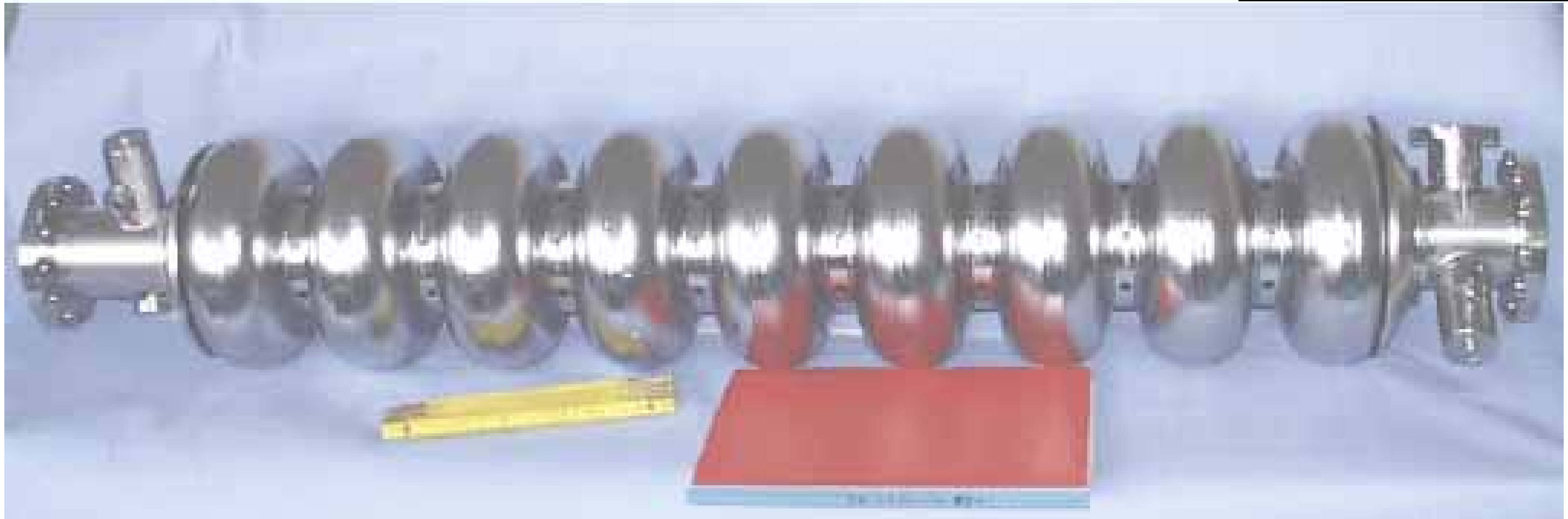

ACD cavity shape : LL

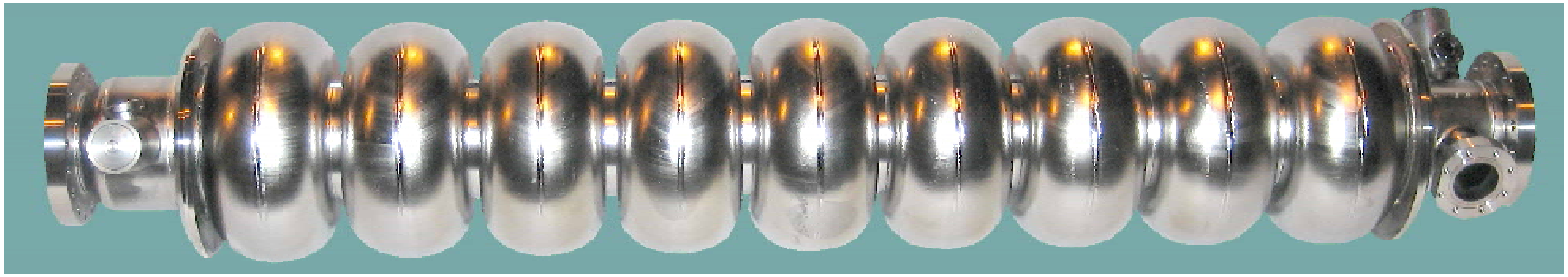

4. HOM Issues

4.1 HOM
4.2 HOM Coupler

4.1 HOM (Higher Order Mode)

The beam will excite HOM modes,
if it passes off beam axis of the cavity.

J.Sekutwitz's Slide

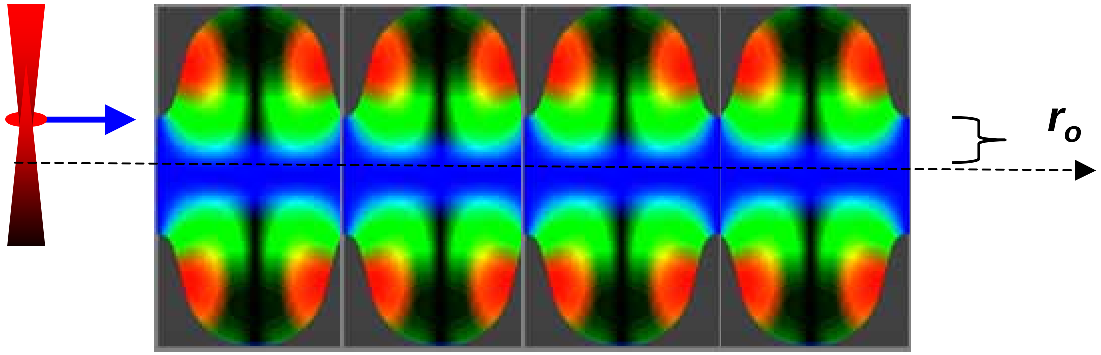

*The amount of induced energy by charge **q** is:*

$$\Delta U_q = k_{/}\cdot q^2 \quad \text{for monopole modes (max. on axis)}$$

$$\Delta U_q = k_{\perp}\cdot q^2 \quad \text{for non monopole modes (off axis)}$$

where $k_{/}$ and $k_{\perp}(r)$ are loss factors for the monopole and transverse modes respectively.

The induced E-H field is a superposition of cavity eigenmodes having the component of the electric field along the trajectory.

HOM Problem

J.Sekutwitz's Slide

Two kind of phenomena can limit performance of a machine due to the beam induced HOM power:

- *Beam Instabilities and/or dilution of emittance*
- *Additional cryogenic power and/or overheating of HOM couplers output lines*

Beam instabilities and/or dilution of emittance

Transverse modes (dipoles) causing emittance growth+ monopoles causing energy spread
This is mainly problem

***in linacs**: TESLA or ILC, CEBAF, European XFEL, linacs driving FELs.*

Additional cryogenic power and/or overheating of HOM couplers output lines

Monopoles having high impedance on axis are excited by the beam and store energy which must be coupled out of cavities, since it causes additional cryogenic load, and induces energy spread.
This is mainly problem

***in high beam current** machines: B-Factories, Synchrotrons, Electron cooling.*

HOM modes has to be taken out from the cavity through HOM coupler.

Spectra of accelerated beams, which bunches are shorter than 1 mm, extend to hundreds of GHz.

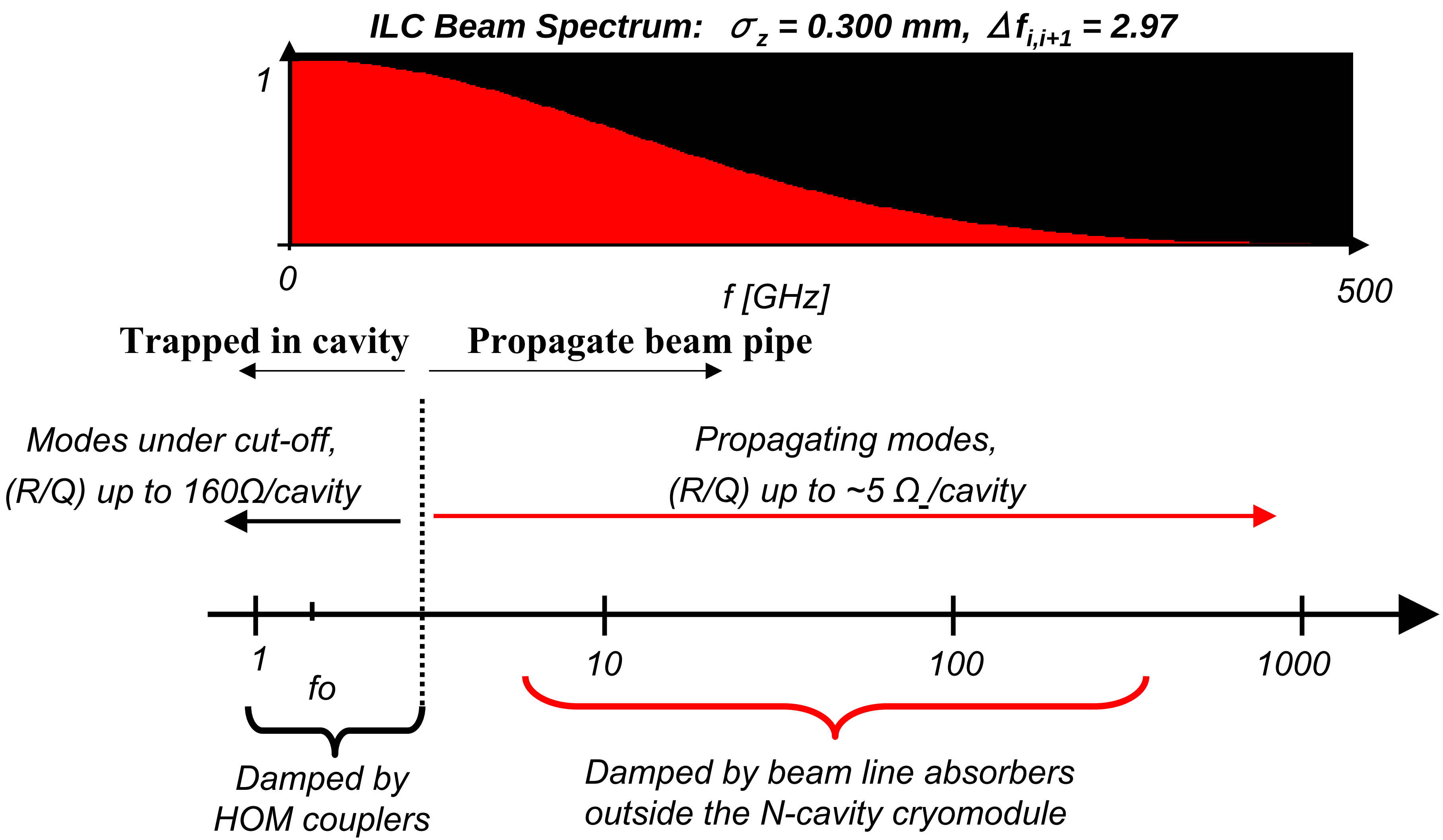

Damping the HOM with higher frequency over than Cut-off frequency

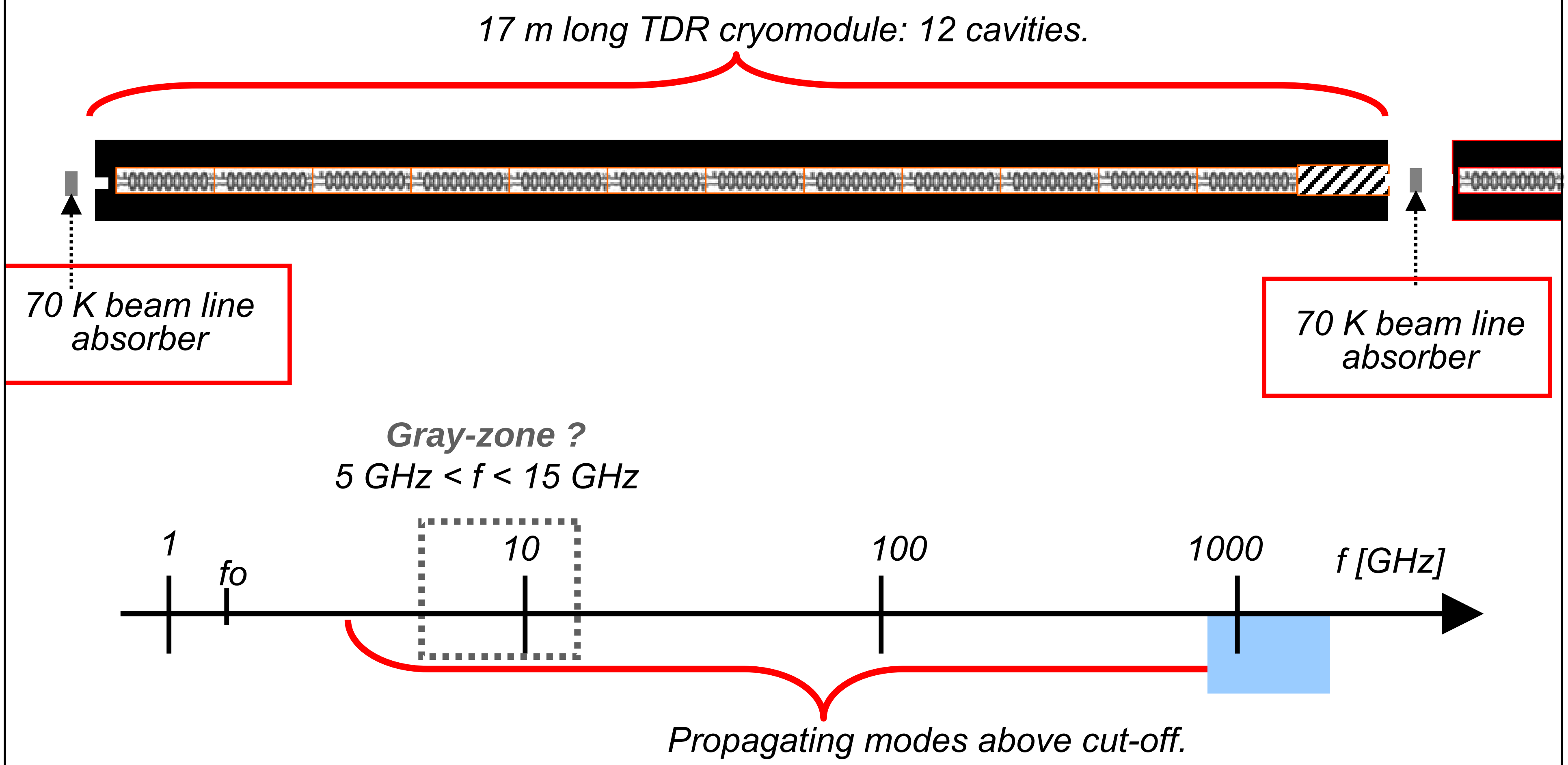

Attention to Trapped modes damping through HOM coupler

HOM couplers limit RF-performance of sc cavities when they are placed on cells

no E-H fields at HOM couplers positions, which are always placed at end beam tubes

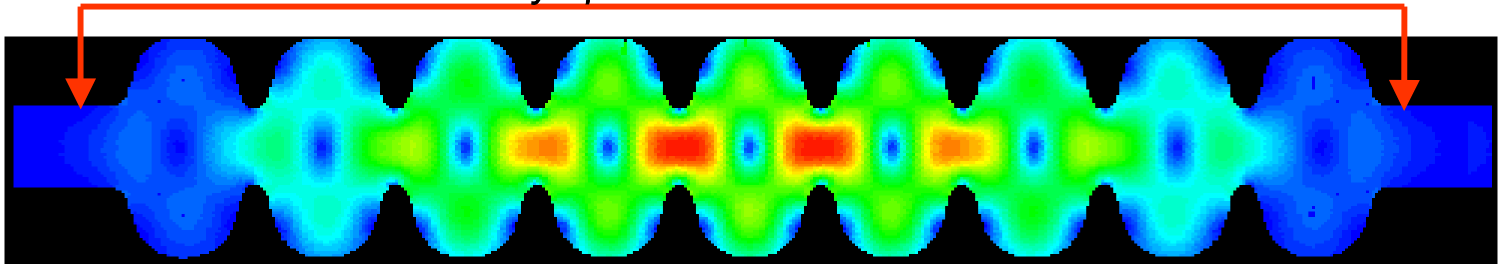

The HOM trapping mechanism is similar to the FM field profile unflatness mechanism:

- *weak coupling HOM cell-to-cell,* $\boldsymbol{k_{cc,HOM}}$
- *difference in HOM frequency of end-cell and inner-cell*

f = 2385 MHz

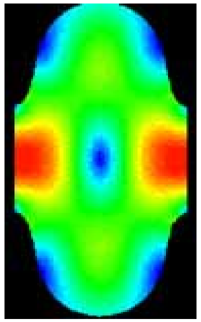

That is why they hardly resonate together

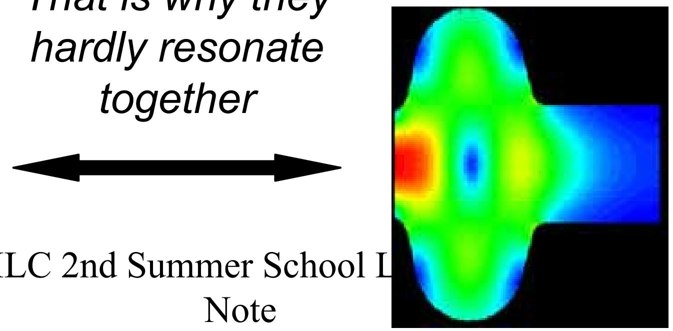

f = 2415 MHz

4.2 HOM Coupler

The TESLA –like HOM couplers are nowadays designed in frequency range: 0.8-3.9 GHz

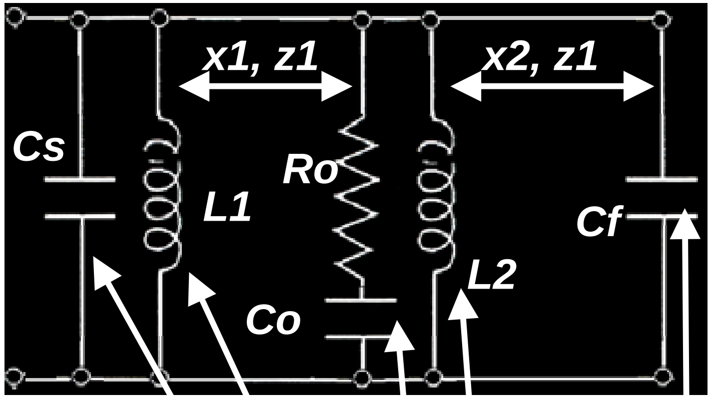

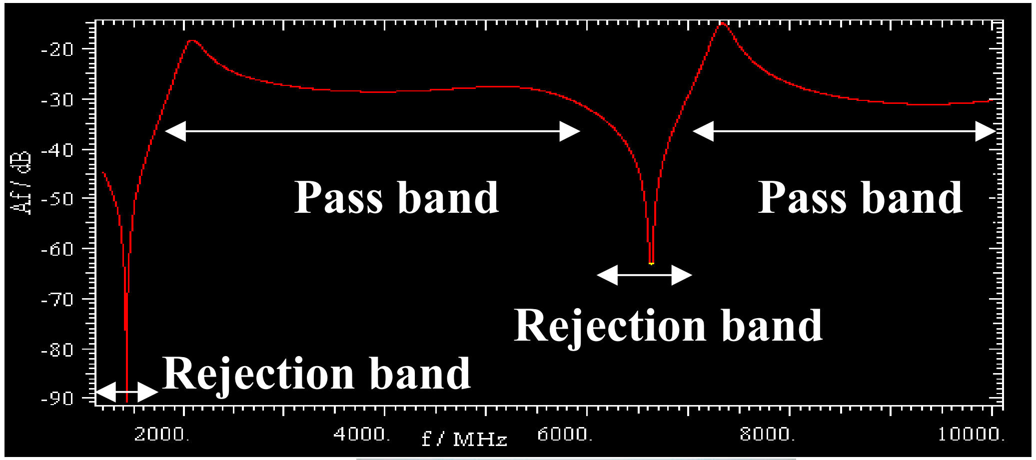

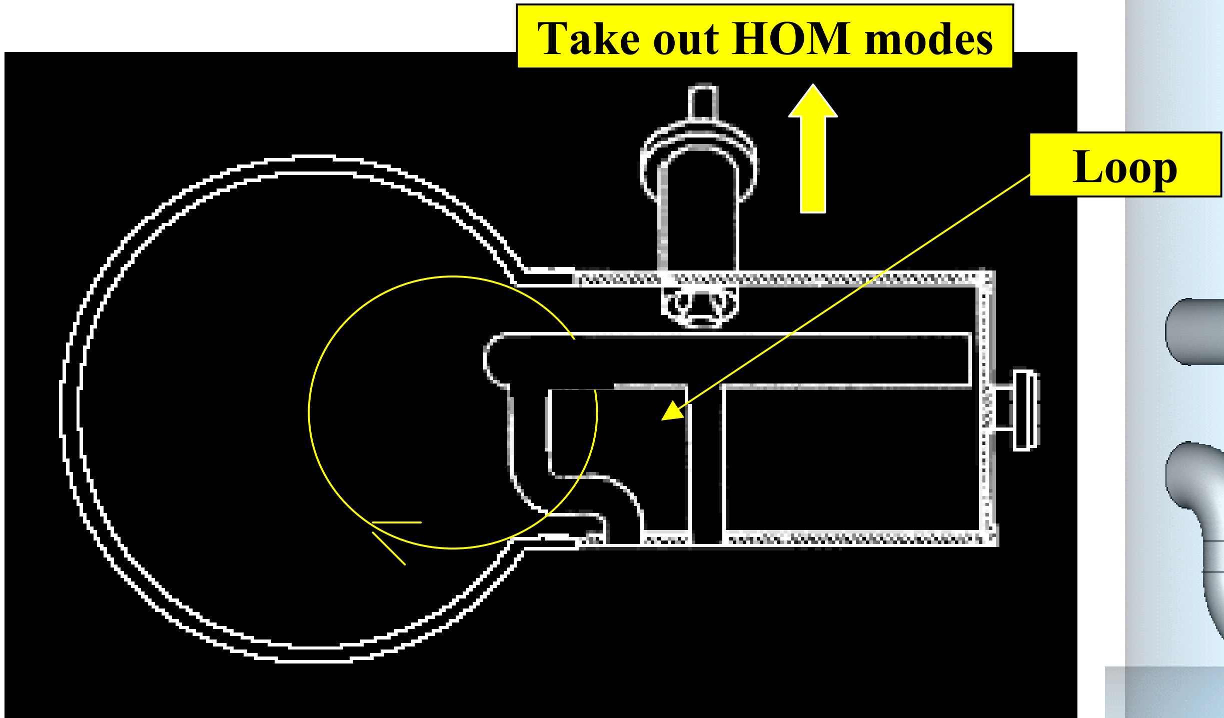

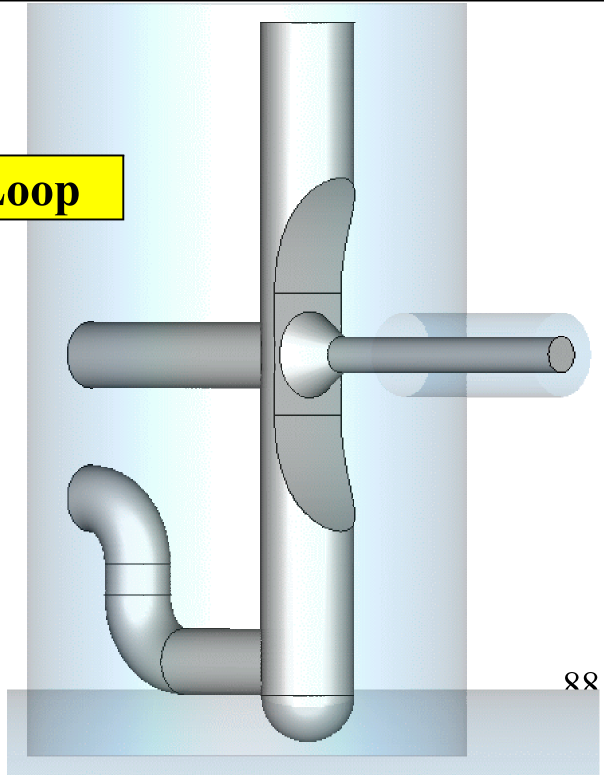

Comparison in Damping Performance of HOMs

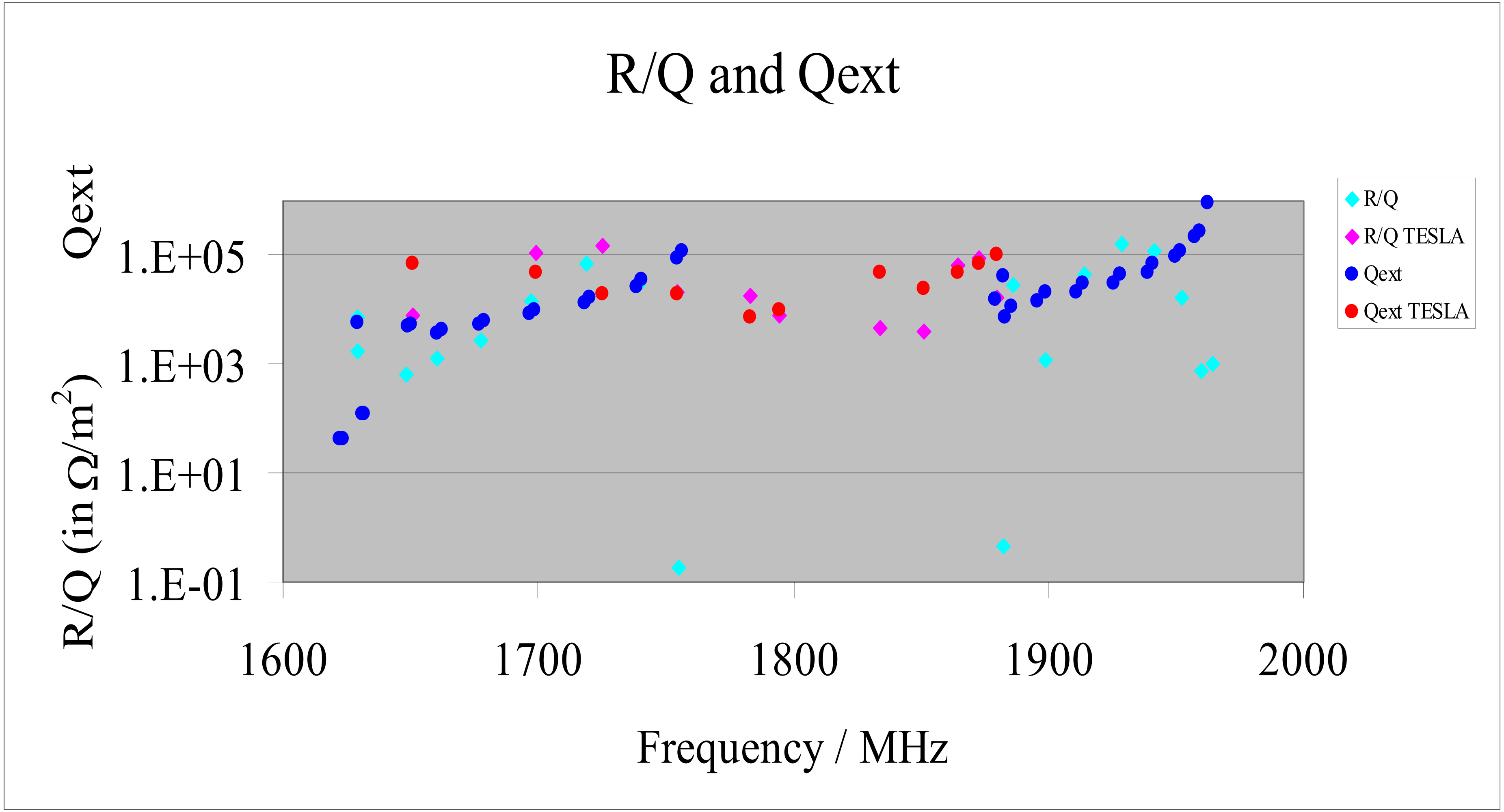

Suppression of Multipacting in HOM Cylinder by better HOM coupler design

By Y.Morozumi @ KEK

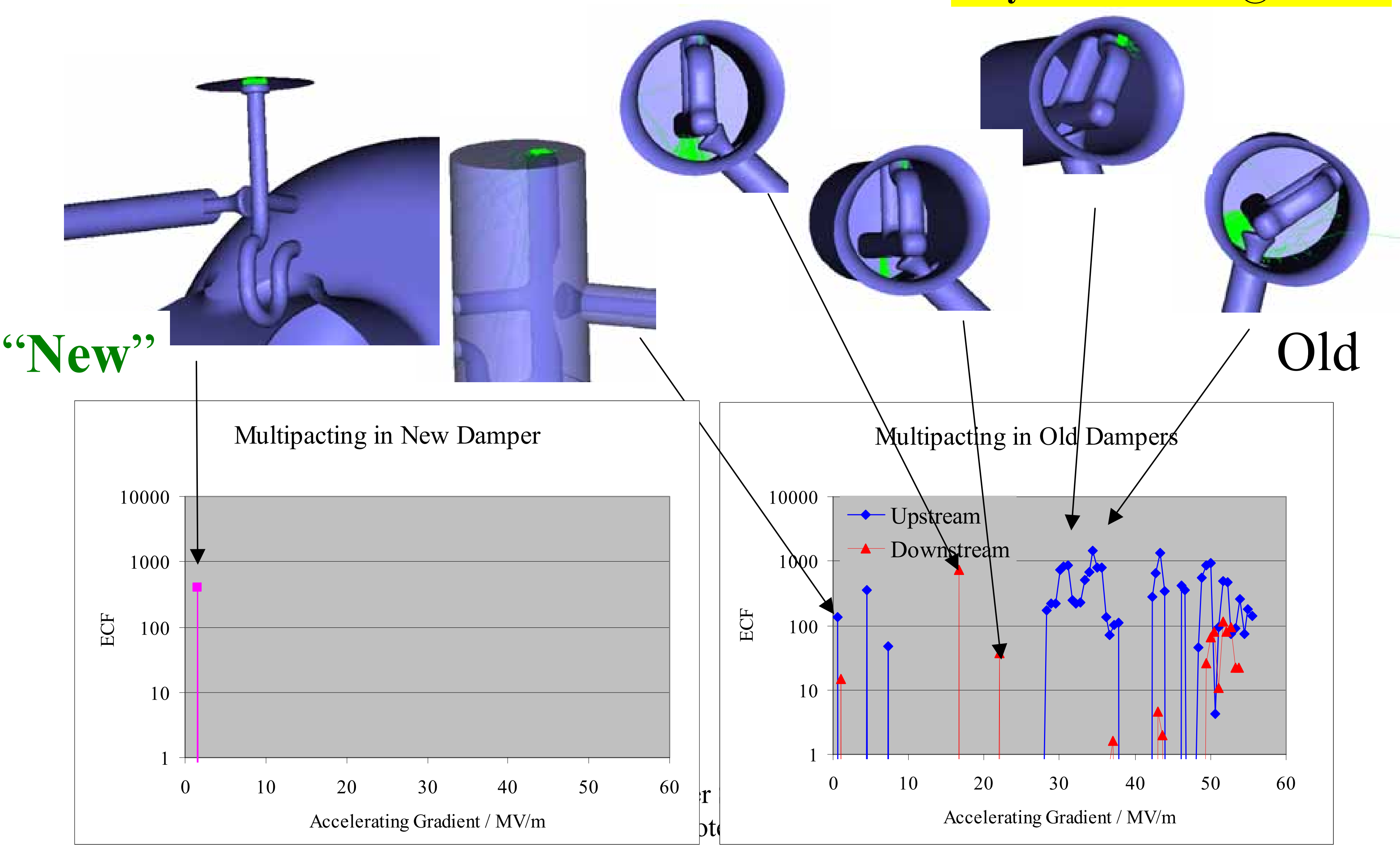

5. Lorentz Detuning

Frequency detuned by Lorentz force

Frequency Detuning during RF Pulse

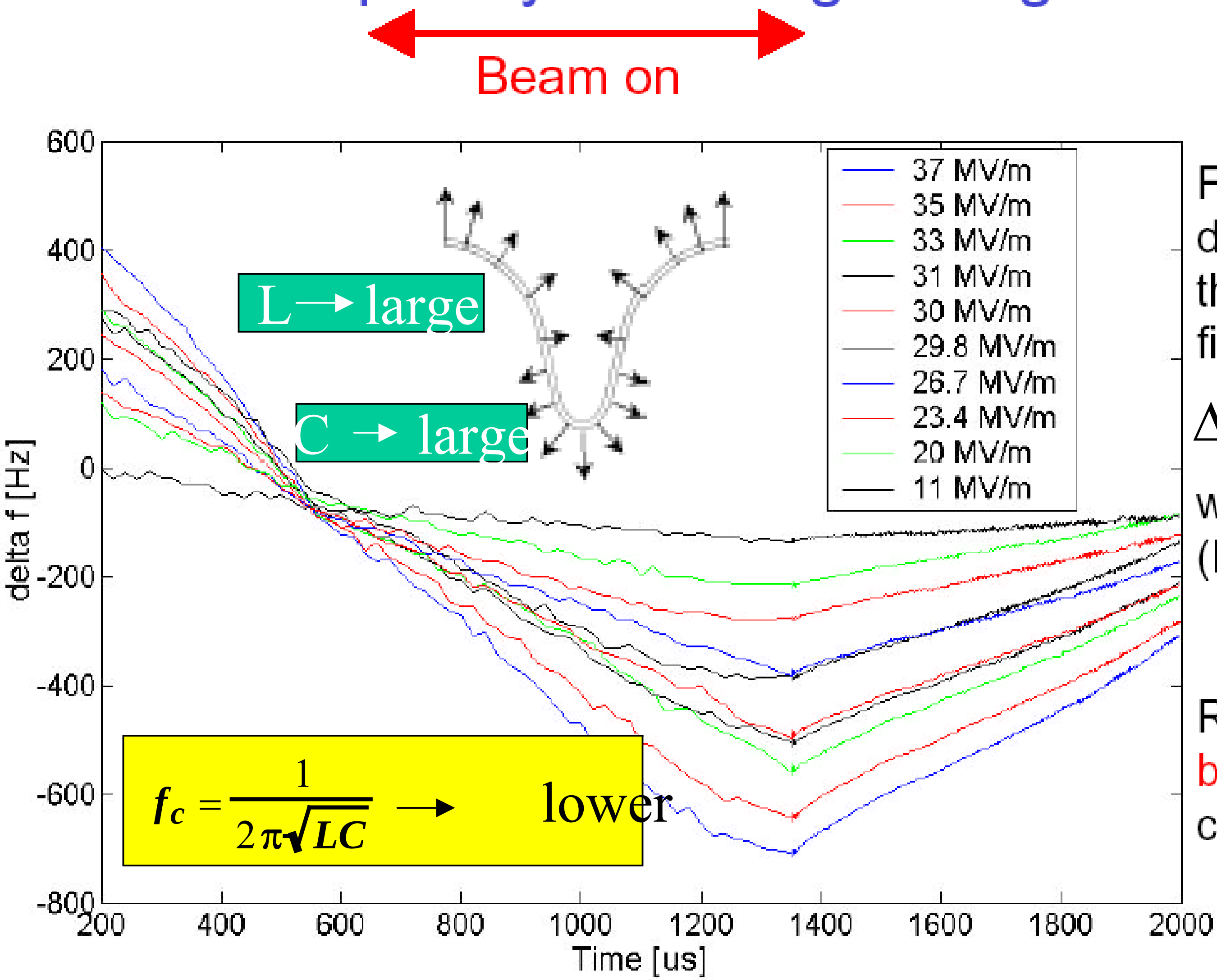

Frequency detuning due Lorentz forces of the electromagnetic field in the cavities:

$\Delta f = -K \cdot E_{acc}^2$

where K " 1 Hz / $(MV/m)^2$

Remember: Cavity bandwidth with main coupler is " 300 Hz

Frequency and Phase Control by Piezo tuner

Lorentz detuning can be compensated with Piezo tuner control

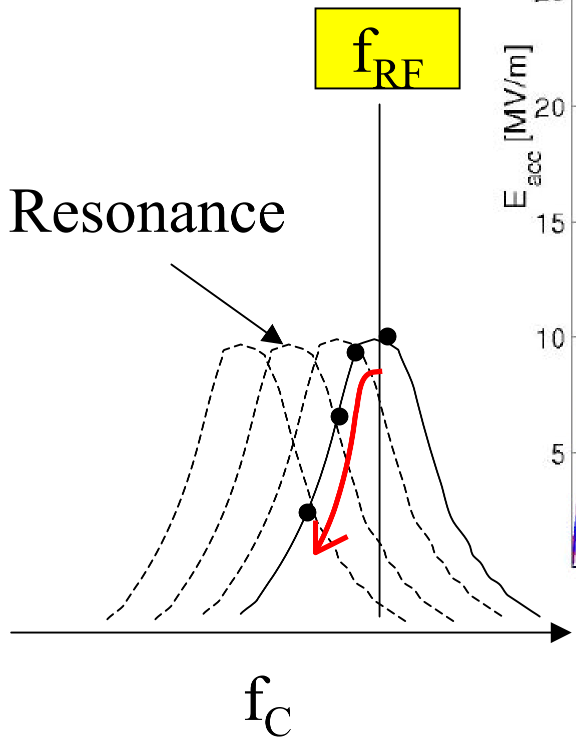

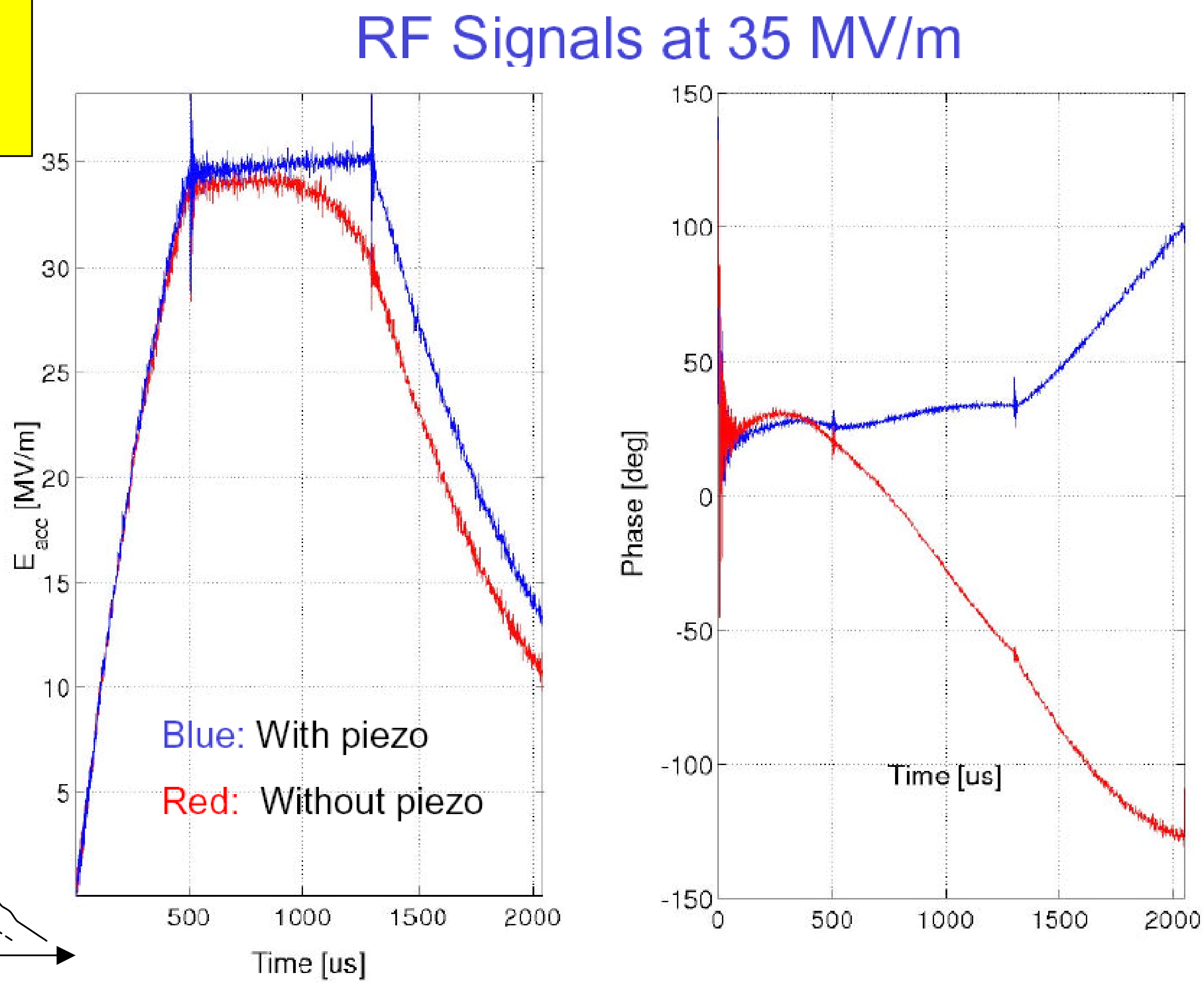

Tow components of Lorentz Deformation

Noguchi's slide in the 1st ILC school

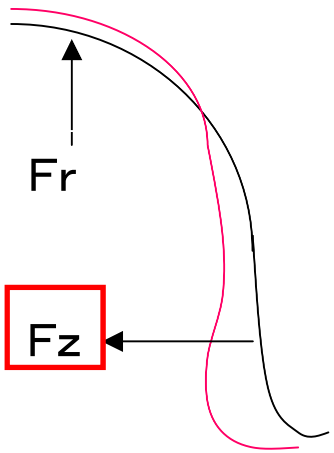

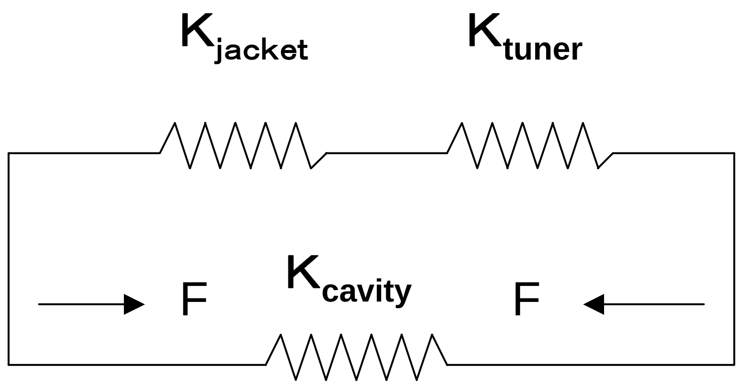

$$\Delta f = \sum_{\text{mode}} a_k \, \delta f_k \approx \sum_{\Delta l = 0} a_k \, \delta f_k + \frac{df}{dl}\frac{dl}{dF} F$$

$$= A E_{acc}^2 + \frac{df}{dl}\frac{B E_{acc}^2}{K_S}$$

Rigid Stiffness at Jacket and Tuner are also Very important against the Lorentz Detuning.

		TESLA Blade	STF Slide Jack	STF Ball Screw
A	Hz/(MeV/m)^2	0.5	0.5	(1.2)
B	N/(MeV/m)^2	0.047	0.047	0.051
df/dl	Hz/μm	320	320	370
dF/dl	N/μm	3	3	1.8
KS	N/μm	13	80	60
Kjacket	N/μm	26	96	58
Ktuner	N/μm	26	500	1700
Δf (30MV/m)	Hz	1490	620	(1360)
Fine Tuning Stroke	μm	3.7	1	2.9

Lorentz Detuning Compensation Tuner System @ KEK

1) Use well established technology
2) Rigidity during handling
3) Wide Range Tuning Design
4) Easy Replacement
5) Less heat loss
6) Less X-ray Damage
7) Keep the possibility to move out of vacuum chamber

1), 2) → Screw Ball Tuner

3) → Mechanical resonance

4), 5), 6) → Locate both tuners around 100K shield

Coaxial screw ball tuner

NO BCD yet for ILC!

Principle of the Lorentz Detuning used mechanical resonance

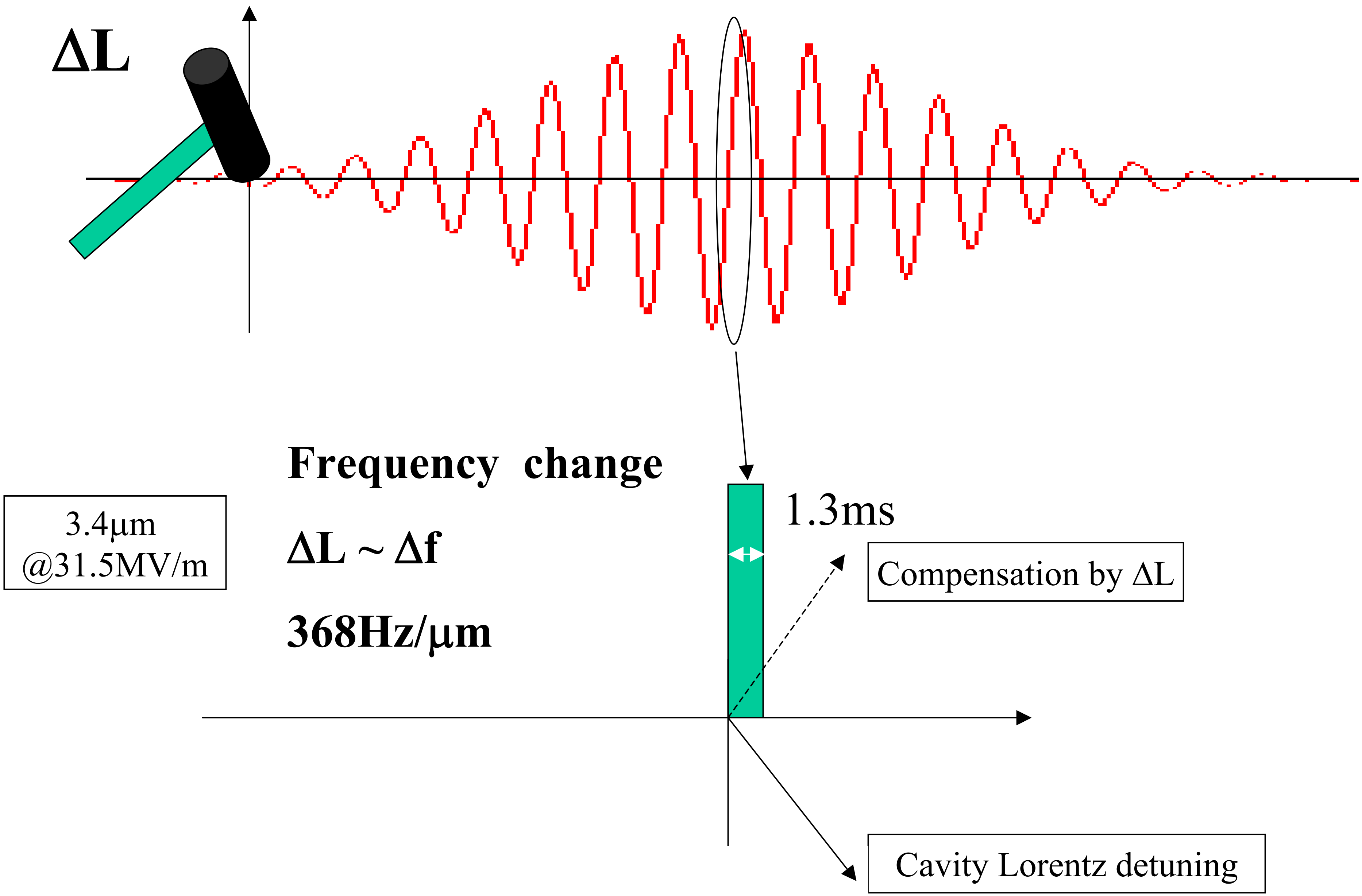

Comparison of Lorentz Force Deformation between different cell shapes

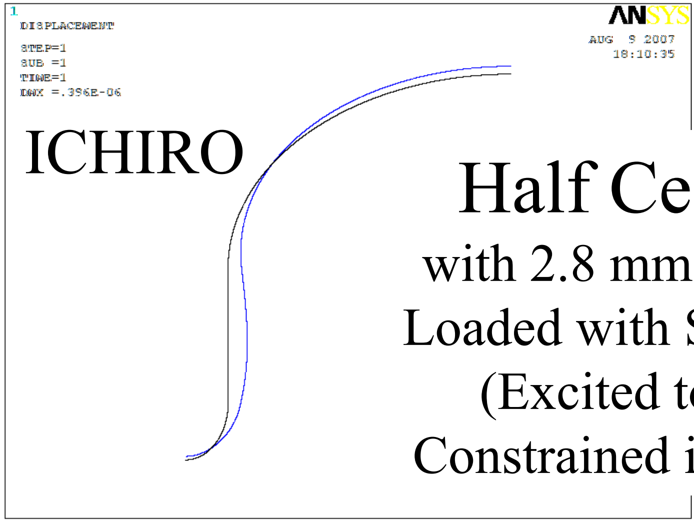

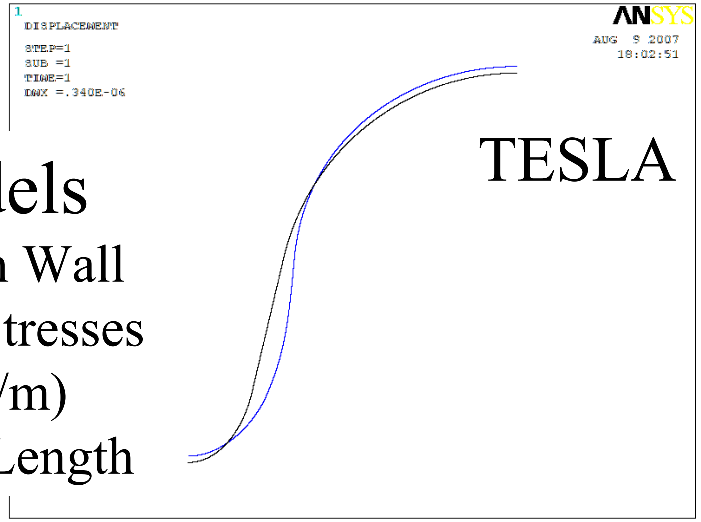

Half Cell Models

with 2.8 mm Niobium Wall

Loaded with Surface Stresses

(Excited to 40 MV/m)

Constrained in Axial Length

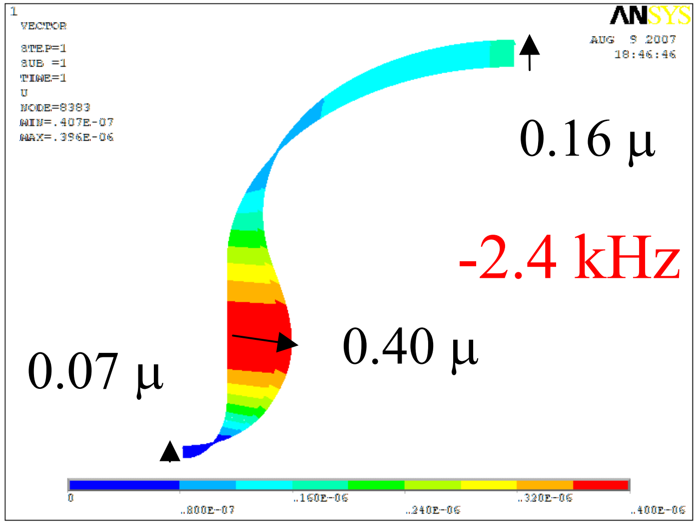

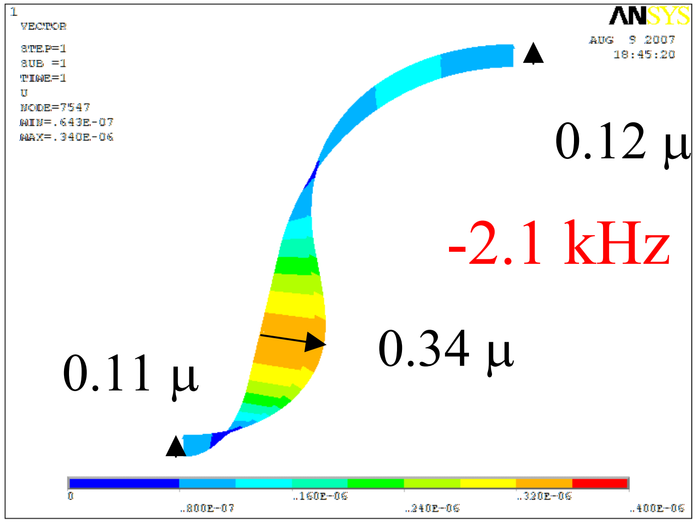

Optimization of Stiffener Location against Lorentz Detuning

Eacc=38MV/m

by H.Yamaoka

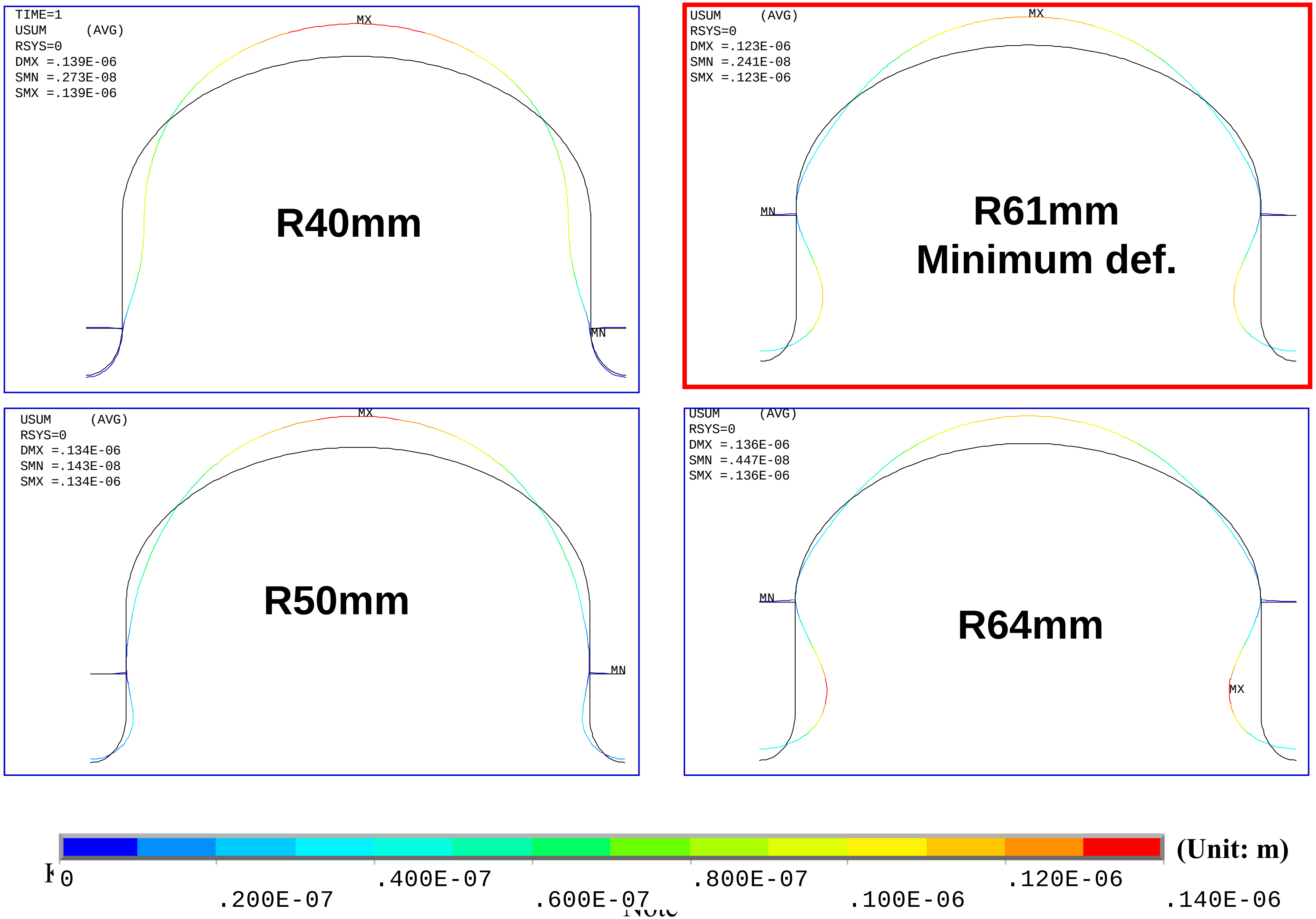

Calculation of longitudinal mechanical resonance w/wo He vessel by H.Yamaoka

Naked Cavity | With He Vessel

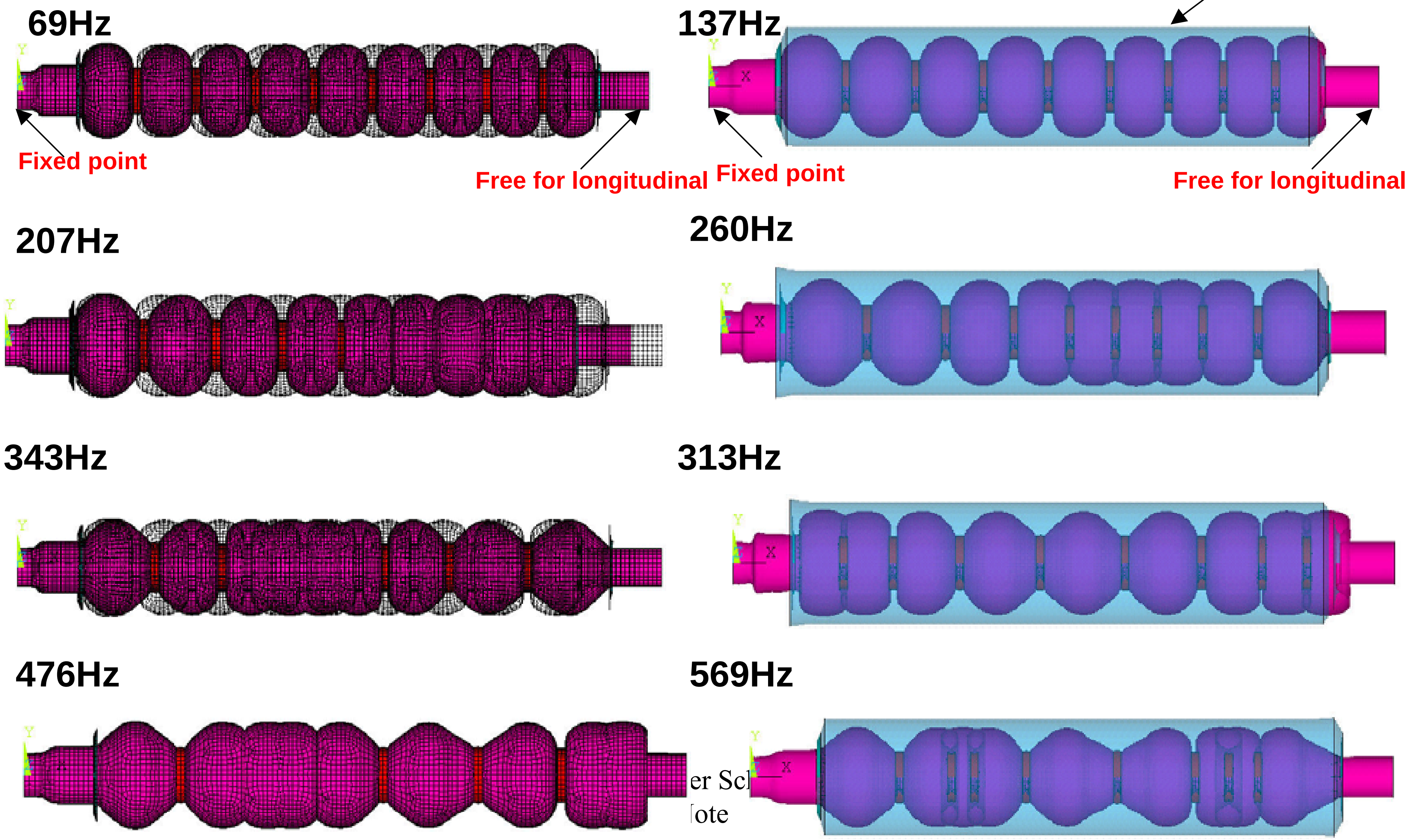

Mechanical Resonance of a multi-cell cavity

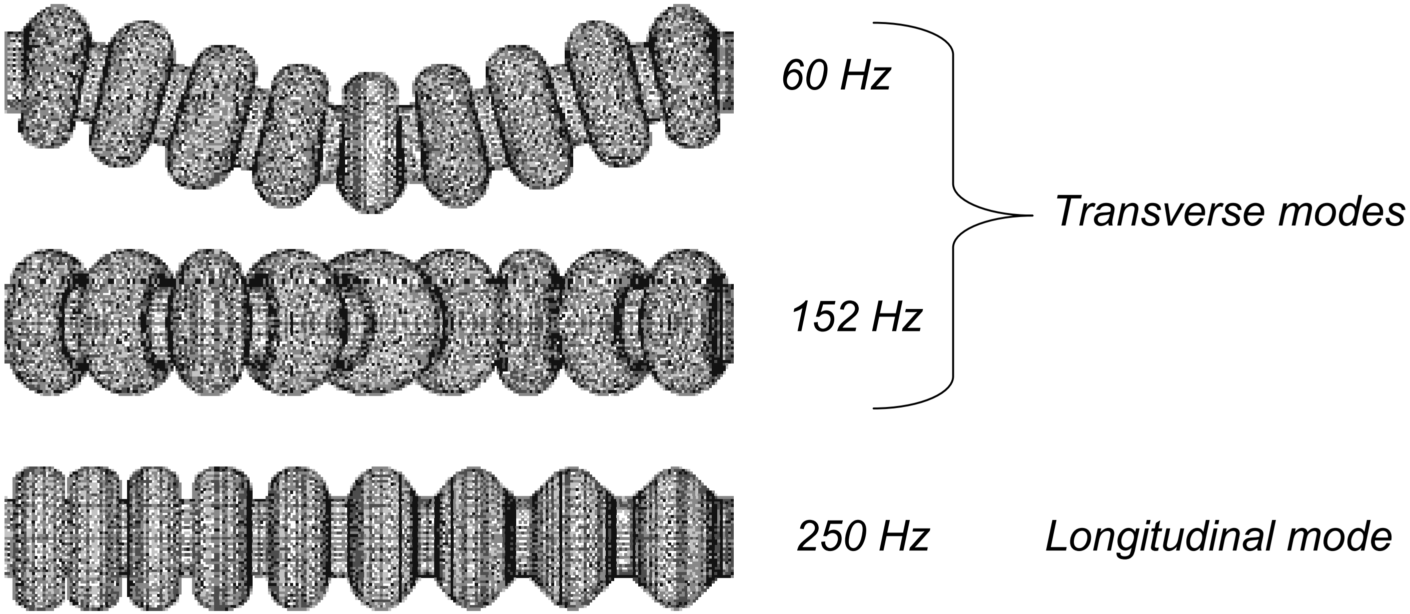

TESLA structure

The mechanical resonances modulate frequency of the accelerating mode.
Sources of their excitation: vacuum pumps, ground vibrations…

Comparison of Tuners (Now NO BCD for ILC)

Screw Ball tuner

Saclay-II

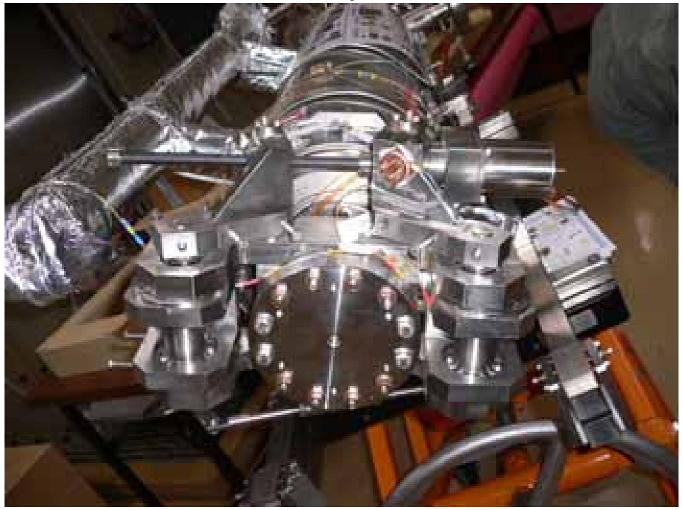

Blade Tuner

Jack tuner

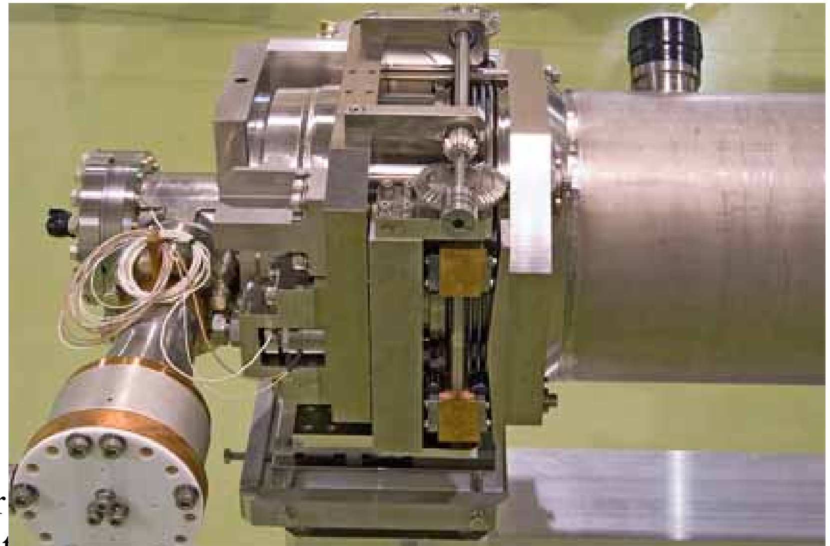

Comparison of Tuner Designs

		Screw Ball	Jack	Blade	Saclay-II
Location	Motor	80K or out of vac. vessel	Out of Vac. vessel	He vessel	Beam tube
	Piezo	80K or out of Vac. vessel	End plate	He vessel	END plate
Tuner mechanism		Coaxial ball screw	Slide Jacky	Twist	Lever type
Motor driving power		0.06gf/μm, 0.1W			
Piezo tuning range		~3000			
Resolution [Hz]	Motor	0.1			
	Piezo	0.1			
$\frac{df}{dl}$ $[\mathrm{Hz}/\mu\mathrm{m}]$		368	320		320
$\frac{dF}{dl}$ $[\mathrm{N}/\mu\mathrm{m}]$		36.4	80	13	

6. RF Input Coupler

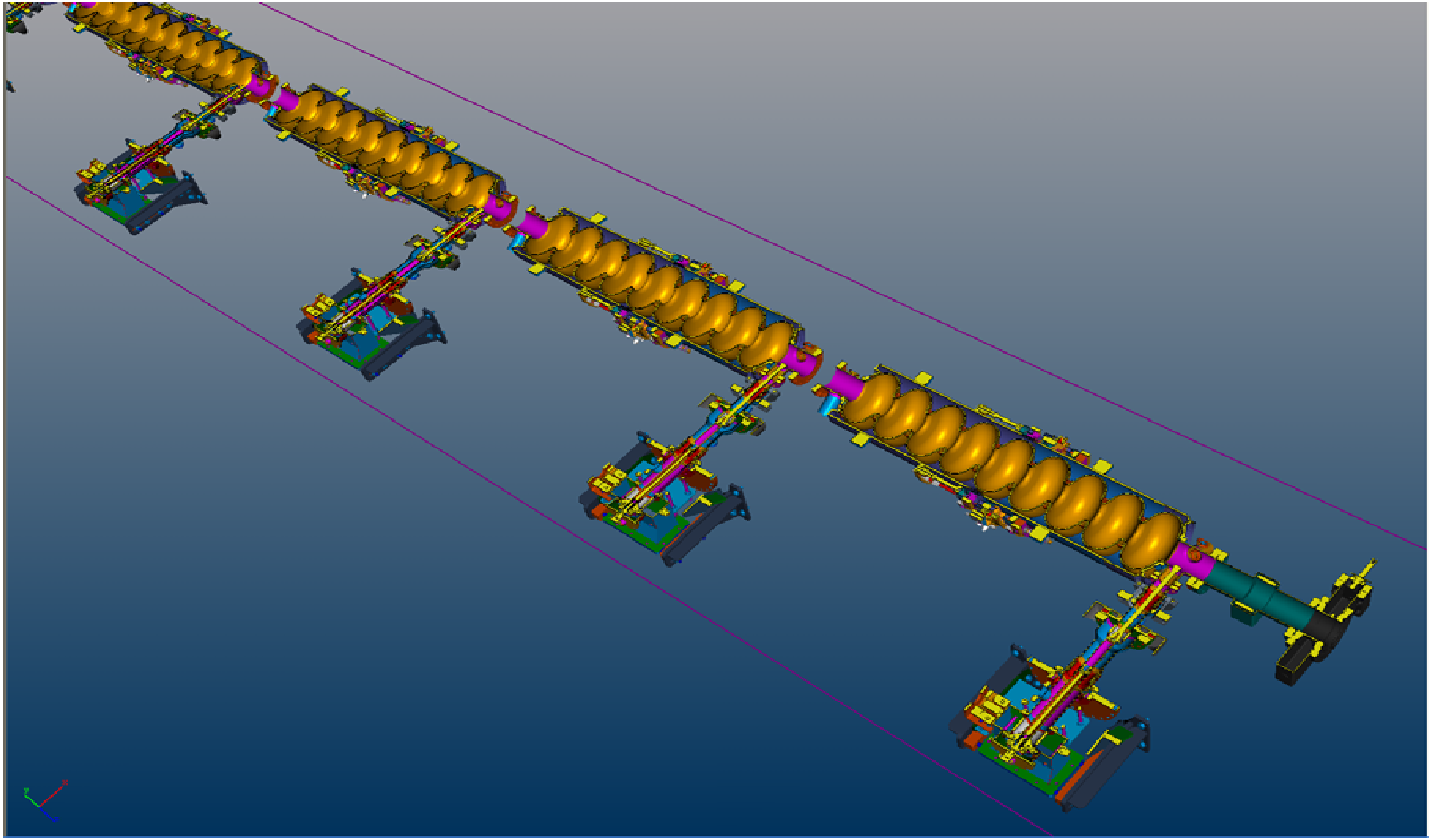

Three types developed for ILC

CC-coupler

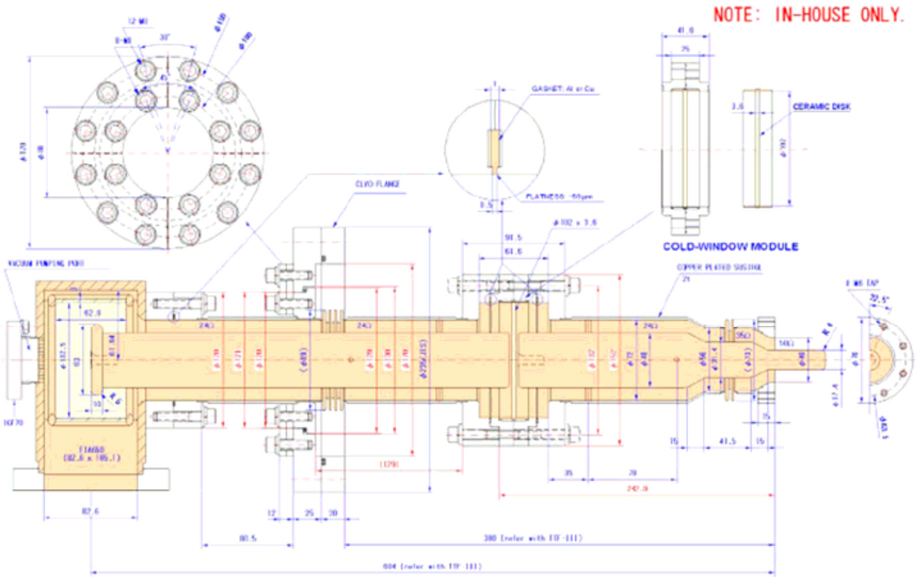

Double disk windows

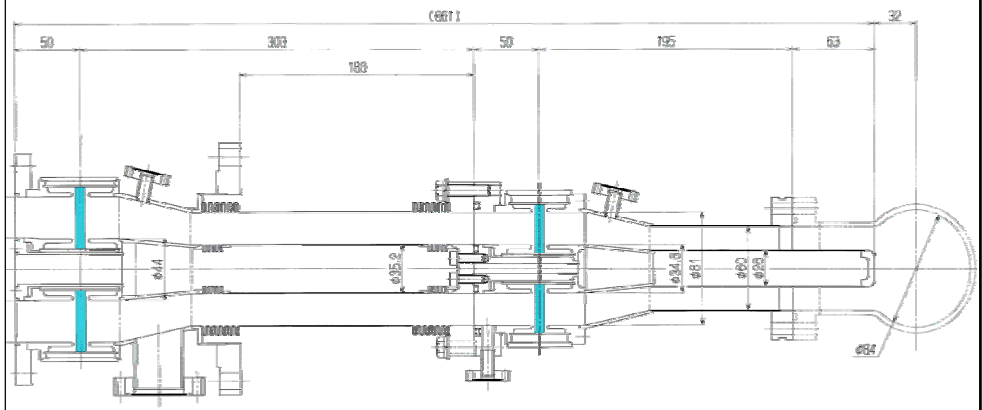

TTF-III (**BCD for ILC**)

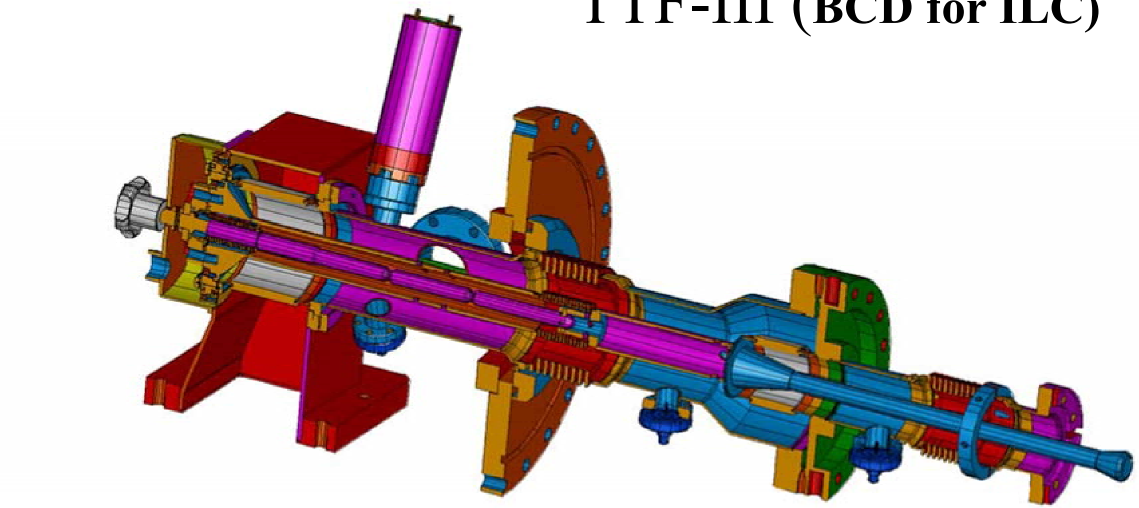

Input Coupler Designs

			CC-coupler	STF-BL	TTF-III
Designed RF Power [kW]			500 (2000)	350(1300)	250(1000)
Pulse width [ms]			1.3 (1.5)	1.3(1.5)	1.3
Repetition [Hz]			5	5	10
Average rf power [kW]			3.25	2.3	3.2
RF processing time [hr]			16	50	20
Thermal Loss [W]	80K	Static	1.24	5	6
		Dynamic	1.5	3	3
	5K	Static	0.54	1.1	0.5
		Dynamic	2.0	0.2	0.1
	2K	Static	1.8e-4	0.05	0.06
		Dynamic	0.18	0.03	negligible

Can be reduced the dynamic loss at 5K and 2K in CC-coupler by using higher RRR cooper material, for example RRR=40.

Input Coupler Design @ KEK

By Matsumoto and Kazakov @ KEK

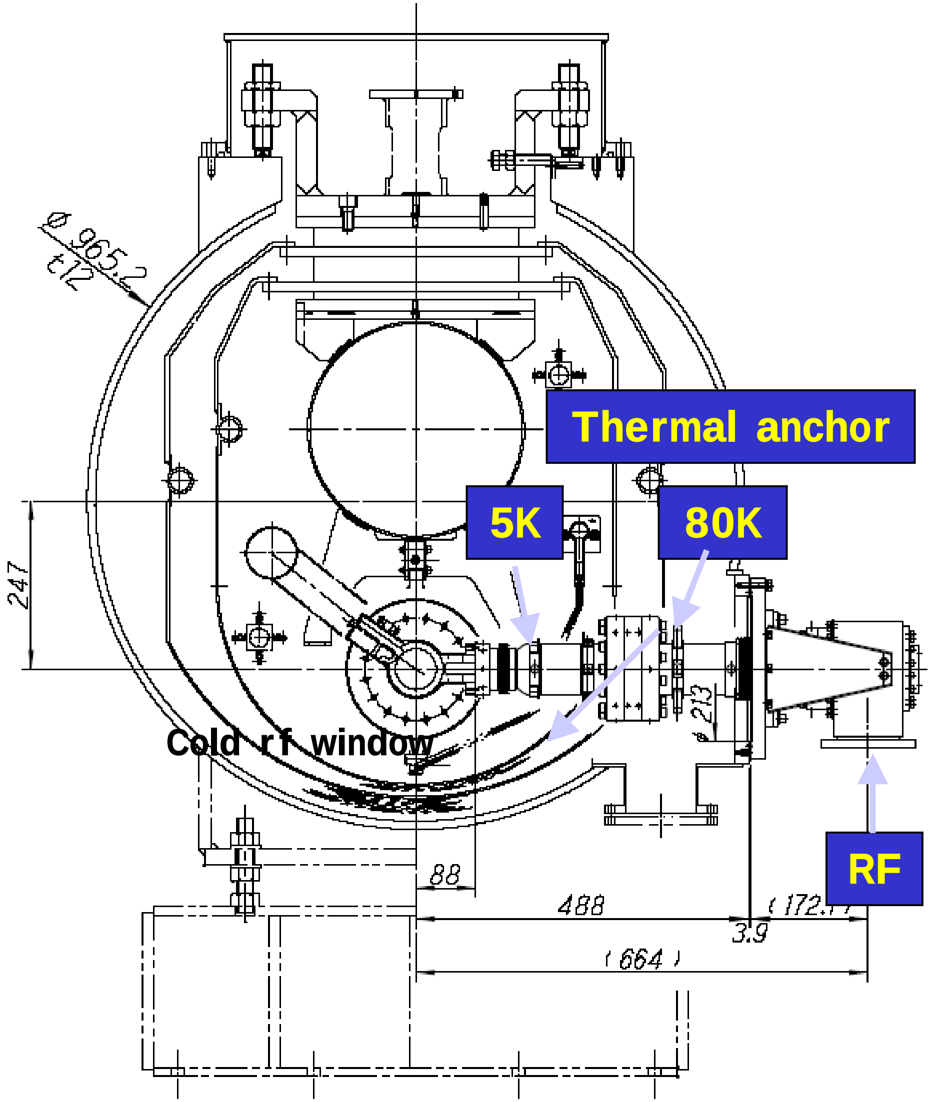

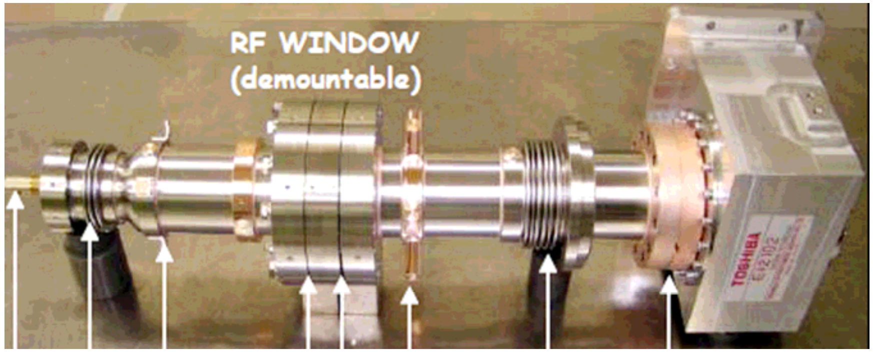

Major Parameters

Input rf power: 500 kW

Pulse width: 1.3 msec

Repetition rate: 5 Hz

Average rf power: 3.25 kW

Thermal loss [W]

	80K	5K	2K
Static:	1.24	0.54	2.6x1e-4
Dynamic:	2.14	2.88	0.25
Total:	3.38	3.42	~0.25

RRR: 3.5 (measured data)

ELECTRIC FIELD GRADIENT AT INPUT POWER OF 500-KW

Maximum electric field gradient in the air side for warm window.

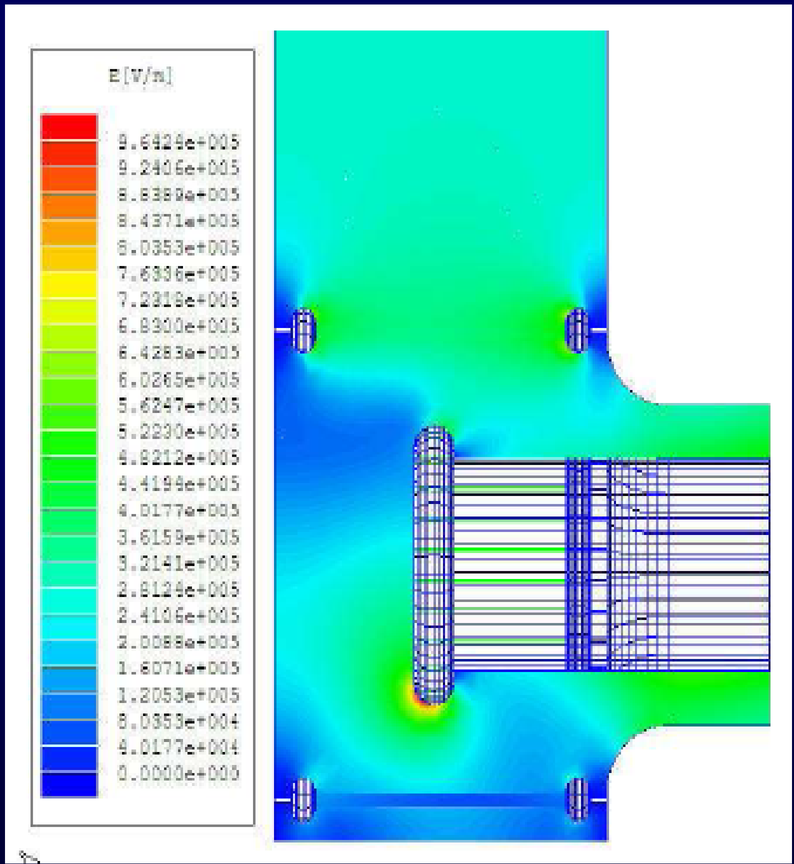

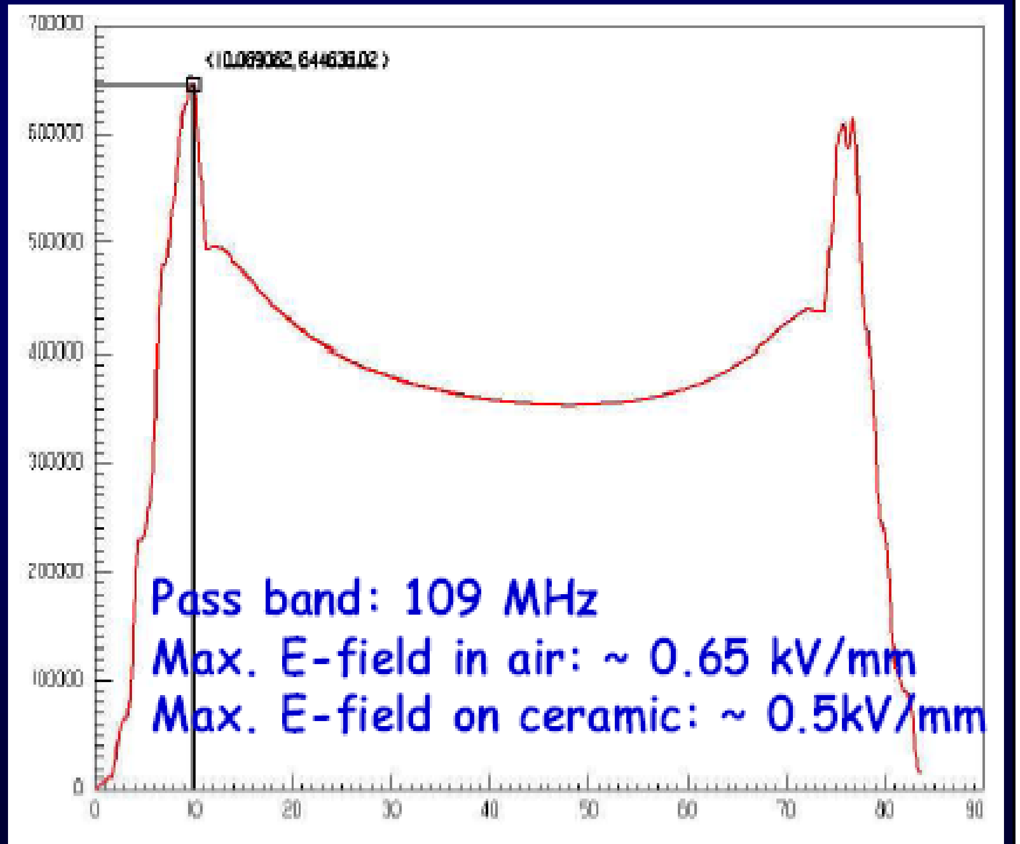

Pass band: 109 MHz

Max. E-field in air: ~ 0.65 kV/mm

Max. E-field on ceramic: ~ 0.5kV/mm

Capacitive Coupling Coaxial Line for Input Coupler

Capacitive coupling coaxial line should have advantages; By H.Matsumoto and S.Kazakov

1) Good thermal insulation ability between the warm and the cold sides.

2) Reduce the brazing difficulty for the ceramic window.

Concept of capacitive coupling coaxial line

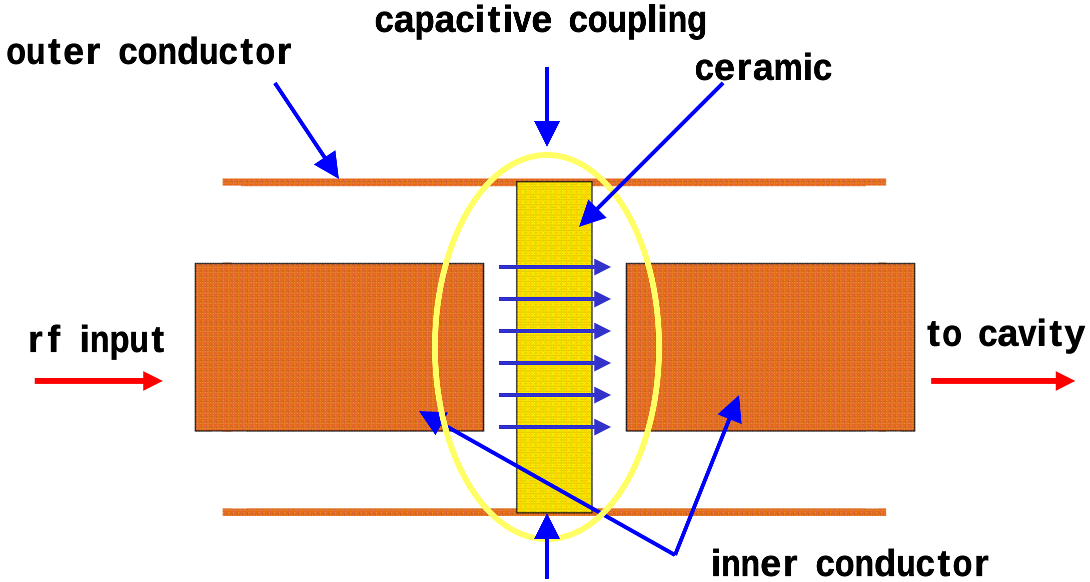

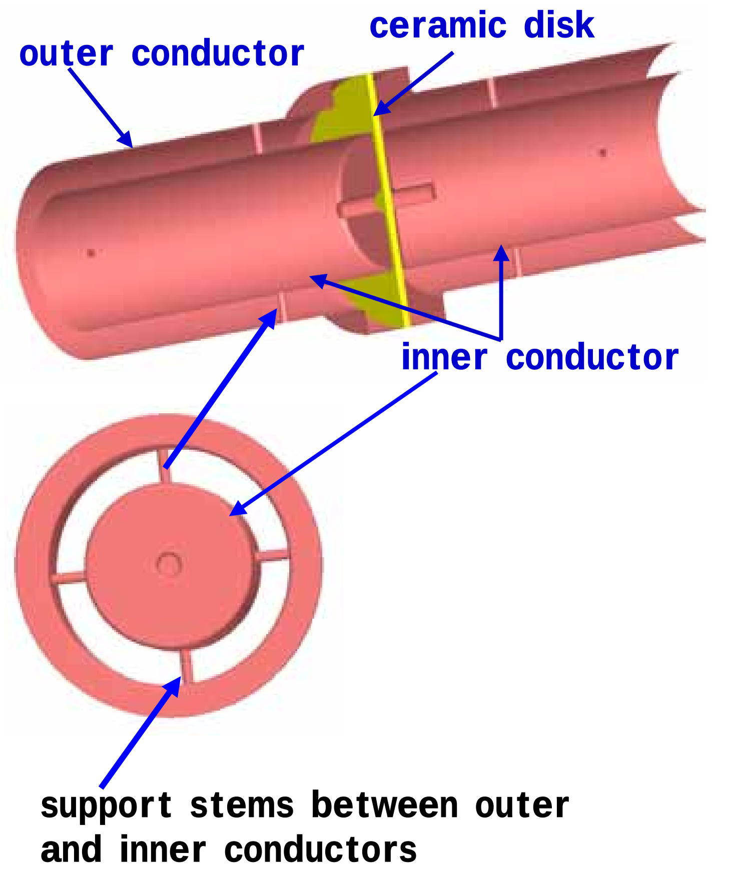

Easy to braze between cooper and ceramic disk.

Well established in warm technology

INDUSTRIALIZATION with MODULAR STRUCTURE

Input coupler comprises of four modules:

1) coaxial transformer
2) coaxial line
3) rf window
4) antenna at cold side

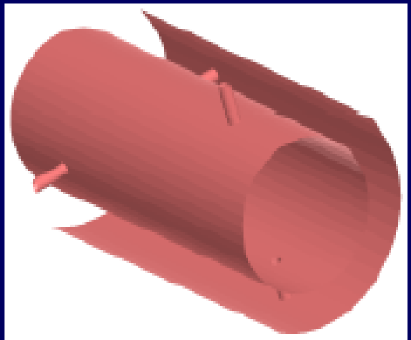

Each pair of rods is mounted in the gap between the inner- and outer-conductors, and are rotated 90 degrees from each other.

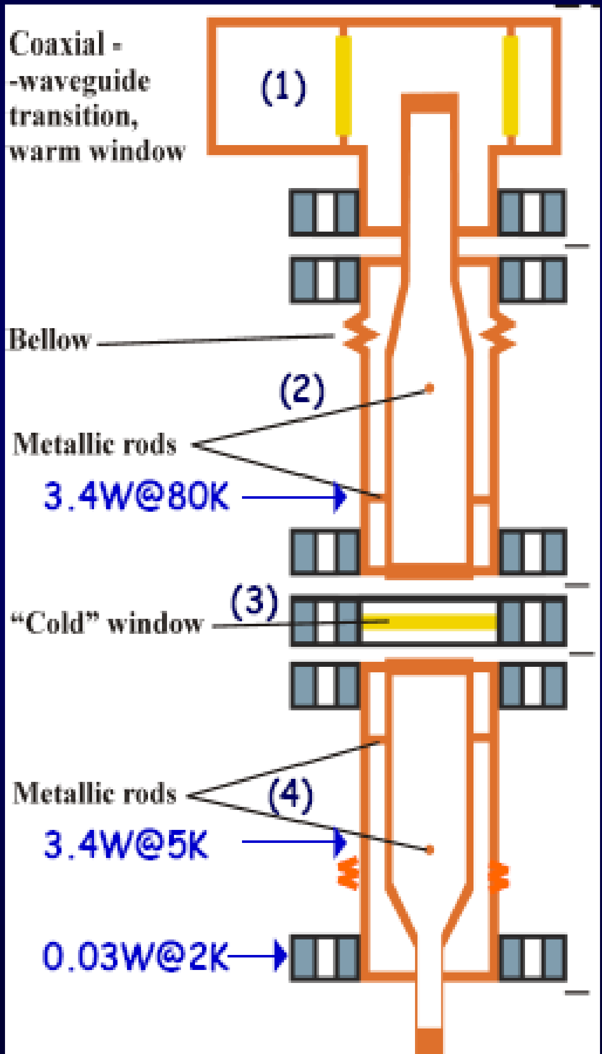

[1] The complete input coupler can be divided into four relatively simple parts to **ease fabrication and assembly**. If we assume that the inner conductors are not attached rigidly to the waveguide, we **need only two**
[2] **bellows to absorb the movement of the coaxial line** due to thermal contaction and
[3] expansion between cool down and warm up.

The fabrication of each module
[4] **technical requirements dose not overlap for each parts.**

Average power: 3.25-kW (500-kW, 1.5-msec, 5-pps) RRR: 3.5 (measured data for copper plated layer)

500kW Input coupler high power test stand @ STF

Coaxial capacitive input coupler

By H.Matsumoto and S.Kazakov

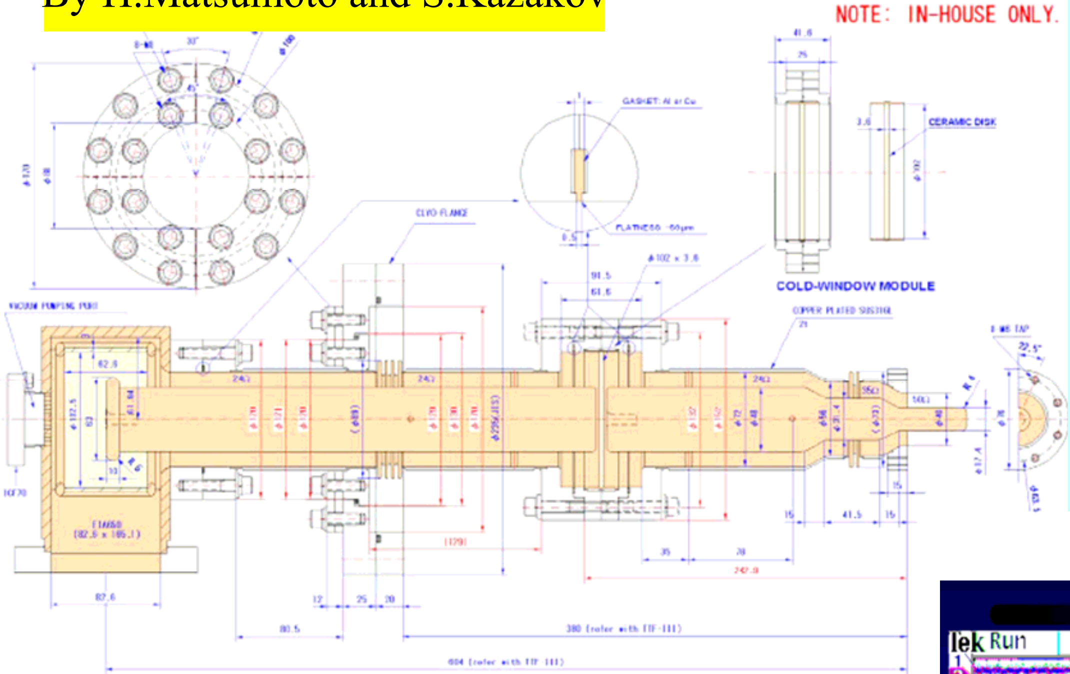

Successfully demonstrated the high power performance up to 2MW!

The specification: 500kW, 1.5msec, 5Hz @ 45MV/m operation

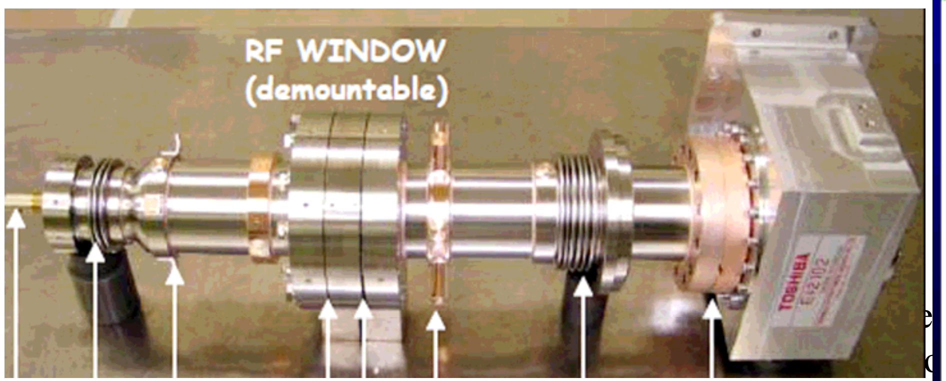

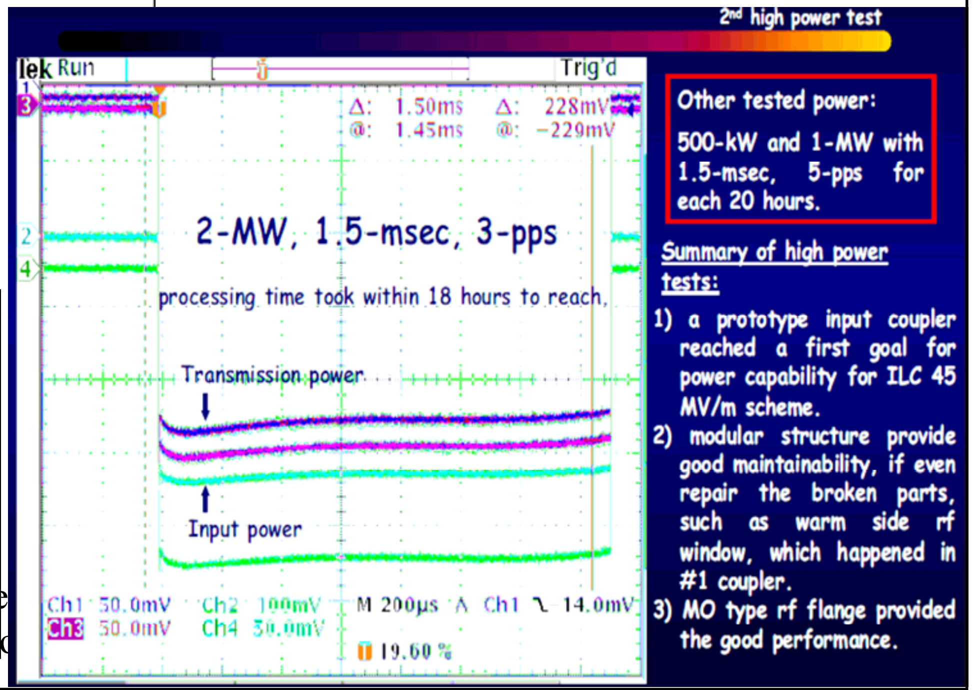

Progress with Input Coupler @ LAL

- Selected recent progress on CARE SCRF:
  3 new prototype designs of power couplers from LAL-Orsay:

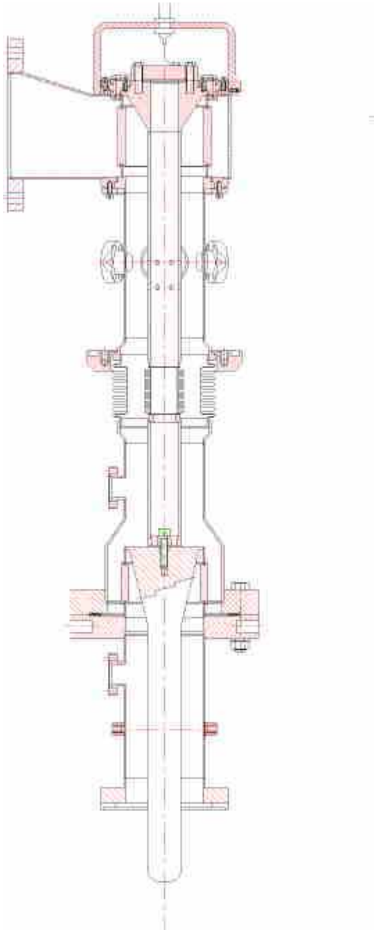

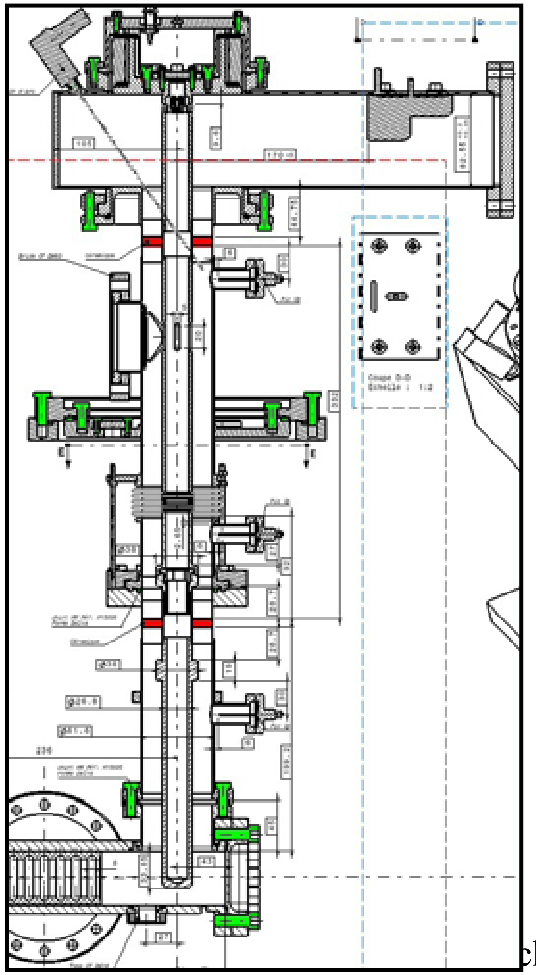

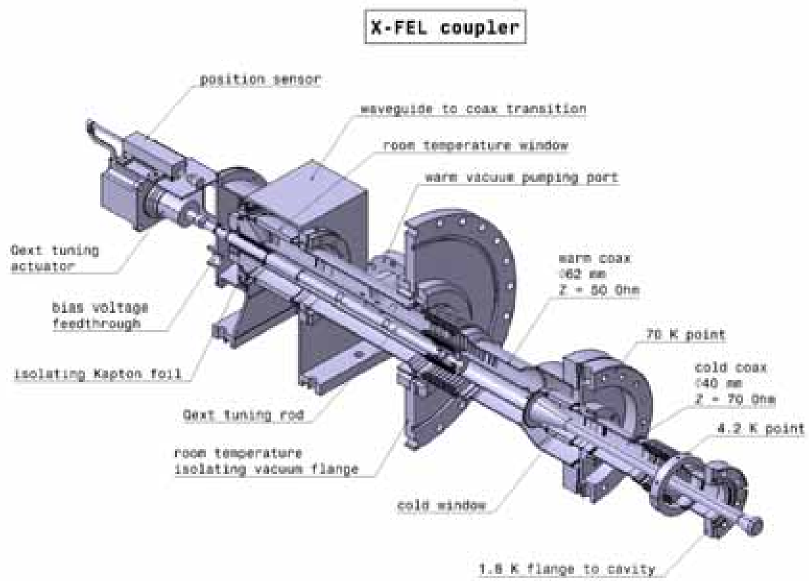

- **To be built in industry and tested in 2006.**

TTF III Coupler Processing Times in CHECHIA

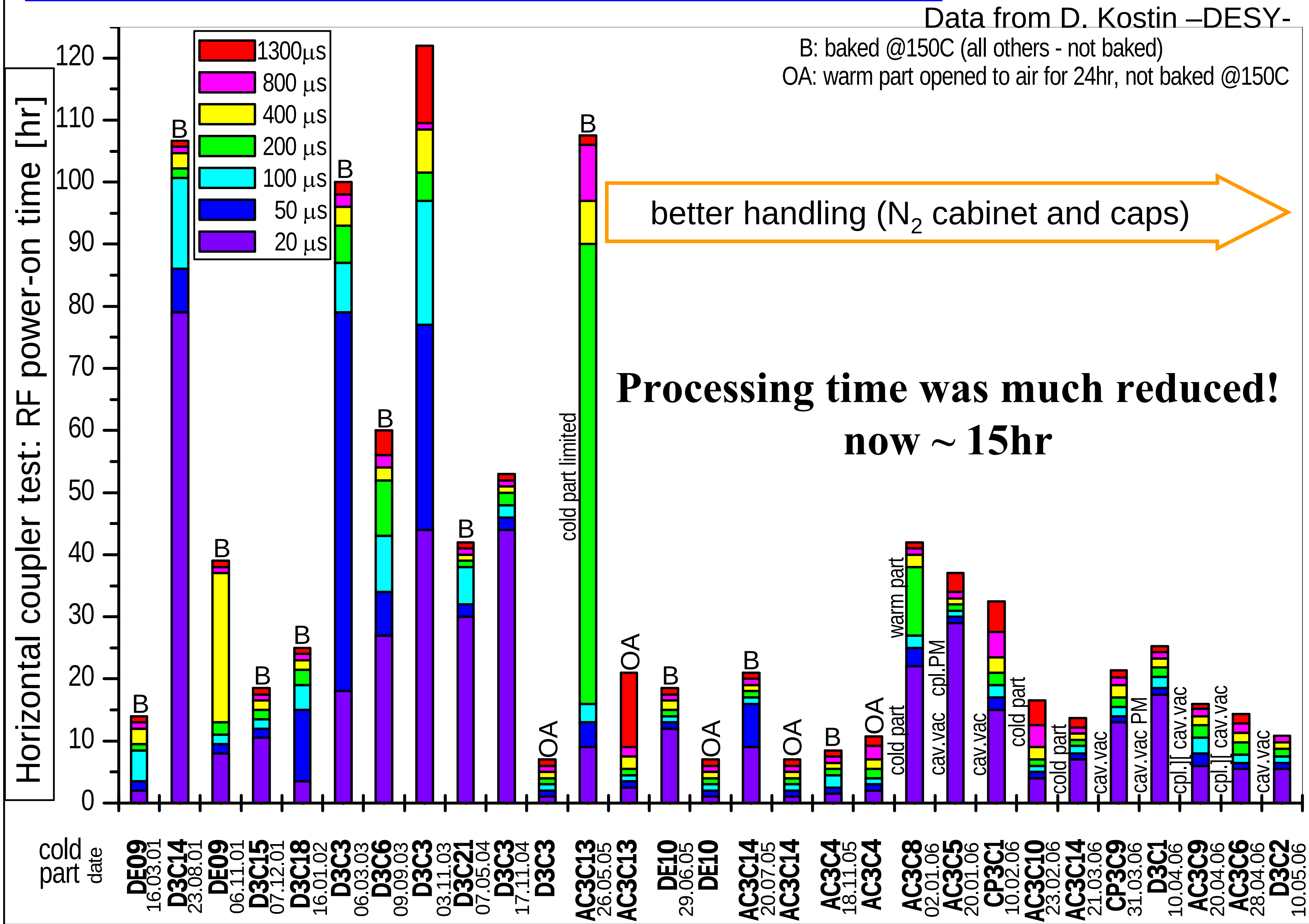

7. Cavity Dressing

7.1 Helium Vessel Assembly at KEK
7.2 Cavity Dressing

Flow of the Cavity Assembly to Cryomodule

TTF

String Assembly

The LC cold option

ITRP Visit to DESY, 5th/6th April 2004

Module Assembly

TESLA

The LC cold option

Helium Vessel Parts @ KEK

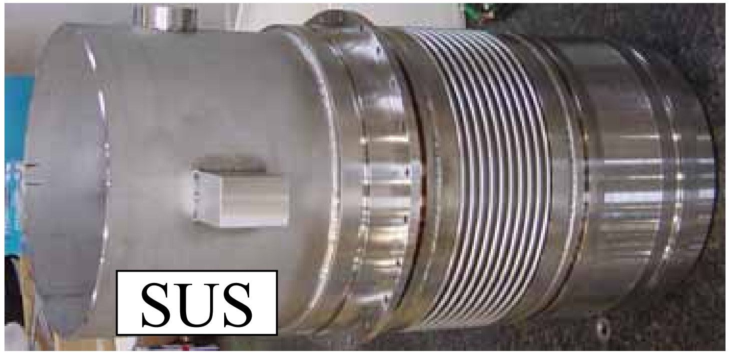

TIG Welding of the Vessel @ KEK

Completed Helium Vessel

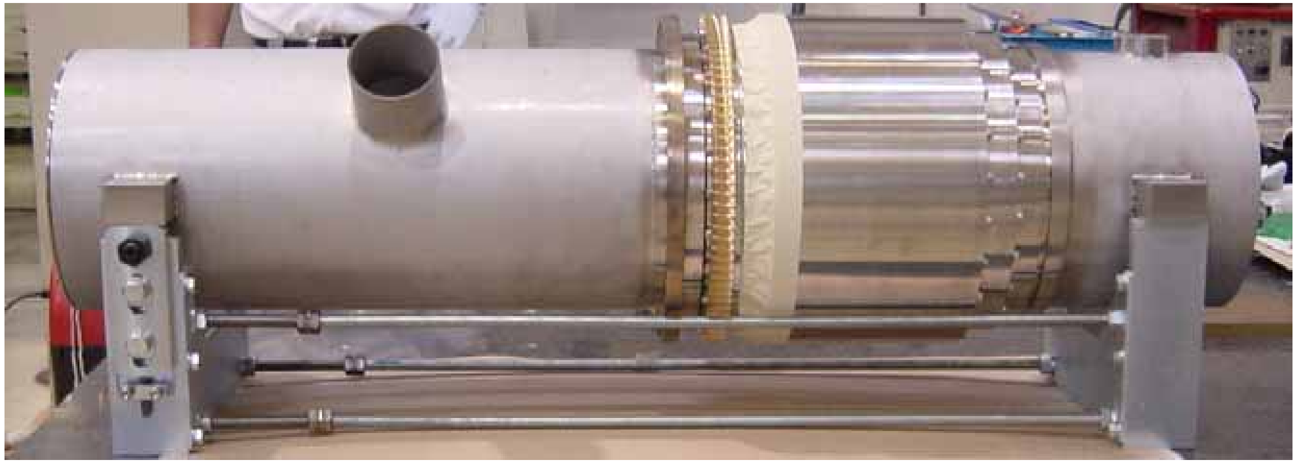

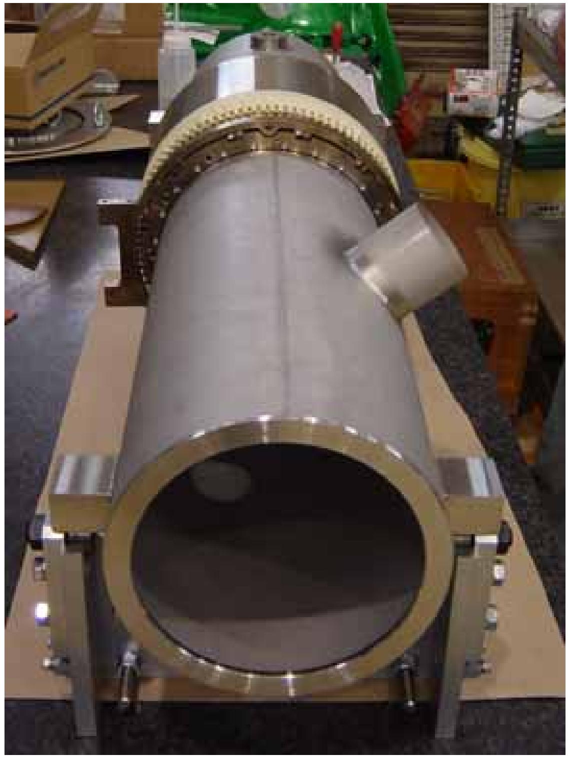

Tuner Dressed Cavity @ KEK

Ichiro Cavity

Cavity String Assembly at DESY

The inter-cavity connection is done in class 10 cleanrooms

Coupler Mounting @ KEK

A Fully Dressed Cavity Holed under He Gas Return Pipe

KEK LL cavity

K

8. ILC Cryomodule

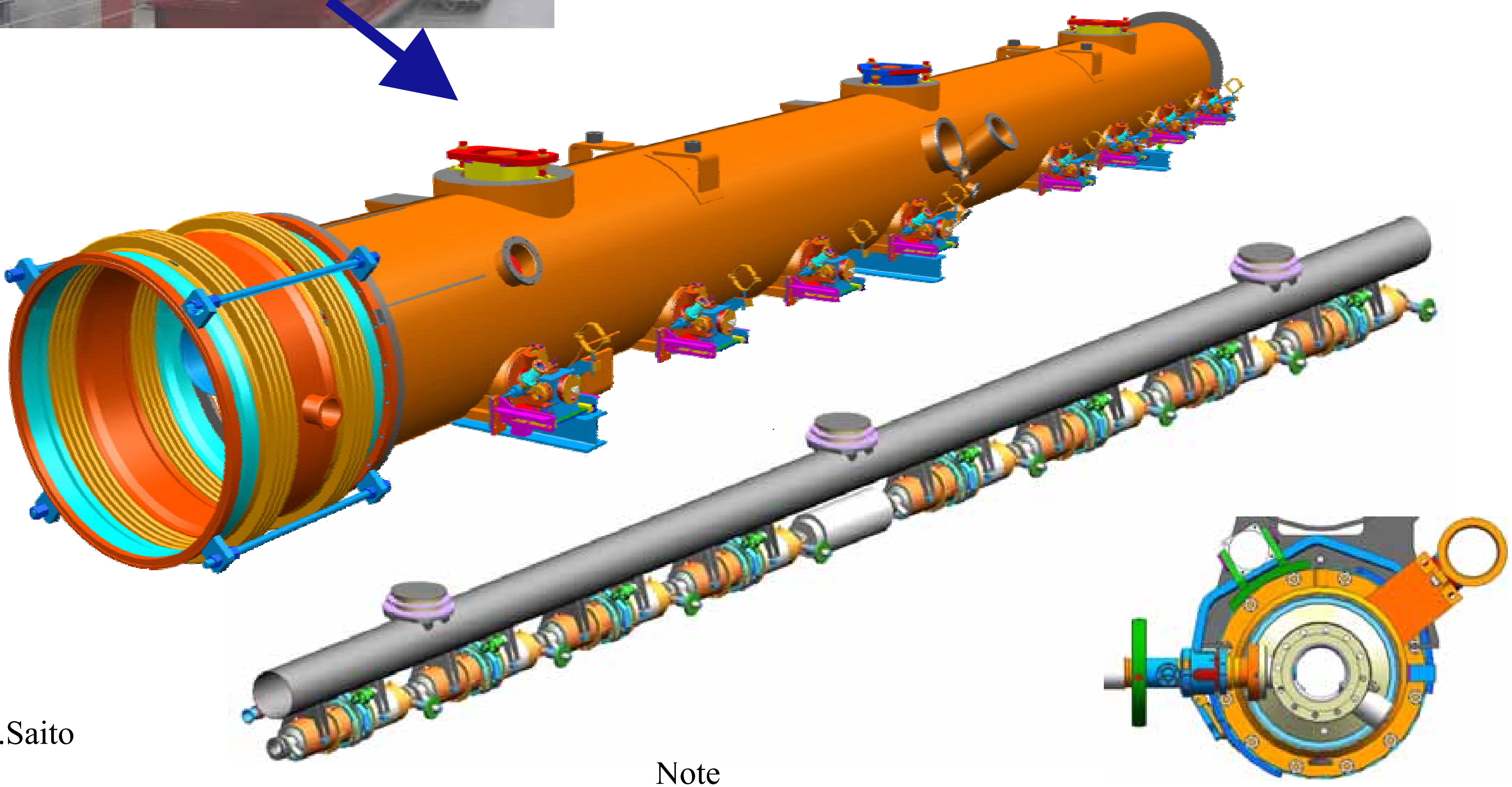

K.Saito

Note

Characteristics of the Liquid Helium

Very small efficiency !

Generation efficiency of LHe: η_{eff}

$$\eta_{eff}(T) = \frac{T}{300\text{-}T} \cdot \eta_{tech}, \quad 6.71E\text{-}3 \ @\ 2T,$$

$$\eta_{eff}(2K) \approx 0.1\% \ @\ \eta_{tech} = 0.2,$$

This means that one needs 1kW energy to remove 1 W of the heating.

Very small Latent heat !

	LHe	LN2
Boiling temp.[K]	**4.22**	**77.35**
Density [kg/L]	**0.125**	**0.809**
Latent heat[kJ/L]	**2.55**	**161**
Volume ratio of Gas/Liquid	**769**	**710**

Cryomodule Design

- **Minimize the radiation energy from outside**
- **Reduce heat leak from outside**
- **Use the material with low thermal shrinkage**

Basics for Cryomodule Design

Radiation energy

Radiation Power: $E_r(T)=\sigma T^4$

(Stefan-Boltzmann law)

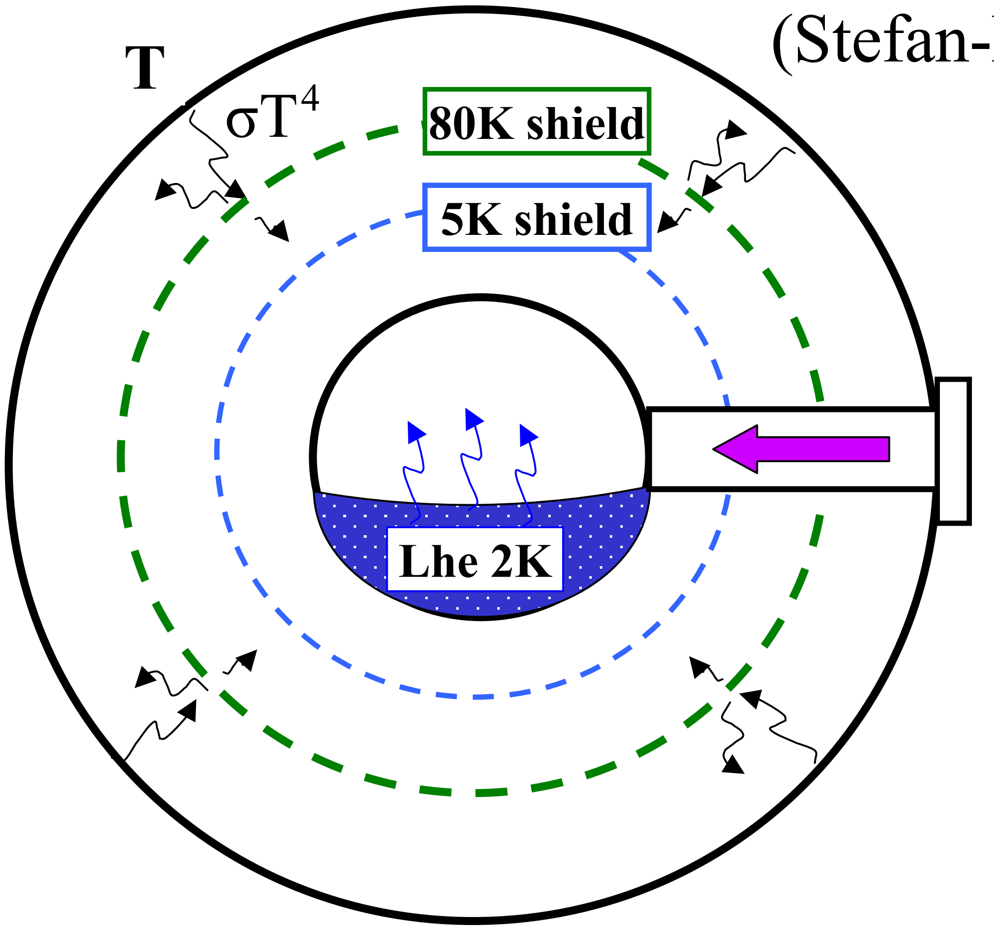

Stop the direct radiation !
Use the reflection shield!

$$\frac{E_r(300K)}{E_r(5K)} = \frac{300^4}{5^4} \approx 13E6$$

$$\frac{E_r(300K)}{E_r(80K)} = \frac{300^4}{80^4} \approx 200$$

$$\frac{E_r(80K)}{E_r(5K)} = \frac{80^4}{5^4} \approx 65500$$

K.Saito

Use the material with small thermal conductivity
Example: SUS, G10….

Cross section

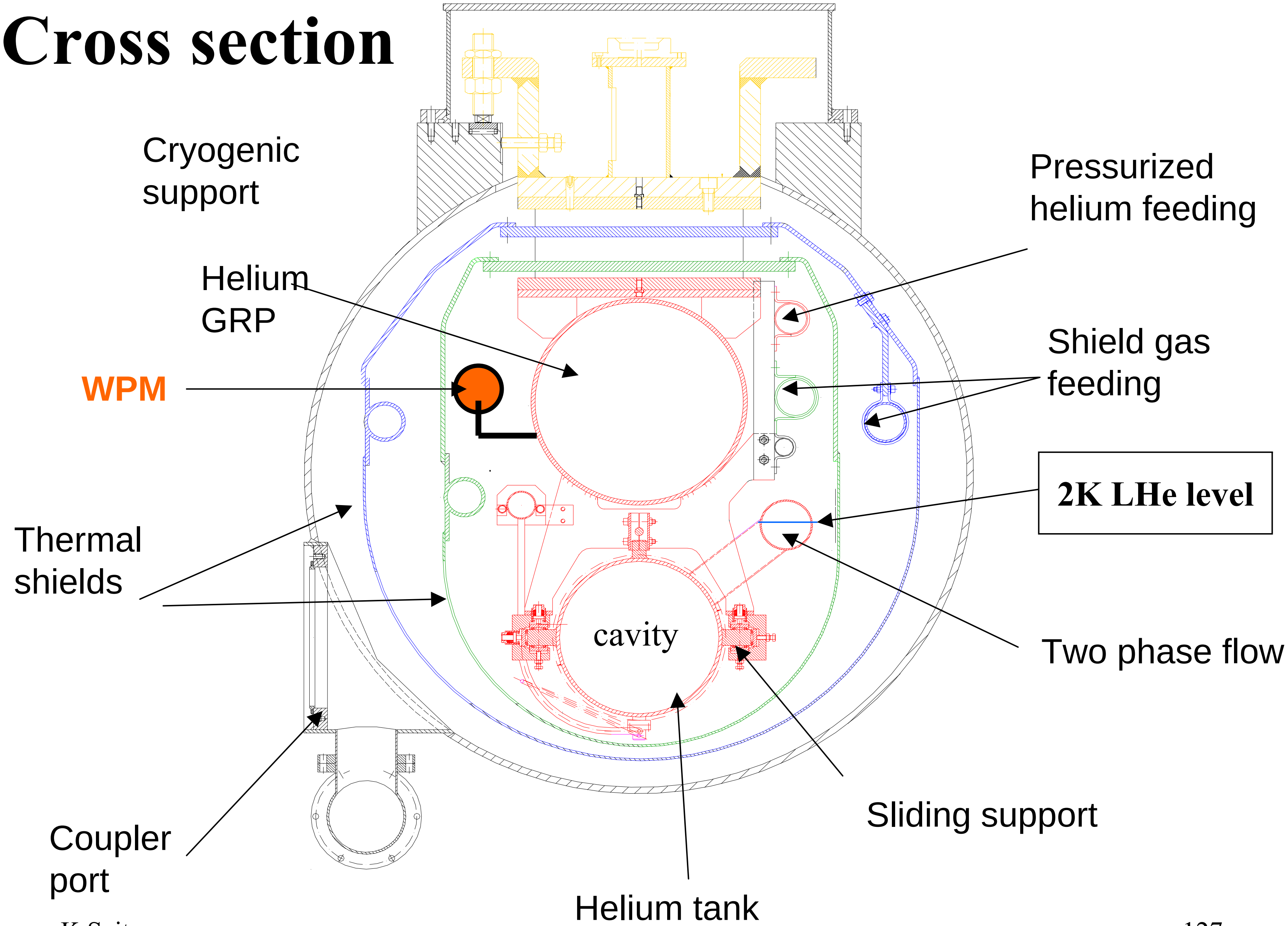

5K Shielding @ KEK

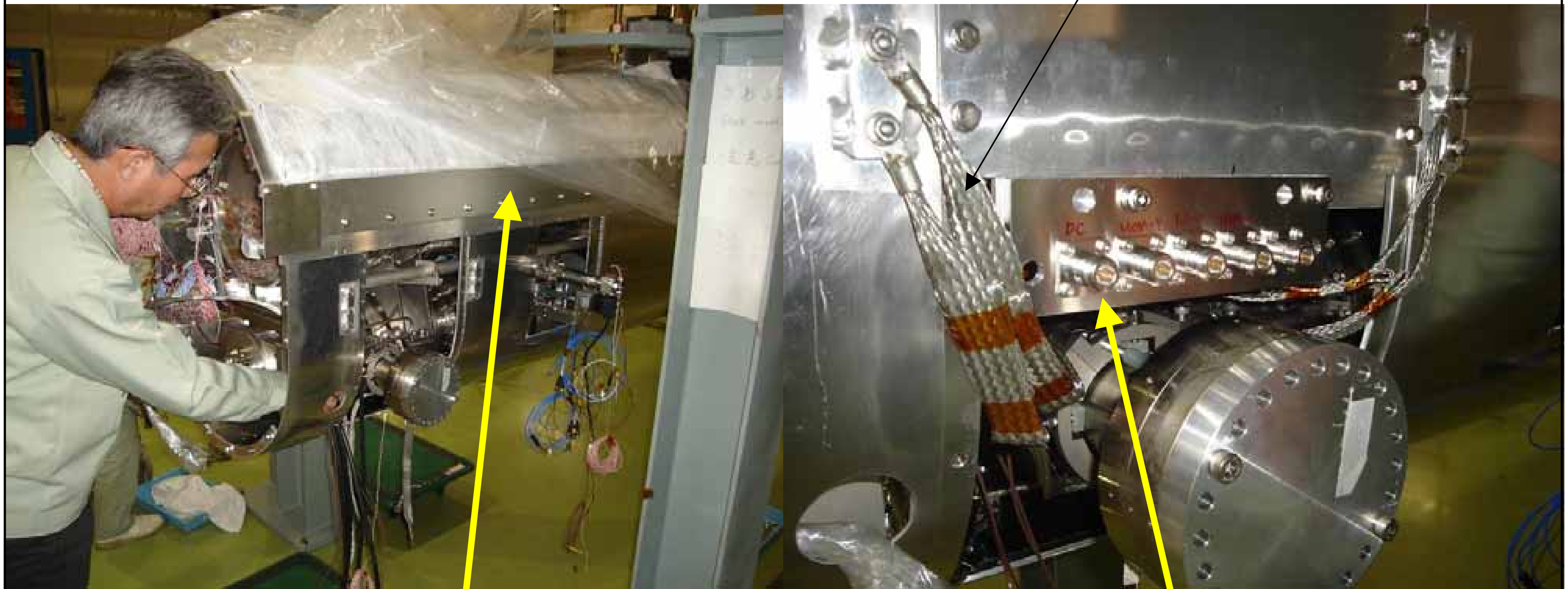

Coupler and Tuner in the cryomodule @ KEK

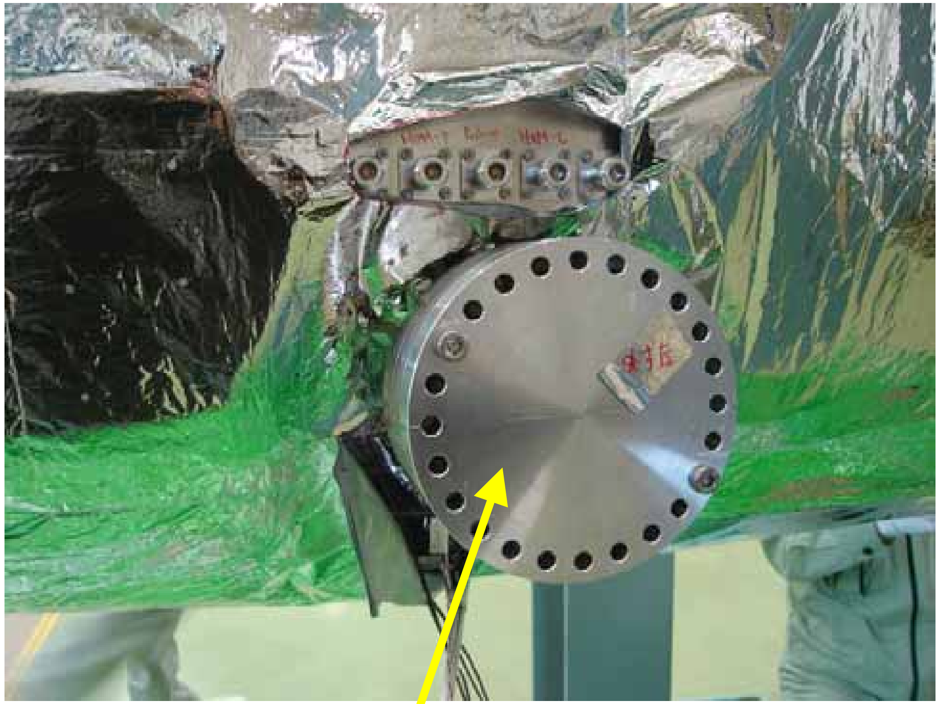

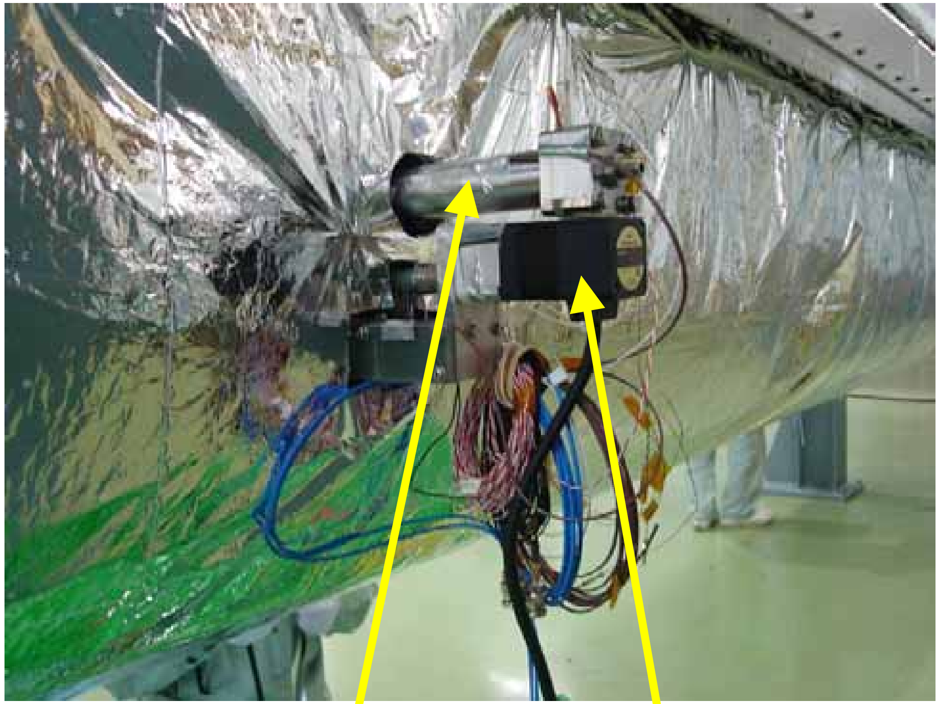

Cold window cover

Piezo Tuner

Motor

80K Shielding

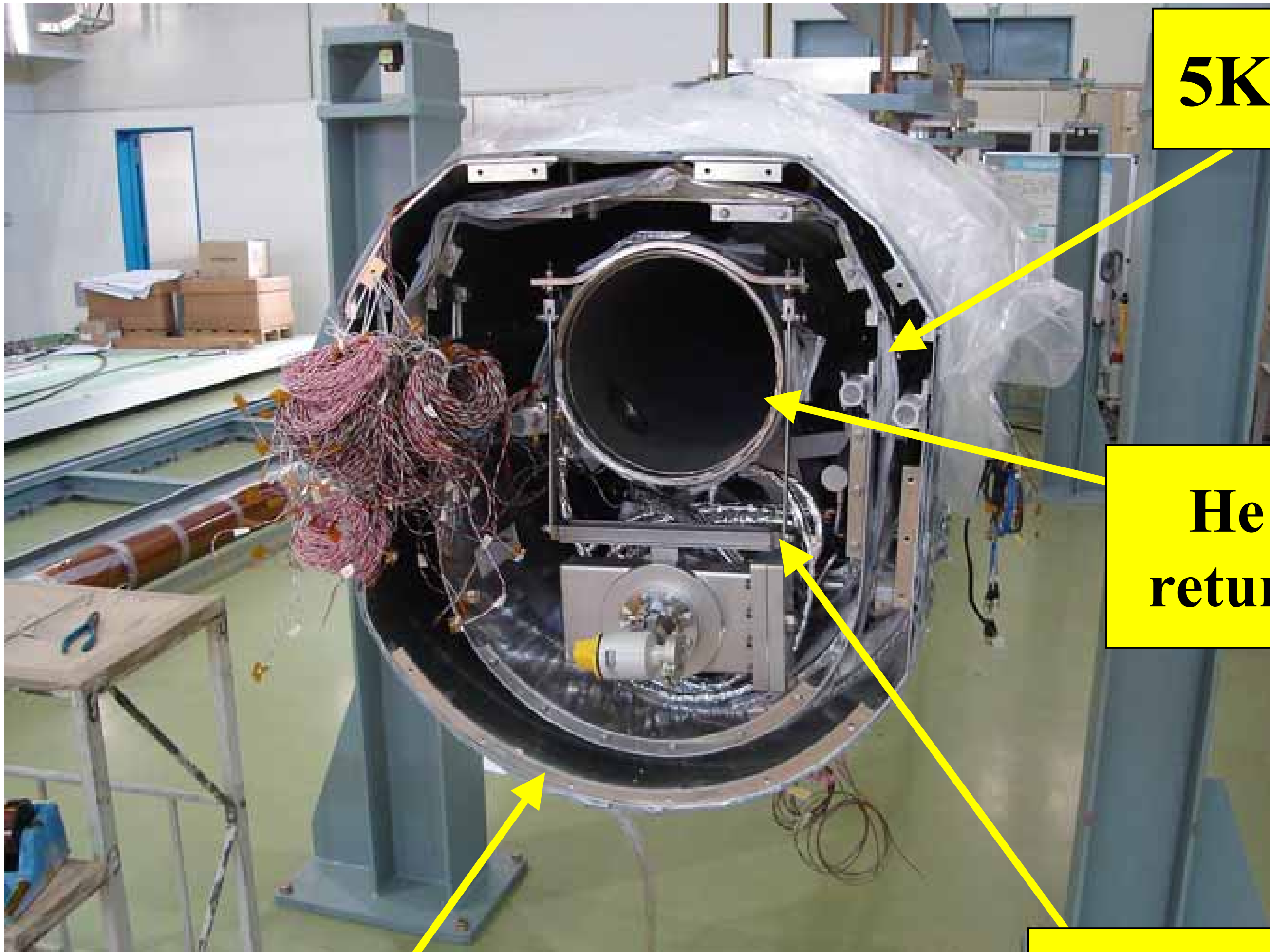

Installation into vacuum vessel

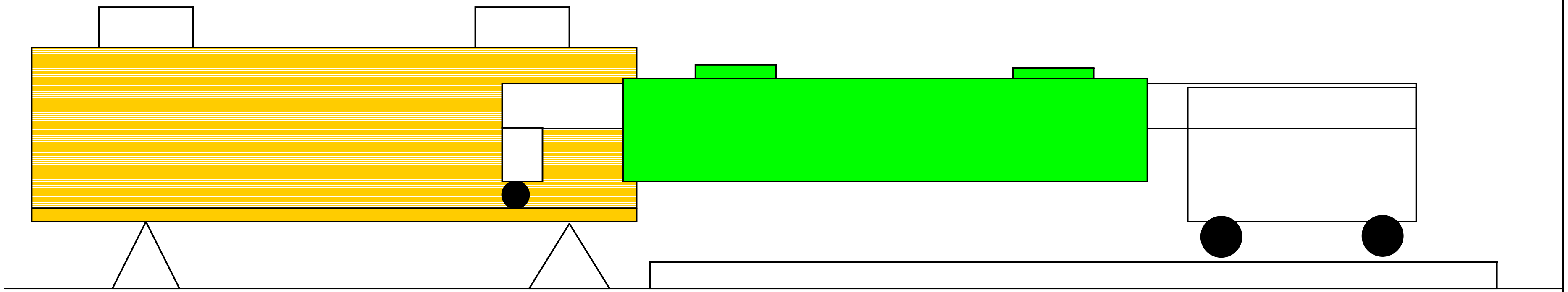

Move into the tunnel

Cryomodule in the STF Tunnel

For ILC Cryomodule Design

Minor changes to address major concerns.

- Magnet alignment and vibration issues.
- Cryomodule with and without magnet package
  - Define BPM, Steering, and Quad parameters
  - Possible option for separate magnet cryo vessel
- Reduced cavity length (which tuner design?)
- Reduced cavity spacing (new interconnect)
- Need for functional Fast-Tuner

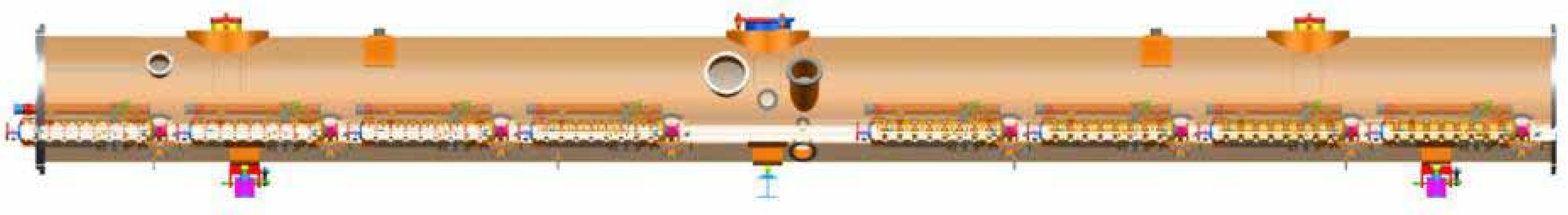

Cryogenics

Completely thermodynamics

Open the JT valve bellow 45K for LHe

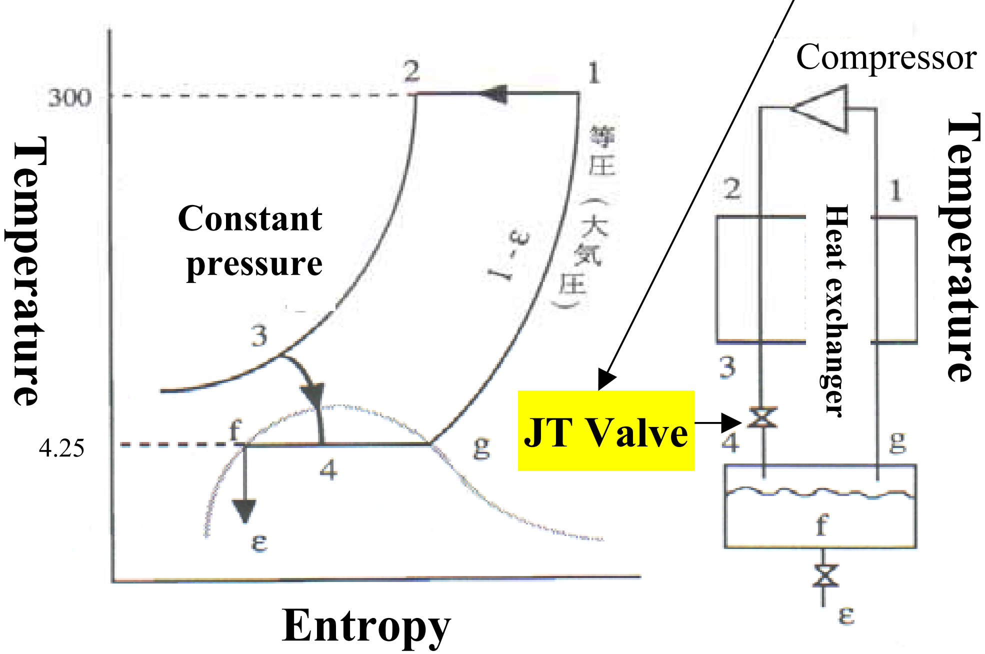

J-T cycle

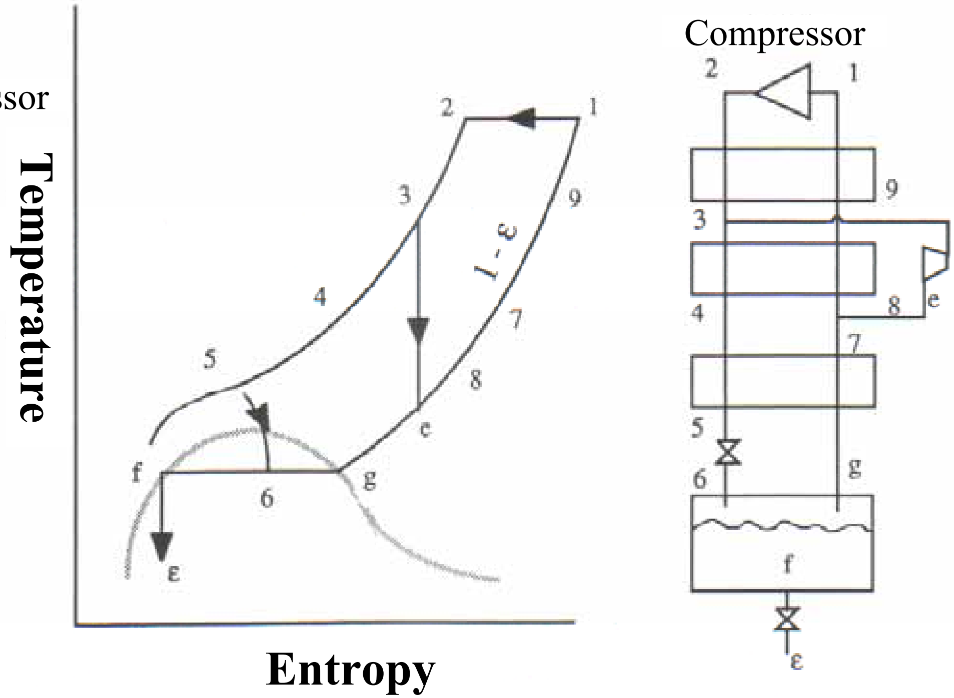

Claude Cycle

Expand the gas by J-T valve, and decrease the temperature

Make work a part of the gas by operating turbine,
Decrease the temperature,
Reduce the temperature of the heat exchanger

2K Liquid Refrigerator (CEBAF)

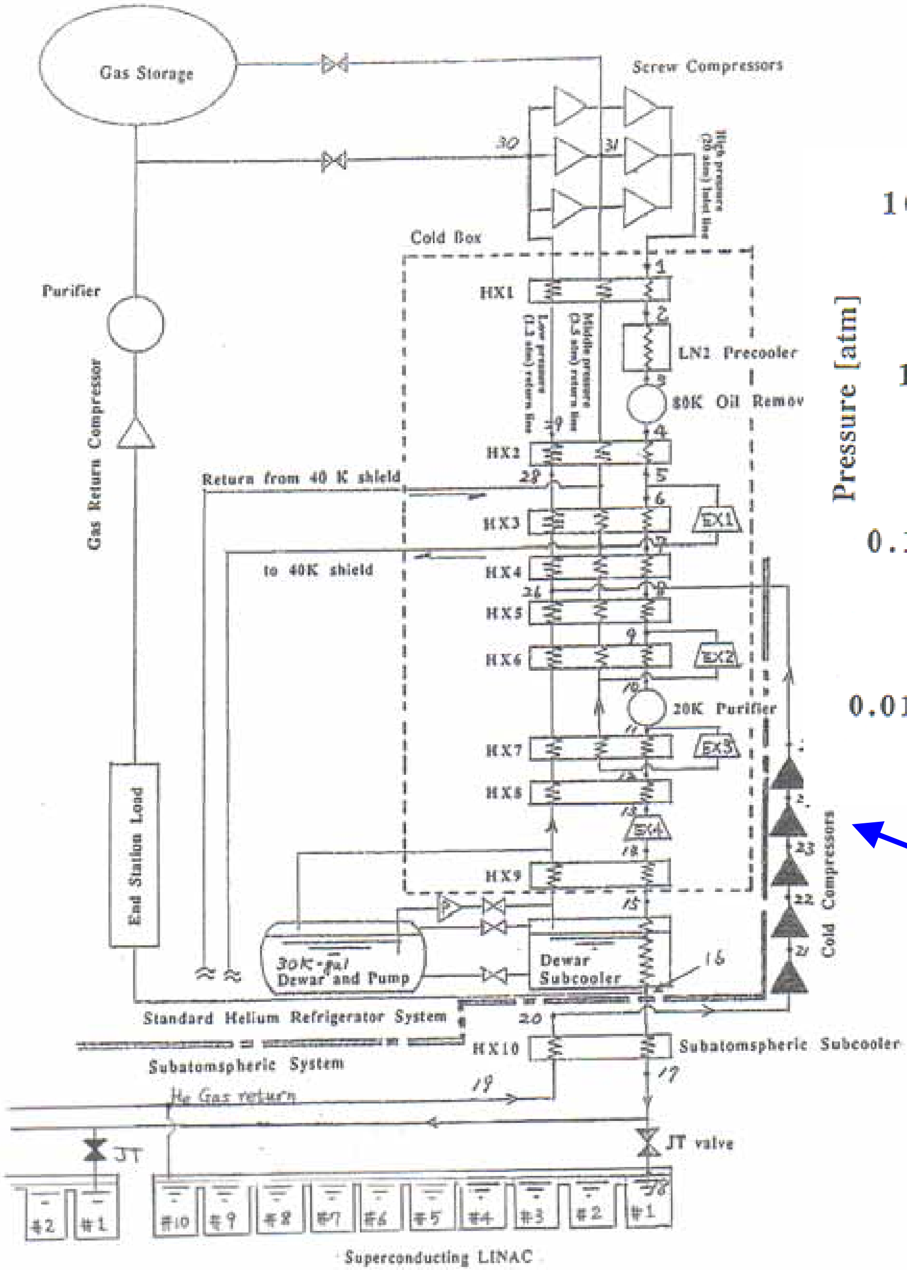

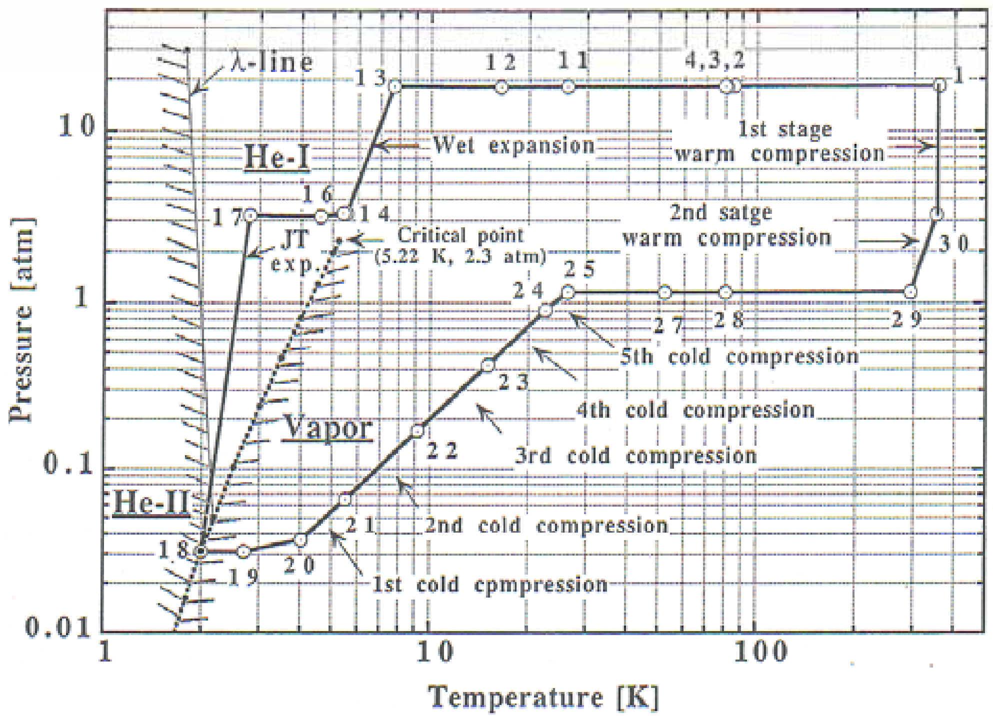

Cold compressor:
Compress the cold gas and
Increase the temperature and pressure up to nearly RT.

LHe Temperature P vs. T

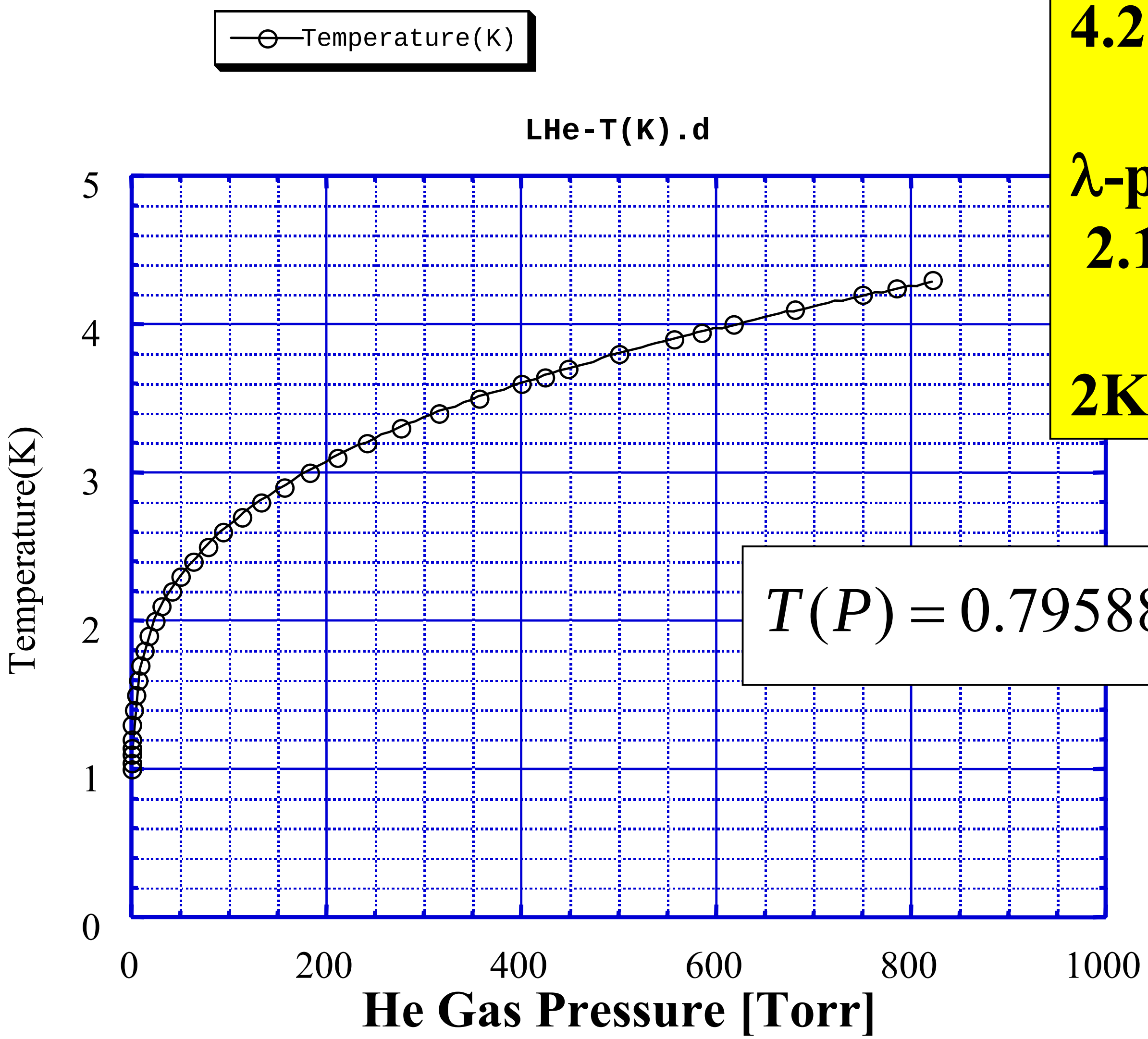

4.25 K = 760 Torr

λ-point :
2.1773K = 38.41 Torr

2K = 23.77 Torr

$$T(P) = 0.79588 + 0.46085 \cdot P^{0.30163}$$

Characteristics of the He-II

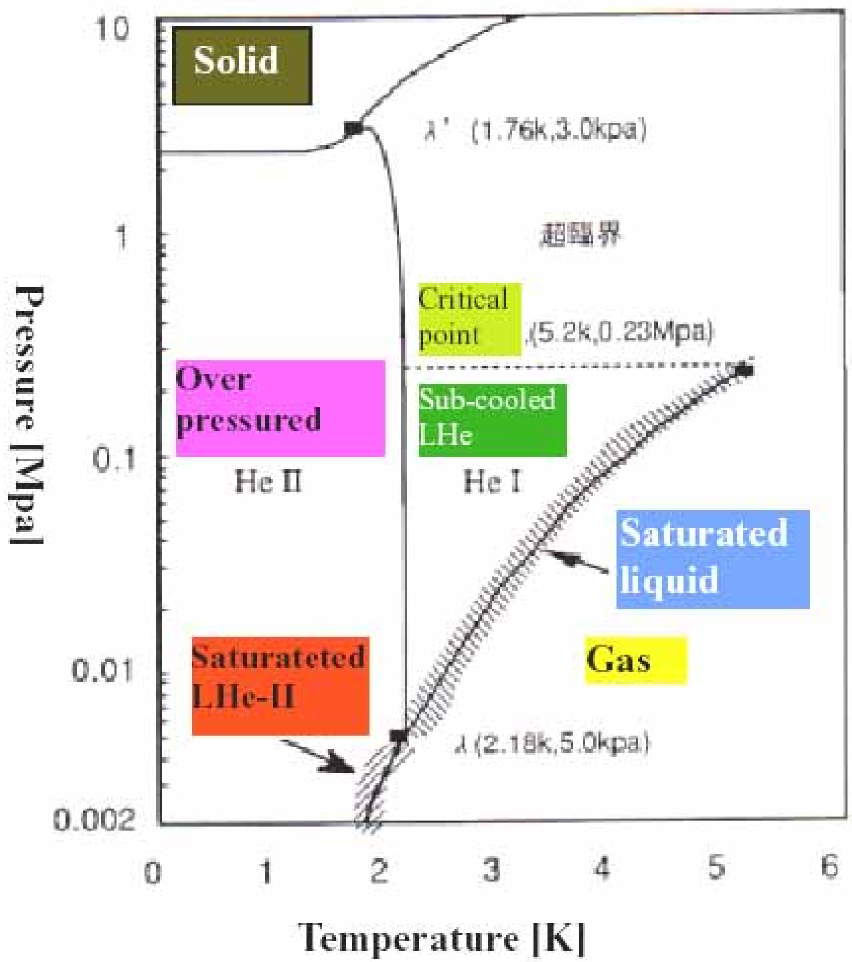

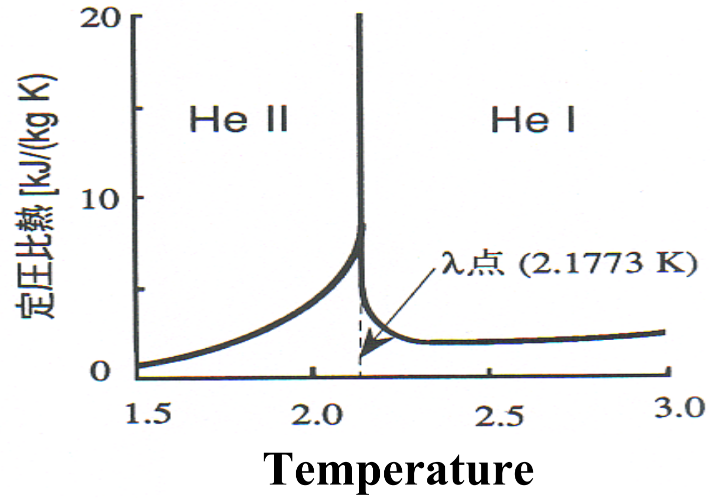

図 5 - 2　ヘリウム 4 の定圧比熱

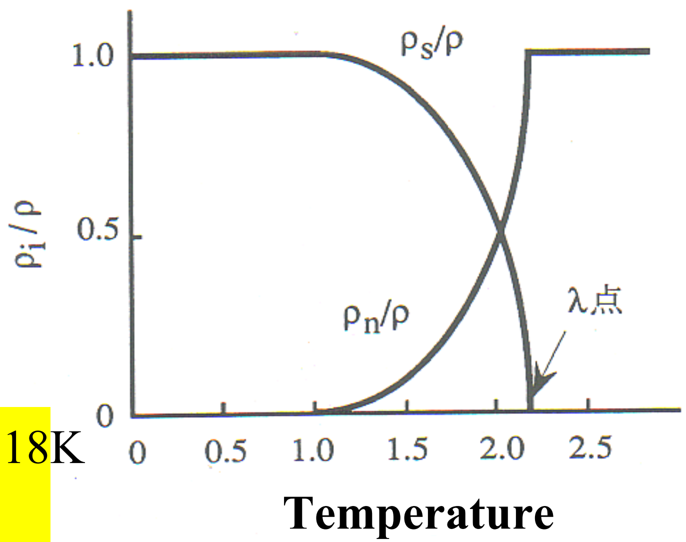

図 5 - 3　He II中での超流動成分（ρ_s/ρ）と常流動成分（ρ_n/ρ）の比率の温度変化

- LHe transits from He-I to LHe-II at Lamda point : T=2.18K
- He-II　has no viscosity and makes easily super-leak.
- He-II has very a large thermal conductivity. which is 100 higher than that of copper at low temperature

Characteristics of thermal conductivity of He-II

$$q^m = f(T)^{-1} \frac{dT}{dx}$$